

THE SEDIMENT BUDGET OF HANAIEI BAY, KAUAI, HAWAII

A DISSERTATION SUBMITTED TO THE GRADUATE DIVISION OF THE
UNIVERSITY OF HAWAII IN PARTIAL FULFILLMENT OF THE REQUIREMENTS
FOR THE DEGREE OF

DOCTOR OF PHILOSOPHY

IN

GEOLOGY AND GEOPHYSICS

DECEMBER 1999

By

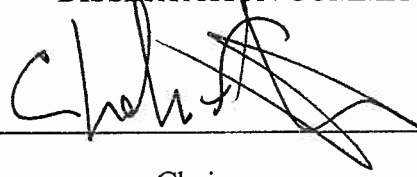
R. Scott Calhoun

Dissertation Committee:

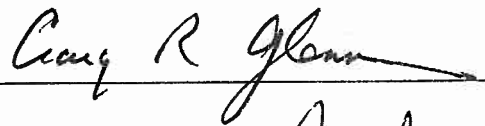
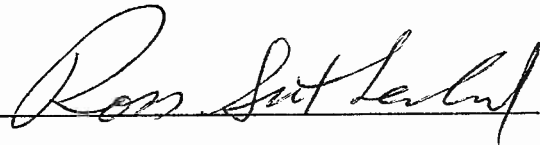
Charles Fletcher, Chairperson
Bruce Appelgate
Craig Glenn
Ralph Moberly
Ross Sutherland

We certify that we have read this dissertation and that, in our opinion, it is satisfactory in scope and quality as a dissertation for the degree of Doctor of Philosophy in Geology and Geophysics.

DISSERTATION COMMITTEE



Chairperson



Dedication

I would like to dedicate this dissertation to and thank the efforts and wisdom of Emmett and Dorothy Calhoun and Paul and Katherine Ashley who recognized my need for an education long before I existed and planned to make it possible. Also to my parents, Kay and Bob Calhoun, for their vision, unwavering support, and occasional defense of my education.

This dissertation also is dedicated to Krister Osterland, Steve Lennon, Trevor Aurand, Karl Bornhoeft, and Gethyn Carr-Harris. Camp Parsons staff members who did not live long enough to fulfill their promise, but set an example for the rest of us.

My finally dedication is to the phenomenal teachers who have been the stepping stones upon which I have traveled. Particularly, to Jean Augustine, who, more than any other person taught me to read and write, and without whose help many years ago this dissertation would never have been possible.

Acknowledgments

I would like to thank Neil Berg of the U.S. Fish and Wildlife Service and Eric Grossman for their assistance in the field; Gary McMurtry, Max Cramer, and Ken Rubin for valuable help in analyzing the cesium-137 data; and Ross Sutherland and Samir El-Swaify for their discussions and critical reviews of early versions of Chapter 1.

Sea Engineering, Inc. conducted the geophysical surveys and provided me with the data. Radiocarbon ages were determined at the NOSAMS facility in Woods Hole, MA under NSF Cooperative agreement number, OCE-9807266. Greg Moore and Denise Hills helped make sense of the seismic data. Alex Ress and Doug Neil spent many weeks in the field with me and managed to keep the sieve...er...boat afloat and running. Alan Friedlander and Ralph DeFelice of the University of Hawaii biology project for MHI-MRI at Hanalei shared valuable insights from their experiences in the bay and data including substrate characteristics and bathymetry. They also kindly allowed me to sleep at their house while I investigated floods. Margarethe Pfeiffer assisted with the grain size analysis and spent many hours wrestling with the “row-smash” shaker. Valuable discussions and field assistance were provided by my fellow Coasties: John Rooney, Melanie Coyne, Clark Sherman, Rob Mullane, Eric Grossman, Jodi Harney, Zoe Norcross, Dolan Eversole, and Ebi Isoun. Denise Hills and Sarah Bean Sherman were very helpful in reading late editions of this dissertation. Although the SOEST Illustrations team of Nancy Hubert, Brooks Bays, and May Izumi made many heroic efforts to make my figures and posters look great, I have foiled them on occasion.

I'd like to thank the “Monday Night Football Crowd” and my dive buddies, Jackie Caplan-Auerbach, James Foster, Gretchen Benedix, Sarah Bean Sherman, Rachel and Eric Lentz, and Jeff Johnson, who managed to keep me sane. Pali Montoya-Bowman shared her home with me for many months while I endlessly filtered water and sediment from the Hanalei River.

Finally, I'd like to thank my advisor, Chip Fletcher, and committee, Bruce Appelgate, Craig Glenn, Ralph Moberly, and Ross Sutherland for their guidance and patience. This research was conducted with funding from the Hawaii State Department of Land and Natural Resources, Division of Aquatic Resources and the U.S. Geological Survey Coastal and Marine Geology Program.

ABSTRACT

The sediments of Hanalei Bay are separated into two groups based on their source: terrigenous and marine. The terrigenous component, primarily from the Hanalei River, was analyzed with measurements of suspended sediment concentration in the river as well as thickness and calibrated radiocarbon ages of the cored fluvial deposits on the coastal plain. An empirical model, the Universal Soil Loss Equation (USLE), was used to describe the erosional characteristics of the Hanalei basin and to estimate the amount of sediment lost from the valley due to water erosion. The marine component was investigated by combining observational data describing sedimentary processes with geophysical surveys. Benthic samples, collected from numerous sites throughout the bay, show physical characteristics of the sediments, while side-scan sonar and seismic reflection surveys disclose the lateral extent and thickness of sedimentary deposits.

Suspended sediment and floodplain volumes indicate $7,560 \pm 2,910$ Mg (metric tons) yr^{-1} are removed from the Hanalei watershed. This is a higher percentage (45-101%) of the USLE-predicted hillslope output ($4,800 \pm 5,600$ Mg yr^{-1}) than would be expected from a watershed the size of Hanalei (54.4 km^2). The excess output of fluvial sediment is likely due to other erosional processes such as mass movement and channel incision. It was not possible to differentiate between hillslope sediments mobilized by water erosion processes, those derived from mass wasting, or those contributed from stream bed and bank erosion.

Calcium carbonate sediments, which comprise approximately 70% of marine sediments in Hanalei Bay, are composed of the skeletal remains of marine organisms such as coralline algae, coral, molluscs, foraminifera, *Halimeda*, bryozoa, and echinoderms. Siliciclastic sediment grains are the most common individual grain type (~27%) and originate primarily from the Hanalei River. The bay holds approximately $45.5 \pm 1.5 \times 10^6$ m^3 of marine sediment while an additional $33.7 \pm 11.2 \times 10^6$ m^3 underlies the modern

coastal plain. Deposition of this sediment likely started soon after the marine environment entered the bay ~11.7 kyr. Based on CaCO_3 production rates in the literature and additional studies in Hawaii (J. Harney, pers. comm.), this is more carbonate sediment than the reefs in Hanalei Bay could have produced in the given time. As a result, an average of $2,490 \text{ m}^3 \text{ yr}^{-1}$ were calculated to have been transported and deposited in Hanalei Bay by the northeast tradewind driven longshore current. This influx of carbonate sediment from the eastern north shore of Kauai is likely to have played a significant role in the mid to late Holocene progradation of the Hanalei shoreline.

Table of Contents

Dedication	iii
Acknowledgements	iv
Abstract	vi
List of Tables	ix
List of Figures	x
 Introduction	 1
 Chapter One: “Measured and Predicted Sediment Yield from a Subtropical, Wet, Steep-sided River Basin: Hanalei, Kauai, Hawaiian Islands”	
Abstract	4
Introduction	5
Geologic Setting	5
Methods	8
Results	10
Discussion	18
Conclusions	26
 Chapter Two: “From Watershed to Reef, A Budget of Carbonate and Terrigenous Sediments, Hanalei Bay, Kauai, Hawaiian Islands”	
Abstract	30
Introduction	31
Geologic Setting	31
Sediment Budget	37
Reef Ecology	38
Methods	39
Results	40
Sedimentology	40
Carbonate Content	40
Composition	43
Texture	46
Beach Volumes	56
Currents	56
Seismic and Sidescan Surveys	60
Coastal Plain Deposition	68
Discussion	68
Sediment Budget	73
Conclusions	79
 Conclusions	 82
Appendix A. Percentage of sediment components	85
Appendix B. Calcium carbonate production rate calculations	86
References	88

List of Tables

Table 1.1. Factors of the Universal Soil Loss Equation.	11
Table 1.2. Estimates of physical erosion rates in Hawaii	19
Table 1.3. Rates of sediment deposition from various environments.....	21
Table 2.1. Hanalei Bay sand texture.	41
Table 2.2. Marine sand composition in Hanalei Bay.	44
Table 2.3. Radiocarbon dates from coral and coralline algae grains.	48
Table 2.4. Marine sediment accumulation in Hanalei Bay and coastal plain system.....	69
Table 2.5. Carbonate sediment production rates.	74

List of Figures

Figure 1.1. Map of the Hawaiian Islands, the island of Kauai, and the Hanalei coastal plain.	7
Figure 1.2. Sediment accumulation rate (mm yr^{-1}) from 7,000 B.P. to the present.	12
Figure 1.3. Profiles of three cores showing depth and lead radioactivity.	14
Figure 1.4. Discharge vs. suspended sediment of the Hanalei River.	16
Figure 1.5. Monthly mean discharge ($\text{m}^3 \text{s}^{-1}$) for the Hanalei River (1963-1995).	17
Figure 1.6. Percent of slope in steps vs. slope gradient, in percentage.	25
Figure 1.7. Schematic diagram of sources and sinks of sediment in the Hanalei basin.	27
Figure 2.1. Map of the Hawaiian Islands, the island of Kauai, and the Hanalei coastal plain.	32
Figure 2.2. Directions of approach by main wave regimes.	33
Figure 2.3. Components of a sediment budget for the Hanalei marine and fluvial system.	36
Figure 2.4. Percent carbonate content of sand.	42
Figure 2.5. Percentage of coral sand grains.	45
Figure 2.6. Percentage of coralline algae sand grains.	47
Figure 2.7. Percentage of siliciclastic sand grains.	49
Figure 2.8. Percentage of mollusc sand grains.	50
Figure 2.9. Mean sediment size and bedform direction.	51
Figure 2.10. Sediment standard deviation and bedform direction.	53
Figure 2.11. Sediment skewness and bedform direction.	54
Figure 2.12. Percentage of silt and clay.	55
Figure 2.13. Sand volume on beach of Hanalei Bay.	57
Figure 2.14. Benthic and surface currents.	58
Figure 2.15A. Selected seismic profiles (A) and survey track lines (B).	61
Figure 2.15B. Seismic survey tracks lines.	63
Figure 2.16. Thickness (m) of marine sediment plotted on a sidescan sonar mosaic.	64
Figure 2.17. Depth (m) below modern sea level to basal reflector in seismic profiles.	65
Figure 2.18. Barbados and Hawaii sea-level curves (20 kyr - present).	66
Figure 2.19. Sea level and topography at 11.2 kyr.	67
Figure 2.20. Sediment accumulation rate in Hanalei Bay and coastal plain.	76
Figure 2.21. Terrigenous sediment budget for Hanalei Bay (5.0 kyr - present).	80
Figure 2.22. The processes and volumes significant to the sediment budget of Hanalei Bay.	84

Introduction

Located on the north shore of the Hawaiian Island of Kauai, Hanalei Bay receives fluvial discharge from three undeveloped watersheds. It is also a part of the oceanic environment of the north shore of Kauai which includes several kilometers of fringing reef and basalt headlands intermittent with pocket beaches to the east and west. Until recently, this area has had relatively low pressure from development. As a result of this and its well defined limits, Hanalei Bay and surrounding watershed provides an excellent location for studying sediment production, transportation, and deposition.

Sediment budgets are principally used to improve the understanding of the sedimentary processes, the sources and sinks that control the variability and evolution of submerged substrates, the coastline, and the watershed to better know their natural history and the potential for anthropogenic impacts. The quantification of sediment sources and sinks to the extent possible is the most important aspect of determining the mass balance of a sediment budget in order to better understand the natural processes involved. The primary components of the Hanalei sediment budget include outputs of terrestrial sediments from the Hanalei River and carbonate contributions from the reefs in and near to the bay. These primary components can presently be analyzed with minimal concern for changes in the natural environment due to anthropogenic impacts on the area.

Prior to the research presented here, complete sediment budgets had not been developed in Hawaii. Several researchers have described individual components and processes of a budget (Inman *et al.*, 1963; Moberly *et al.*, 1965; Kraft, 1982; McMurtry *et al.*, 1995; Sea Engineering, 1996), but, without additional components of the budget to form a cohesive picture, these efforts address a limited set of questions.

Sediment budget studies in the continental United States have ranged from terrestrial drainage basins (Clarkin *et al.*, 1986; Prestegard, 1988; Phillips, 1991) to littoral cells and long stretches of coastline (Shepard, 1973; Dean, 1988; Inman and Dolan,

1989; Best and Griggs, 1991; Peterson *et al.*, 1991; Kana, 1995; Komar, 1996; Komar, 1998). Budgets emerge from the practice of quantifying sediment gains and losses for a defined area. General processes that must be addressed in coastal budgets include sediment production or introduction to the area of interest, transport within and out of the area, and storage within the area. Some processes, such as beach erosion or longshore drift, are well recognized budget components. Others, like biological production or chemical dissolution, may not be as readily apparent or easily measured. In general, the area defined for a budget is constrained into littoral cells by physical boundaries. These boundaries may be, but are not necessarily, comprised of rocky headlands or other sections of coastline that interrupt the supply of sediment. Sediments may enter a littoral cell situated between two headlands from terrestrial runoff, fall from an eroding bluff within the cell, or biological production. Additionally, sediments may enter a cell as part of the longshore drift which bypasses the upcurrent headland. Sediment may be lost to the cell through longshore drift around the downcurrent headland, transport into deep water beyond the influence of littoral processes, removal from the beach system by the wind to form dunes, or abrasion of sediment particles to a size too fine to be maintained in the littoral cell. Sediments may have residence times of various lengths in the beach or in offshore bars.

Although it is not currently a problem in Hanalei, anthropogenic activities may disrupt any one of these processes that in turn is likely to influence the others. Since coastal erosion is a common reason to investigate sediments in an area, budgets are frequently a major consideration in the design of erosion control plans (Kana, 1995). Human influences may be caused by local activities such as groin fields on Long Island (Kana, 1995) and seawalls on Waikiki Beach and elsewhere on Oahu (Gerritsen, 1978; Fletcher *et al.*, 1997) or far removed from the locations of impact such as the cutting off of sediments by the Aswan High Dam on the Nile River (Frihy *et al.*, 1991) or the Akosombo Dam of the Volta River of West Africa (Ly, 1980).

It is notoriously difficult to measure all components of a sediment budget. Some studies do attempt to explain all components in their budget, but, instead of independent field measurements, some components are arrived at by subtraction. These components are called “unmeasured residuals”, and they have comprised as much as 94% of the budget in some studies (Kondolf and Matthews, 1991). These residual terms must be carefully examined. If errors have occurred in the compilation of the other components, these errors will be compounded together and hidden in the residual term (Kondolf and Matthews, 1991).

For Hanalei, I address the most significant processes to develop a better understanding of the major influences governing sediment characteristics. Improved management practices may be implemented based on this knowledge of sediment production, transportation, and storage.

Chapter 1. Measured and predicted sediment yield from a subtropical, wet, steep-sided river basin: Hanalei, Kauai, Hawaiian Islands¹

Abstract

To determine the sediment yield of the 54.4 km² Hanalei River basin, three methods were employed: 1) the Universal Soil Loss Equation (USLE), which uses natural characteristics of the basin such as the amount of rain, slope steepness and length values, and soil types to predict water erosion from certain hillslope processes in a basin; 2) the thickness and calibrated radiocarbon age of fluvial deposits cored from the coastal plain; and 3) field measurements of river suspended sediments. Method 1 (USLE) provides a model prediction of sediment yield that is tested with observational data from methods 2 and 3. Several curves, including one by the U.S. Soil Conservation Service, predict a sediment delivery ratio (measured sediment yield: gross erosion) between approximately 15% and 50%. With 5,260±2,210 Mg (metric tons) per year of suspended sediment output from the Hanalei River and 2,300±700 Mg per year deposited on the coastal plain, however, the delivery of sediment in the Hanalei basin ranged between 45% and 101% of the maximum predicted USLE value (88±103 Mg km⁻² yr⁻¹). This higher than predicted yield may be the result of mass movement. It is not possible to differentiate, however, between erosion and mass movement as the principal agent of denudation. Measurements indicate a sediment yield of 140±55 Mg km⁻² yr⁻¹ for the Hanalei Valley.

¹ Calhoun, R.S. and C.H. Fletcher. in press. Measured and predicted sediment yield from a subtropical, heavy rainfall, steep-sided river basin: Hanalei, Kauai, Hawaiian Islands: *Geomorphology*.

Introduction

In the Hawaiian Islands, limited research exists describing the erosion of sediments on a basin or island-wide scale. Denudation of the Kaneohe Bay drainage basin on windward Oahu was examined by bedrock analysis, soil and soil-forming processes, and the concentration of detrital sediment in the bay (Moberly, 1963). Sediment yields from the Makiki, Manoa, and Palolo Valleys of central Honolulu were analyzed using sediment deposition rates, determined by ^{210}Pb and ^{137}Cs dating techniques, in the Ala Wai Canal (McMurtry *et al.*, 1995). Li (1988) calculated island-wide rates of denudation for the islands of Hawaii, Oahu, and Kauai based on measurements of dissolved and suspended sediment concentrations in multiple rivers and groundwater wells.

The physical loss of sediment from the Hanalei River basin was determined using observations of floodplain sedimentation and the delivery of suspended sediment to Hanalei Bay. These are, in turn, used to test the predictions of sediment yield by the Universal Soil Loss Equation (USLE). This combination of measured and predicted sediment erosion and deposition has not been previously attempted in Hawaii to describe non-agricultural wildlands.

Geologic Setting

The Hanalei River basin, extending north from Mt. Waialeale near the center of the Hawaiian Island of Kauai, receives rainfall volumes that are among the highest on Earth ($>10 \text{ m yr}^{-1}$). The basin is comprised predominantly of steep-sided mountain walls plunging into deep, fluvially-cut gorges. Though heavily vegetated, the steep slopes and high rainfall ensure a steady supply of sediment to the river. At 25.2 km in length and with a planimetric drainage area of 54.4 km^2 , the Hanalei River is one of largest river systems in the Hawaiian Islands. Over much of its length, the Hanalei River flows

between canyon walls with little or no floodplain. Below the ~61 m (200 ft) contour, however, the canyon begins to widen and the river forms a floodplain over its final 12 km. In its lowest reach, the river traverses 6.6 km of the Hanalei coastal plain, defined by the ~6 m (20 ft) contour, before entering the east side of Hanalei Bay (Figure 1.1).

The upper-most sedimentary facies of the coastal plain is a red-brown mud derived from the overbank flow of the Hanalei River (Calhoun and Fletcher, 1996). The top facies is generally underlain by a carbonate sand that is marine or fluvial-marine in origin. This carbonate sand is a relic of former marine influence that has been interpreted as showing net shoreline progradation over the last 4,000 years (Calhoun and Fletcher, 1996). The well-dated contact between the fluvial and marine lithosomes provides an excellent base from which to calculate the volume and rate of recent Hanalei River sedimentation.

Three general spacial scales and mechanisms of subaerial mass movement have been identified in the steep valleys in Hawaii. The smallest mechanism, called soil avalanches by Wentworth (1943) and soil slips by Ellen *et al.* (1993), involves movement of only the top soil and range in size from a few cubic meters up to approximately 1,000 m³. During studies of the Honolulu District of Oahu, Scott (1969) and Ellen *et al.* (1993) calculated the mean volume of 201 slips to be 120 m³. An average of between 30 and 40 of these soil slips occur each year in this district depending on the number and severity of rain events (Ellen *et al.*, 1993; Peterson *et al.*, 1993). Landslides resulting from the second mechanism, the failure of weathered basalt (saprolite), occur in the Honolulu District approximately once a decade and have volumes in the tens of thousands of m³ (Peterson *et al.* 1993). Both of these types of mass movement are related to times of severe rainfall events. The third type of mass movement is massive rock avalanches which occur when unweathered basalt bedrock fails. These are not associated with rainfall events and probably result from gradual undercutting. The location of these

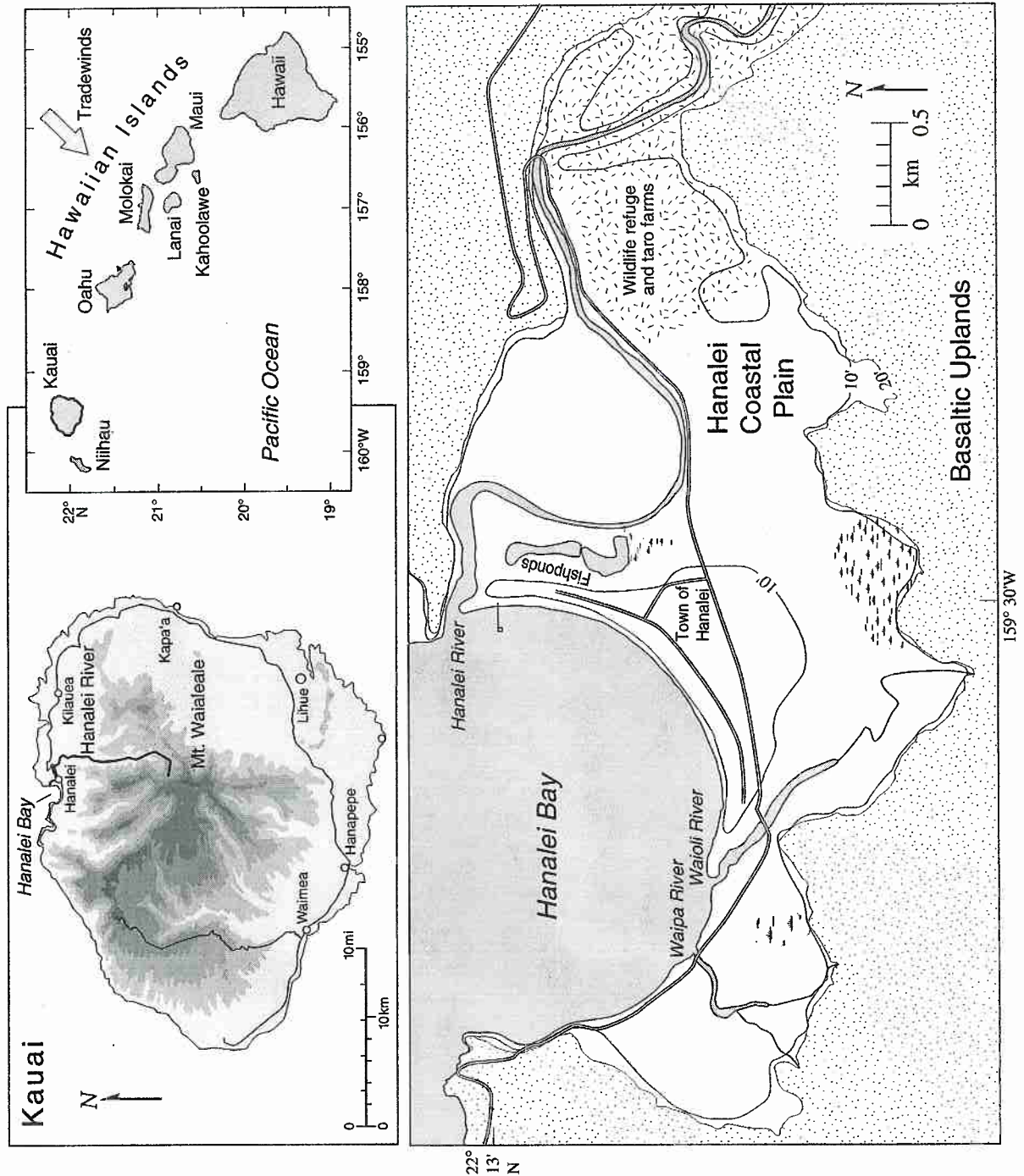


Figure 1.1: Map of the Hawaiian Islands, the island of Kauai, and the Hanalei coastal plain on the north shore of Kauai, Hawaii. Also shown are the town of Hanalei, major roads, and the areas of disturbed stratigraphy associated with the waterfowl refuge and the Hawaiian fishponds. The 10 and 20 ft (3.0 and 6.1 m) contours were obtained from U.S. Army Corps of Engineers contoured orthophotoquads (1:4800).

infrequent massive avalanches have been linked with ash layers in the bedrock and are associated with earthquakes. They may include hundreds of thousands to millions of m³ of rock and soil (Jones *et al.*, 1984). Analysis of geologic maps (Macdonald *et al.*, 1960), descriptions and maps from the US Soil Conservation Service (1972), and aerial photographs indicates that all three mass movement types described elsewhere in Hawaii do or should occur in the Hanalei Valley.

Several studies (Scott and Street, 1976; Jones *et al.*, 1984; Ellen *et al.* 1993; Peterson *et al.* 1993) have described the frequency and volume of mass movement. A few have computed the total rate of denudation from individual valleys or islands (Moberly, 1963; Li, 1988; Hill *et al.*, 1997). Although White (1949) addresses it, this is the first study to quantify denudation of a pristine Hawaiian valley based upon soil erosion.

Methods

Several methodologies were used to determine the sediment yield of the Hanalei watershed. Cores were obtained with a gouge auger at 104 sites throughout the coastal plain to determine subsurface stratigraphy. These were 2.54 cm in diameter and typically between 3 and 7 m in length. Core penetration was limited by sediment density, most often after encountering marine sands. Samples of cored sediments were radiocarbon dated to provide long-term rates of the accumulation of sediment and to determine the transition from marine to fluvial sedimentation. Short-term rates of sedimentation were obtained at three locations by means of short (<1 m), thick (6.5 cm) cores. The shallowest depth of zero ²¹⁰Pb activity in each core was used to mark the 150 year level to calculate sedimentation rates.

Isopach mapping of the coastal plain provides an estimate of the volume of fluvial sediment deposited. Combining this information with radiocarbon ages at the

base of the fluvial lithosome (Calhoun and Fletcher, 1996) allows the calculation of the annual sedimentation rate on the coastal plain during the late Holocene.

Discharge and crest-stage data on the Hanalei River are recorded at two U.S. Geological Survey (USGS) stations. The first is a water-stage recorder located 7.89 km from the river mouth and 10.91 m above mean sea level. At this station, the instantaneous discharge and the crest height are recorded every half hour from water year 1962 to 1994, although only the daily mean discharge is preserved in the long-term record. In addition, from 1962 to 1979, the maximum discharge and crest height for each year are recorded. From 1980 to 1994, every discharge above $261 \text{ m}^3 \text{ s}^{-1}$ (9,200 cfs) and its accompanying crest height are recorded. The second station is located 3.86 km above the river mouth on the Highway 56 bridge near the town of Hanalei. This gage measures only crest-stage and records the maximum crest-heights for water years 1963 through 1994. It uses mean sea level as its datum. Although during normal conditions of discharge one sample was taken per day, at times of high discharge, samples were collected throughout the day to more accurately measure the sediment flux of an event. A total of 127 samples were taken from the river.

A record of suspended sediment was gathered from the Hanalei River using a U.S.D.H. 48 hand-held water sampler. Integrated depth (0-100 cm) water samples were collected from the center of the Highway 56 bridge next to the crest-stage gage on 90 consecutive days from January 21 to April 20, 1995, considered the approximate rainy season on Kauai. Approximately 950 mL of water were collected per observation under normal conditions. Five hundred mL or less were collected when the water was particularly turbid. A vacuum of $\sim 33 \text{ kPa}$ ($\sim 5 \text{ psi}$) was used to aid in the subsequent filtering of the water samples through a preweighed $0.45 \text{ }\mu\text{m}$ filter. The filters were then dried for 48 hours at 60° C and the mass measured to the nearest 0.0001 g. Repeated filtrations with distilled and deionized water indicate that the technique was accurate to

0.001±0.0005 g. The mass of the sediment left on the filters was used to calculate the concentration of suspended sediment in g L^{-1} of water discharged by the Hanalei River. This, in turn, was combined with the daily discharge data from the USGS discharge station (7.84 km from mouth) to calculate the mass of suspended sediment load of the Hanalei River. Stream discharge was then compared to the measured concentration of suspended sediment to derive a regression equation. A 31.75 year record of USGS discharges formed the basis for obtaining a longer-term estimation of suspended sediment output.

To characterize the collection site for suspended sediment, five samples were taken from evenly spaced locations laterally across the bridge. Additionally, daily water conductivity and temperature measurements were obtained. The thickness of the fluvial water column and the basal marine wedge in the channel could then be calculated. A 290 g grab sample of river bottom sediment was obtained and sieved with a ro-tap sieve shaker, with sieves ranging in size from -1.0 to 4.0 phi in 0.5 phi increments. The moment method was used to describe the sample's texture.

In addition to these field methods, an empirical model, the Universal Soil Loss Equation (USLE), was used to estimate the mass of rill and interrill erosion from the Hanalei basin, and to facilitate comparisons with other basins. The factors of the USLE (Table 1.1) were determined using data from U.S. Soil Conservation Service (1972) soil descriptions, field observations, and tables, graphs, and equations from Foster and Wischmeier (1974), Wischmeier (1975), Wischmeier and Smith (1978), and Dissmeyer and Foster (1980).

Results

Late Holocene rates of fluvial sediment accumulation on the Hanalei coastal plain, covering thousands of years and calculated with radiocarbon dates, range from 0.07

Table 1.1: Factors of the Universal Soil Loss Equation.

The Universal Soil Loss Equation: $A = R \cdot K \cdot L \cdot S \cdot C \cdot P$; from Wischmeier and Smith (1978)

Factor	Value for	Source
R (rainfall and runoff)	Hanalei Basin (units) 1,070 (100 N hr ⁻¹)	Lo <i>et al.</i> (1985) and NWS rain gage data
K (soil erodibility)	0.148 - 0.458 (tons per index unit)	U.S. Soil Conservation Service descriptions and figure 3 acre per erosion from Wischmeier and Smith (1978)
LS (slope length and steepness)	120 (unitless ratio)	Equations from Foster and Wischmeier (1974) and measurements from U.S.G.S. topographic maps
C (cover and management)	$1.01 \times 10^{-5} \pm 0.908 \times 10^{-5}$ (unitless ratio)	Fractional Uncertainty Multiplication from Taylor (1982)
P (support practice)	- incorporated into C	Dissmeyer and Foster (1980)
C subfactors: (percentage used in calculation)		
bare soil (90-100%)	0.03 - 0.07	Figure 2 from Wischmeier (1975) and field observations
canopy (80-90%, 0.5 m understory)	0.34 - 0.40	Figure 1 from Wischmeier (1975) and field observations
soil reconsolidation	0.45	Dissmeyer and Foster (1980)
high organic content	0.7	Dissmeyer and Foster (1980)
fine roots (80-90%)	0.26 - 0.32	Figure 15 from Dissmeyer and Foster (1980) and field observations
onsite storage (70-90%)	0.10 - 0.30	Dissmeyer and Foster (1980) and field observations
steps (80-90%)	0.0112- 0.0483	Equations from Foster and Wischmeier (1974), measurements from U.S.G.S. topographic maps, equations derived from table 7 of Dissmeyer and Foster (1980), and field observations
residual binding effect	not used in forest environment	Dissmeyer and Foster (1980)
contour tillage	not used in forest environment	Dissmeyer and Foster (1980)
A (eroded sediment)	0.391 ± 0.457 tons acre ⁻¹ yr ⁻¹ or 88.2 ± 102.9 Mg km ⁻² yr ⁻¹	Fractional Uncertainty Multiplication from Taylor (1982)

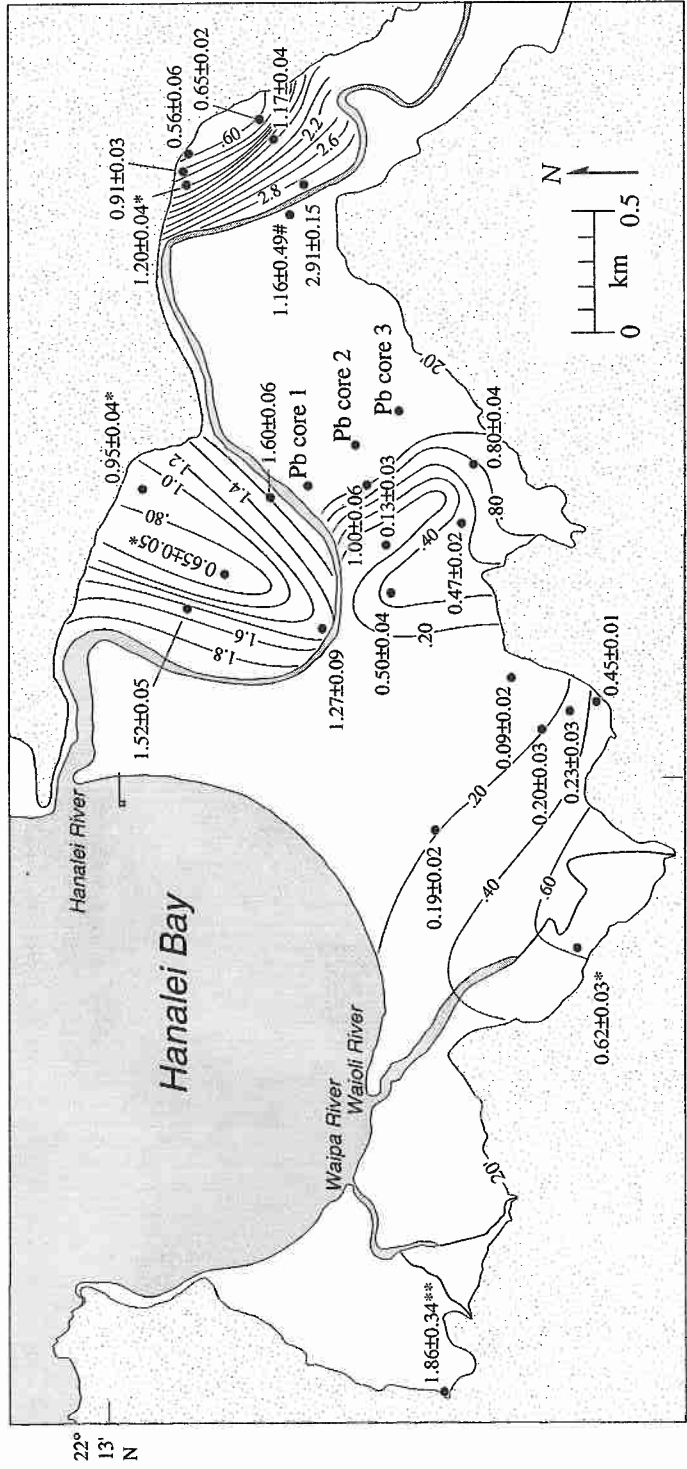


Figure 1.2: Sediment accumulation rate in mm/yr from 7000 yr B.P. to the present. Contour interval = 0.20 mm/yr. All accumulation rates are based on surface to depth interval except where noted. * = Cores containing inverted dates. ** = Cores with rates derived from a dated interval. # = The average of three rates obtained from core.

to 3.06 mm yr^{-1} with rates generally highest near river channels and decreasing with distance from the river banks (Figure 1.2). Minimum rates are found in the center of the coastal plain far from any immediate source. Short-term sedimentation, measured with short cores, covering less than 150 years, and calculated with ^{210}Pb dating techniques, also indicate a decrease in the rate of sedimentation as the distance from the Hanalei River increases. These short-term rates, 0.82 to 3.09 mm yr^{-1} (Figure 1.3), correlate well with calculations of long-term accumulation using radiocarbon.

From the isopach map derived from core data, it was estimated that the Hanalei River deposited $7,520,000 \text{ m}^3$ of sediment on the coastal plain over the past 4,000 years. Measurements of 21 oven dried sediment samples indicate that the average bulk density is $1.22 \pm 0.38 \text{ Mg m}^{-3}$ (2 sigma). Hence, the river has deposited $\sim 9,170,000 \text{ Mg}$ of sediment on the coastal plain during the last 4,000 years, or an average of $2,300 \pm 700 \text{ Mg yr}^{-1}$.

At the bridge sampling site, a wedge of marine water was present during 76% of the sampling days with an average thickness of 1.54 m and a maximum thickness of 2.37 m. The river flowing over this wedge averaged 1.52 m thick with a minimum of 0.60 m. During times of increased flow, the marine wedge was pushed down river by the freshwater. Several days of low flow were needed to allow the wedge to return to its original thickness.

Bottom sediments immediately upriver from the bridge consist of moderately sorted, very coarse, rounded, basalt sands and granules with a mean phi size of -0.23 (very coarse sand), a standard deviation of 0.90 phi (moderately sorted), and skewness of 0.53 (strongly fine skewed).

Suspended sediment samples from the four locations to either side of midchannel were found to contain slightly less suspended sediment than simultaneously collected

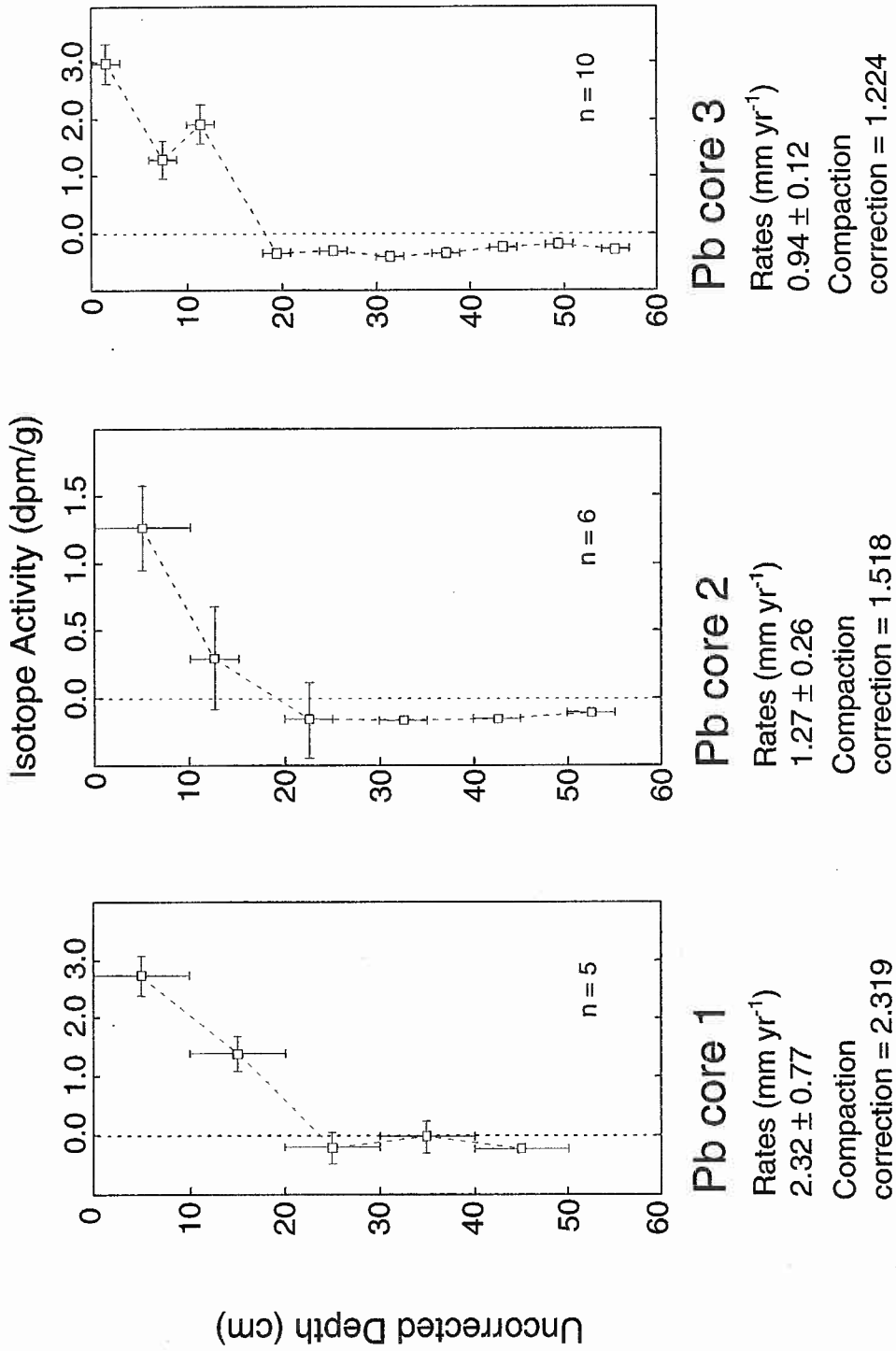


Figure 1.3: Profiles of three cores showing depth and ^{210}Pb activity. The horizontal errors in many of the samples are smaller than the squares used to show their locations. Core locations on the coastal plain are shown in Figure 1.2.

samples from the standard midchannel station. The mass of sediment obtained from the side locations was, however, well within the range normally found at the midchannel station.

To calculate the mass of suspended sediment transported by the Hanalei River, records of discharge from the USGS were regressed against suspended sediment concentration data collected during 90 days of measurement. Only discharges greater than $2.83 \text{ m}^3 \text{ s}^{-1}$ (100 cfs) were used to eliminate the random variability of concentrations found at low discharge levels. The regression (Figure 1.4) yields: $Y = 1.39 X + 17.98$ where Y = suspended sediment concentration (g m^{-3}) and X = river discharge in $\text{m}^3 \text{ s}^{-1}$. The average daily mean discharge is $6.38 \text{ m}^3 \text{ s}^{-1}$ (225 cfs) with a range of $2.83 \text{ m}^3 \text{ s}^{-1}$ (100 cfs) to $24.1 \text{ m}^3 \text{ s}^{-1}$ (852 cfs). This relationship has a correlation coefficient (r) of 0.76, a probability (p) value of less than 0.001, and the standard error of estimate is 5.53 g m^{-3} . The mean daily discharge of each month from January, 1963 through September, 1995 was calculated and averaged with the other monthly mean discharges from a given year (Figure 1.5). The suspended sediment load of the Hanalei River from 31.75 years of data was estimated to be $5,260 \pm 2,210 \text{ Mg yr}^{-1}$ using the regression equation.

The USLE predicts erosion in short tons (2,000 lb) per acre per year. Using fractional uncertainty multiplication (Taylor, 1982) on the USLE factors yields a prediction that 0.39 ± 0.46 tons per acre per year ($88.2 \pm 103 \text{ Mg km}^{-2} \text{ yr}^{-1}$) of sediment will be eroded from the Hanalei basin. By design of the USLE, this figure is total hillslope erosion that includes only rill and interrill erosion and does not account for redeposition and storage within the basin.

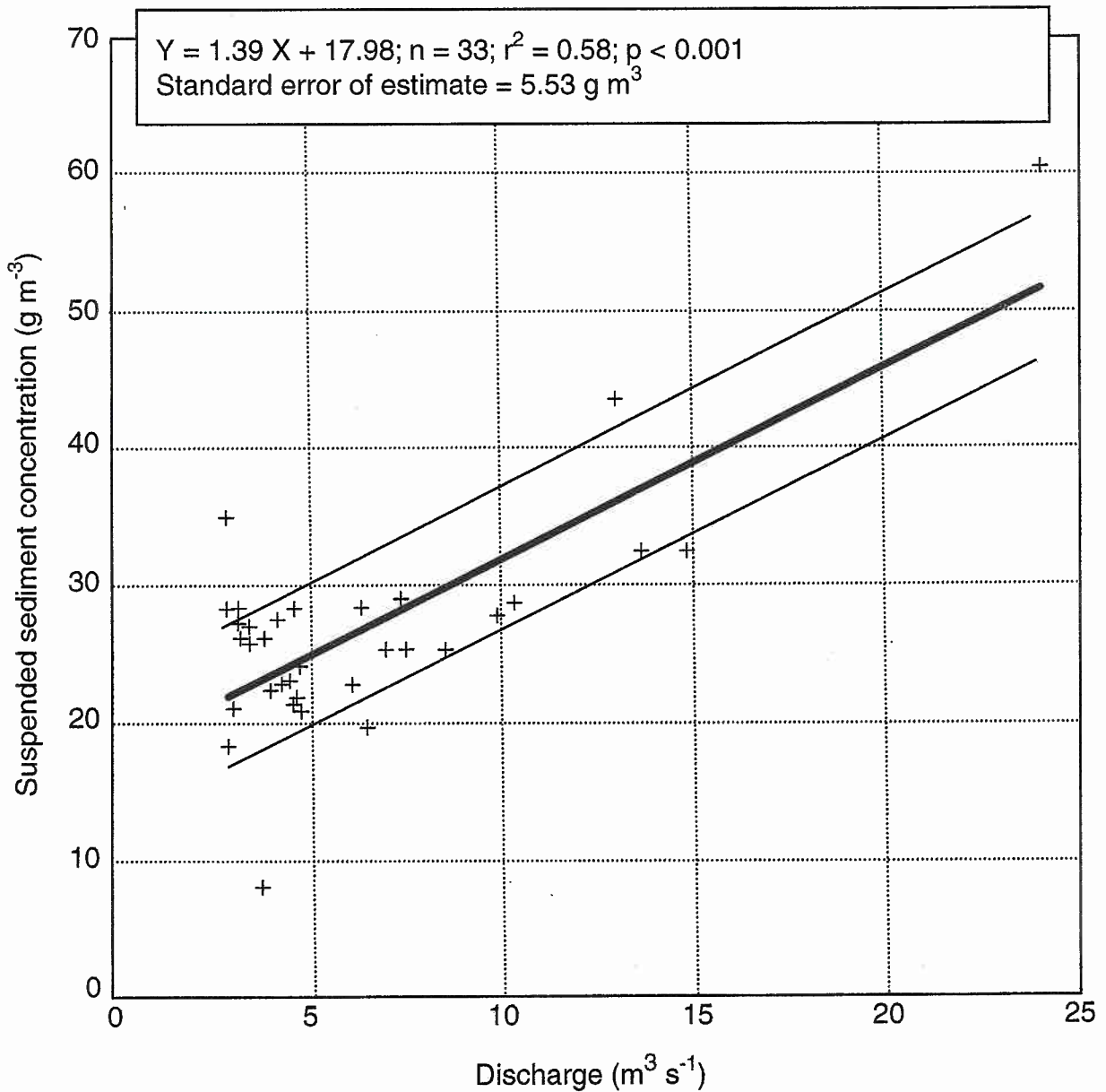


Figure 1.4. Discharge vs. suspended sediment concentration for the Hanalei River. Discharge ranges between 2.83 m³ s⁻¹ (100 cfs) and 24.1 m³ s⁻¹ (852 cfs). Data were collected between January 21 and April 20, 1995. Bold line shows the regression equation and the two thin lines represent the standard error of estimate of 5.53 g m⁻³.

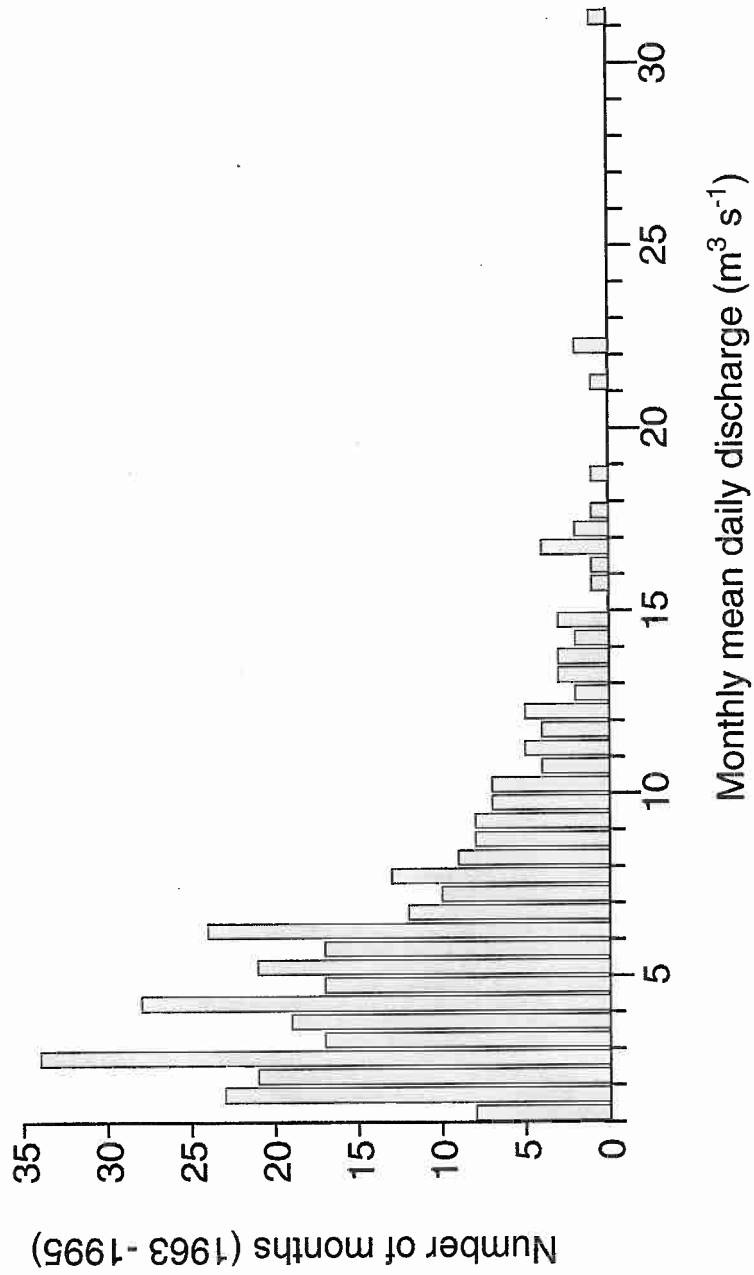


Figure 1.5: Monthly mean discharge ($\text{m}^3 \text{s}^{-1}$) for the Hanalei River (1963 - 1995). Data are from the USGS discharge station on the Hanalei River (station# 16103000) (USGS Water-Data Reports, 1963-1995).

Discussion

Li (1988) calculated a maximum rate of physical denudation of $400 \pm 200 \text{ Mg km}^{-2} \text{ yr}^{-1}$ for the island of Kauai. In the Hanalei valley, this is equivalent to $21,760 \pm 10,880 \text{ Mg yr}^{-1}$. A minimum rate was not calculated. From this study, estimates of sediment deposited on the Hanalei coastal plain combined with the suspended sediment output from the basin indicate that at a minimum $4,650\text{-}10,470 \text{ Mg yr}^{-1}$ ($140 \pm 55 \text{ Mg km}^{-2} \text{ yr}^{-1}$) are removed from the upper valley. Measurements from Hanalei, despite being on the windward side of the island, should not be equal to Li's (1988) maximum rates for two reasons. First, in using the USLE, no estimates of mass movement were included as was done by Li (1988). Mass movement is considered to be a significant method of sediment movement on steep mountain slopes in the Hawaiian Islands (Scott and Street, 1976). Second, no sediment concentration data are available for high discharge events because the sampling interval covered an El Nino year, known to be a period of reduced rainfall in the Hawaiian Islands. Given the limited temporal measurement period and other constraints previously discussed, the measured values should be considered minimum estimates. Additionally, no measurement of bedload transport was made. Inclusion of this component would increase sediment output, although some evidence suggests that this increase would be well within the error found in the suspended sediment measurements (Meade *et al.*, 1990).

McMurtry *et al.* (1995) calculated $2,630 \text{ Mg yr}^{-1}$ of detrital sediment are deposited in the Ala Wai Canal on the island of Oahu (Table 1.2). The canal drains 42.9 km^2 of urbanized central Honolulu and nearby steep undeveloped mountains. This results in a sediment yield of $61.2 \text{ Mg km}^{-2} \text{ yr}^{-1}$ from the Ala Wai drainage basin compared to $140 \pm 55 \text{ Mg km}^{-2} \text{ yr}^{-1}$ in the Hanalei valley. The drier climate and heavy urbanization of central Honolulu are likely to be contributing factors to the lower

Table 1.2: Estimates of physical erosion rates in Hawaii.

Author	Island	Area drained (km ²)	Sediment yield (Mg km ⁻² yr ⁻¹)	Sediment load (Mg yr ⁻¹)	Denudation (mm yr ⁻¹)	Method
This study	Kauai	54.4	140±55	7,560±2910	0.05-0.23	Fluvial yield
Hill et al. (1997)	Oahu	10.4	330±130 200±100	3,400±1,350 2,080±1,040	0.30-0.70 0.1-0.3	Fluvial yield Aerosol quartz and ¹³⁷ Cs concentrations ²¹⁰ Pb and ¹³⁷ Cs concentrations
McMurtry et al. (1995)	Oahu	42.9	61.2 #	2,630	0.08	concentrations in sediments
Ellen et al. (1993)	Oahu	Koolau Range	--	--	0.02-0.15 ##	K-Ar dates for original Koolau volcano surface and sequential digital simulations of erosional development
Li (1988)	Kauai	Island wide	? - 400±200	--	0.18±0.08	Cation and SiO ₂ concentrations
Li (1988)	Oahu	Island wide	60-300	--	0.10±0.06	in rivers and groundwater
Scott and Street (1976)	Oahu	7	760±621	5,290±4350 *	0.16-0.86	Field measurement of soil avalanche scars
Moberly (1963)	Oahu	82	340±50 **	27,900±4,100	0.13	Dissolved calcium
Wentworth (1943)	Oahu	38.8	690±215	26,800±8,350 ***	0.76	Estimate number of slides and their volumes

= adapted from McMurtry et al. (1995).

= adapted from figure 5 by Ellen et al. (1993).

* = adapted from Scott and Street (1976) assuming a soil density of 1.22±0.38 Mg m⁻³.

** = adapted from Moberly (1963) based on rates from removal of dissolved weathering products, and assuming basalt density of 2.60±0.35 Mg m⁻³.

*** = adapted from Wentworth (1943) assuming a soil density of 1.22±0.38 Mg m⁻³.

sediment yield from the Oahu basins. Values of sediment yields from McMurtry *et al.* (1995) are at the lower end of the range (60-300 Mg km⁻² yr⁻¹) predicted for Oahu by Li (1988). Li (1988) does not give a minimum rate of denudation for Kauai, but the rate computed here (140±55 Mg km⁻² yr⁻¹) is substantially below Li's (1988) Kauai maximum of 400±200 Mg km⁻² yr⁻¹ and well above his minimum rate of denudation of 60 Mg km⁻² yr⁻¹ predicted for the islands of Hawaii and Oahu. High end yield estimates by Wentworth (1943) and Scott and Street (1976) are based on direct field measurements of mass movement scars. They reflect a maximum rate of denudation and may indicate that portions of soil avalanches are stored low in the valley for periods longer than a thousand years.

Comparisons of the rates of sediment deposition on the Hanalei coastal plain with other rates of deposition in various environments from around the world are shown in Table 1.3. Hanalei has a low rate of deposition relative to other depositional environments, but has a range similar to those found on other floodplains. The high rates found by Goodfriend and Stanley (1996) on the Nile River delta could be the result of being measured in a lake on the floodplain and, therefore, more closely resemble those in the open water section of the table. Despite the differences in characteristics in size and area, the Hanalei River (length: 25.2 km; area: 54.4 km²), the Colorado River of Texas (1,400 km and 110,000 km²), and the Ganges River of India and Bangladesh (2,500 km and 952,000 km²) (Showers, 1979) have remarkably similar rates of sediment deposition. The Ganges River is among the largest continental rivers in the world, draining high mountainous terrain and includes seasonal monsoon and snowmelt runoff, whereas the Colorado River drains the semi-arid plains of west and central Texas accustomed to episodic heavy rains before crossing the more humid Texas gulf coast region. The Hanalei River valley is characterized by steep, humid, forested mountainsides where

Table 1.3: Rates of sediment deposition from various environments.

Location	Rate of Deposition (mm yr ⁻¹)	Author (year)	Method
<u>Open Water (Oceans, Bays, Lakes)</u>			
Skagerrak and Oslofjord (Norway)	1.0-11.0	Pederstad <i>et al.</i> (1993)	Seismic profiles, zinc presence
Northeastern Skagerrak (Norway)	0.8-11.0	Van Weering <i>et al.</i> (1993)	²¹⁰ Pb and ¹³⁷ Cs
Lillooet Lake (British Columbia, Canada)	7.0-28.5	Desloges and Gilbert (1994)	Varves, seismic profiles, ¹³⁷ Cs
Barmouth Bay (Wales)	2.3-3.1	Larcombe and Jago (1994)	Radiocarbon, seismic profiles (?)
<u>Estuaries and other confined bodies of water</u>			
Illinois River (Illinois, U.S.A.) measurements(?)	2.0-79.2	Bhowmik and Demissie (1989)	Bathymetry
Paleolakes and wetlands (Mangaia, Cook Islands)	0.58-12.1	Ellison (1994)	Radiocarbon
Mawddach estuary (Wales)	~82.0	Larcombe and Jago (1994)	Radiocarbon, seismic profiles (?)
Hamble estuary (England)	4.0-8.4	Cundy and Croudace (1995)	²¹⁰ Pb and ¹³⁷ Cs
Ala Wai Canal (Hawaii, U.S.A.)	20-220	McMurtry <i>et al.</i> (1995)	²¹⁰ Pb and ¹³⁷ Cs
<u>Floodplains</u>			
Ganges delta (Bangladesh)	0.3-4.0	Umitsu (1993)	Radiocarbon
Colorado River (Texas, U.S.A.)	0.24-3.12	Blum and Valastro (1994)	Radiocarbon
Nile delta (Egypt)	0.51-19.0	Goodfriend and Stanley (1996)	Radiocarbon, amino acid racemization, stable isotope analysis
Hanalei coastal plain (Hawaii, U.S.A.)	0.07-3.06	this study, Calhoun and Fletcher (1999)	Radiocarbon
Hanalei coastal plain (Hawaii, U.S.A.)	0.82-3.09	this study, Calhoun and Fletcher (1999)	²¹⁰ Pb

mass movement and soil erosion, encouraged by copious volumes of rainfall, are significant means of sediment mobilization.

Because the long-term rates of sediment accumulation and the short-term rates of sedimentation overlap on the Hanalei floodplain, compaction and erosion of the fluvial coastal plain sediments are not considered to be significant processes. As a result, the volume of fluvial sediment present on the modern coastal plain represents the total deposited during the last 4,000 years. Prior to 4,000 years ago, Hanalei Bay covered much of the modern coastal plain and limited significant fluvial deposition to the extreme eastern portion (Calhoun and Fletcher, 1996). These middle to late Holocene fluvial sediments represent the deposition of suspended sediment during flood conditions, a major constituent of the sediment budget missed by the daily observations of suspended sediment. Neither the $2,300 \pm 700 \text{ Mg yr}^{-1}$ deposited on the coastal plain nor the measured $5,260 \pm 2,210 \text{ Mg yr}^{-1}$ of suspended sediment lost to the bay, however, account well for the large volumes of suspended sediment which pass completely through the Hanalei River system and into the bay during extremely high discharge events. One high discharge event was sampled in the field, but it was a bankfull event and cannot accurately be compared with the massive discharges that reach heights of up to 2.5 m above flood stage. Even this bankfull event, however, contained nearly seven times the concentration of suspended sediment that would be predicted for such a discharge based on interpolations from normal flow conditions. This relatively high concentration of suspended sediment shows that high discharge events cannot be adequately explained by simple extrapolation from normal flow discharges. These events, which range in frequency from 0 to 5 events per year, have yet to be adequately sampled, and, as a result, the contribution of sediment to the bay, though almost certainly significant, must remain speculative.

The USLE was designed for and empirically tested on the gently sloping, deep soiled, agricultural fields of the American midwest and eastern seaboard. It describes soil loss only by rill and interrill erosion. It does not describe sediment loss due to mass movement, stream channel and bank erosion, or gully erosion. In this study, it was applied to the steep, thin soiled, wildlands of the Hanalei Valley. This study may, therefore, serve as a test of the validity of the USLE in such an environment as well as the applicability of the similar Modified Universal Soil Loss Equation (MUSLE) (Williams, 1975) and the Revised Universal Soil Loss Equation (RUSLE) (Renard *et al.*, 1994). The use of these equations would greatly simplify the field measurements and calculations of sediment loss from the valley because of individual high-intensity storms in addition to long-term erosion.

The USLE calculates the total mass of sediments eroded in a specific area by specific processes. Drainage basins the size of Hanalei tend to have sediment delivery ratios (SDR = sediment yield / gross erosion) of 15% to 50% (Walling, 1994) which means the erosion predicted by the USLE will be approximately two to seven times the sediment yield. In the case of the Hanalei Valley however, the 95% confidence band of suspended sediment and storage (4,650 - 10,470 Mg yr⁻¹) is 45% to 101% of the upper 95% confidence band of the USLE prediction (i.e. 10,400 Mg yr⁻¹). This is not an entirely unexpected result. The consistently steep mountain sides and general lack of a floodplain in the Hanalei Valley results in few areas for the systematic redeposition of eroded sediments. Additionally, because the USLE was established to calculate only sheet and rill erosion, the processes of mass movement, stream bank and bed incision, and gully erosion were not included in the calculation. These processes will increase basin sediment output, but not effect the USLE estimate of "gross" erosion.

In the Hanalei basin, the R and K factors fit within expected ranges. The C factor and the combined LS factor are extreme values. The C factor is several orders of

magnitude lower than normally calculated. Usually C values smaller than 1×10^{-3} are considered too small to have been accurately measured (El-Swaify, personal communication, 1996). Despite this, higher “normal” C values would render the final calculation far too high to be of any practical use. Additionally, the use of a lower than “normal” C value in Hawaii is consistent with the findings of Cooley and Williams (1985), and the C value was calculated using the same equations and graphs that would be used on any forested land (Figure 1.6) (Dissmeyer and Foster, 1980). The LS factor was calculated using the mean LS factor from six representative profiles in the basin. These profiles had a mean length of 1,910 m, 62% slope, and change in height of 690 m. They ranged from 680 to 3,060 m in length, 35 to 146% slope, and 290 to 1220 m height variation. These are extremely long, steep profiles and this is reflected in the extreme value for the LS factor.

With a water erosion estimate of $4,800 \pm 5,600 \text{ Mg yr}^{-1}$, the USLE appears at first to reasonably reflect the physical characteristics of the Hanalei Valley. Water erosion, however, is not the sole process mobilizing sediment in the basin. Mass movement also contributes to sediment mobilization and must be addressed.

Mass movement has long been recognized as an important process in steep valleys of Hawaii (Stearns and Vaksvik, 1935; Wentworth, 1943; White, 1949; Scott and Street, 1976; Ellen *et al.*, 1993; Peterson *et al.*, 1993, and Hill *et al.*, 1997). Several of the more recent authors (Scott and Street, 1976; Ellen *et al.*, 1993; and Peterson *et al.*, 1993) have attempted to quantify the volume of denudation because of mass movement. Li (1988), Moberly (1963), and Hill *et al.* (1997) all quantify the total volume lost from an area, but do not distinguish the losses by type. Between 15% and 50% of the maximum USLE-predicted gross erosion ($10,400 \text{ Mg yr}^{-1}$), or 1,560 to $5,200 \text{ Mg yr}^{-1}$, should be output from the basin (Walling, 1994). If mass movement does account for the apparent excess sediment found in the Hanalei River and coastal plain, the difference

100% in steps: $Y = 12.081 X^{(-1.552)}$; $r^2 = 0.995$

90% in steps: $Y = 4.851 X^{(-1.052)}$; $r^2 = 0.997$

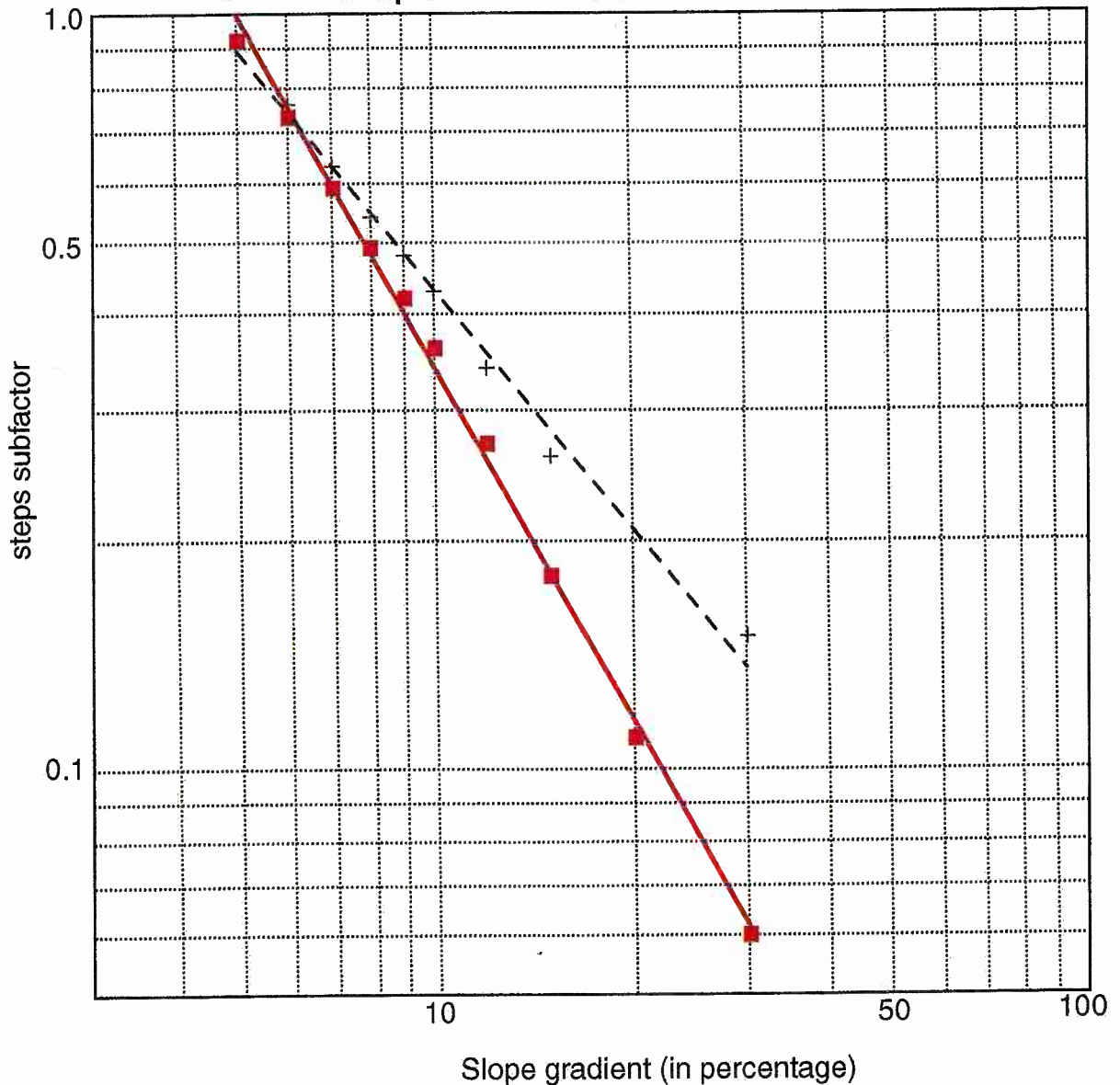


Figure 1.6. Steps subfactor value vs. slope gradient, in percentage. Curves are used to derive steps subfactor of C. Estimates of the percentage of slope that are that are stepped range between 90 and 100%, while estimates of slope gradient, in percentage, are 80 to 90%. Data points are from Table 7 of Dissmeyer and Foster (1980).

between the total measured sediment (4,650 - 10,470 Mg yr⁻¹) and the SDR-predicted eroded sediment (1,560 - 5,200 Mg yr⁻¹) is the result of mass movement. The result is that between 0 and 8,910 Mg yr⁻¹ appear to be removed from the Hanalei Valley by mass movement. Mass movement, however, is not the only process likely to be producing this apparently extra sediment. Stream channel and bank erosion, as well as gully erosion also factor into this mass. These four processes should be grouped together into what Kondolf and Matthews (1991) term "unmeasured residuals". Caution must be taken when using unmeasured residuals because, while they may help balance a sediment budget, hidden errors are often enclosed within these budget components (Kondolf and Matthews, 1991). It is also apparent from comparing the total measured yield, the expected volume of mass movement (and other processes), and the expected volume of erosion that the ability to differentiate denudation processes in the Hanalei Valley is not precise enough to warrant practical application.

From the measured yield of $7,560 \pm 2,910$ Mg yr⁻¹, a total denudation rate of 0.05-0.23 mm yr⁻¹ may be calculated for the 54.4 km² Hanalei Valley (1.22 ± 0.38 Mg m⁻³). This agrees very well with the rates calculated by others (Table 1.2). It may be surprising to find such good agreement given the direct influence of total rainfall on sediment yield (Scott and Street, 1976; Ellen *et al.*, 1993) and the much higher rainfall volumes in the Hanalei Valley.

Conclusions

From calculations based on field data, $7,560 \pm 2,910$ Mg of sediment per year, or 140 ± 55 Mg km⁻² yr⁻¹, are removed from the upper Hanalei River valley by the river (Figure 1.7). This is higher than the sediment yield from three central Honolulu drainage basins (McMurtry *et al.*, 1995) as is to be expected because of the lower rainfall and

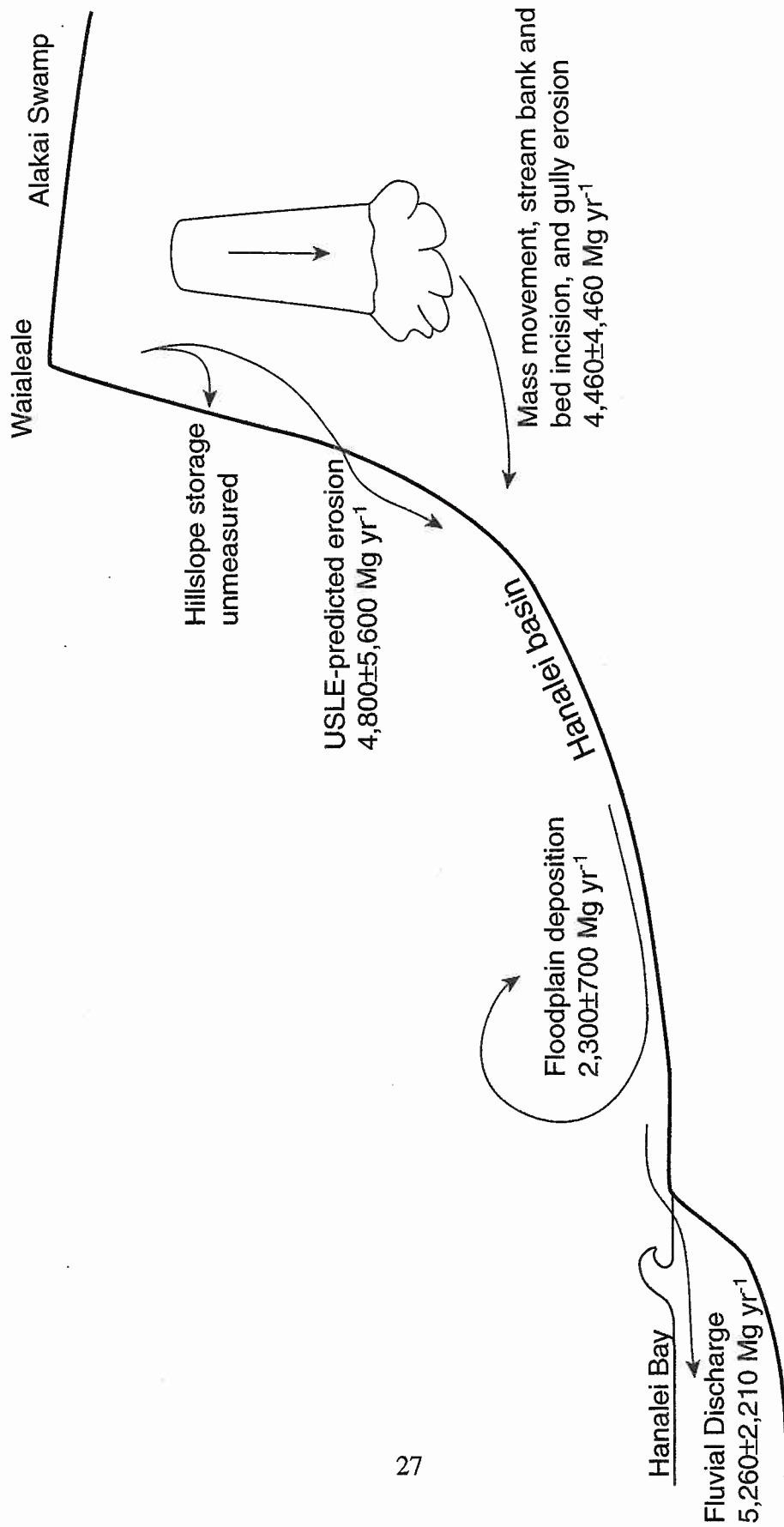


Figure 1.7: Schematic diagram of the sources and sinks of sediment in the Hanalei basin.

higher degree of urbanization found in the Honolulu watersheds. It also fits within the expected range for Kauai based on Li's (1988) measurements and calculations.

As the rates of deposition indicate, "overbank" events on the Hanalei River are a common and important characteristic of the lower reaches of the river. While these events may presently be described as yearly averages by what they have left behind (i.e., deposited sediments), "overbank" events cannot yet be individually characterized in terms of frequency and magnitude. It is in these terms that the river must be described to be of practical use for land use managers.

The USLE was applied in an attempt to test the validity of its assumptions in an environment significantly different from that for which it was developed. If the equation was able to describe erosion in the valley, other equations with similar assumptions, such as the RUSLE and MUSLE, could be used in the valley and greatly simplify the fieldwork necessary to describe the "overbank" events of the Hanalei River. The measured sediment yield is 45% to 101% of the maximum predicted rate of hillslope rill and interrill erosion of $4,800 \pm 5,600 \text{ Mg yr}^{-1}$. The higher than expected sediment delivery ratio may reflect the importance of mass movement in Hanalei Valley, but which is not accounted for by the USLE. Additionally, when the important process of mass movement is addressed, it becomes apparent that data presented herein are not able to differentiate between sediment movement due to water erosion and that due to mass movement. As a result, the USLE equation provides a description of sediment erosion that does not appear to be of practical use in the Hanalei watershed.

Calculations show that approximately 30% of the yearly sediment arriving at the coastal plain ($7,560 \pm 2,910 \text{ Mg}$) is deposited. The remaining 70% is discharged into the ocean. Because of biases inherent in the field measurements, more accurate and detailed observations of high discharge events are likely to lower the percentage of total sediment

deposited on the coastal plain by increasing the measured volume of sediment passing through the Hanalei River system to the ocean.

Chapter 2. From watershed to reef, a budget of carbonate and terrigenous sediments, Hanalei Bay, Kauai, Hawaiian Islands

Abstract

Surficial sediments of Hanalei Bay on the north shore of Kauai are dominated by carbonate grains made of coralline algae, coral, and mollusc fragments as well as foraminifera, *Halimeda*, bryozoa, and echinoderm tests comprising approximately 70% of the grains. Siliciclastic grains from the Hanalei River watershed draining the shield volcanic highlands of Kauai are the most common individual grain type and form a zone of high concentration from the mouth of the Hanalei River into the center of the bay.

The post-glacial sea-level transgression began in the bay soon after 11.7 kyr and resulted in the deposition of $45.5 \pm 1.5 \times 10^6 \text{ m}^3$ of sediment in the bay and approximately $33.7 \pm 11.2 \times 10^6 \text{ m}^3$ of sediment on the Hanalei coastal plain since that time. The total volume of carbonate sediment stored in the bay and coastal plain is greater than the volume likely to have been produced exclusively in the bay during the same time according to published carbonate sediment production rates. Calculations indicate that approximately $2,490 \text{ m}^3 \text{ yr}^{-1}$ have been imported into the bay or coastal plain and deposited since 11.7 kyr. The majority of this sediment influx is likely delivered from the east by the strong tradewind currents that characterize Kauai's north shore. Excess carbonate sediment flux into Hanalei Bay peaked at a rate of $15,530 \text{ m}^3 \text{ yr}^{-1}$ between 5.0 kyr and 3.0 kyr (when sea level may have been 2 m above present) diminishing to $3,890 \text{ m}^3 \text{ yr}^{-1}$ from 1.0 kyr to the present. This influx is likely to have played a significant role in the mid to late Holocene progradation of the Hanalei shoreline.

Introduction

The close proximity and high gradient of marine and terrestrial environments at Hanalei Bay on the north shore of Kauai, Hawaii, combine to form a unique system in which to study sedimentary processes (Figure 2.1). The watershed adjacent to Hanalei Bay contains several rivers: the Hanalei River, one of Hawaii's largest rivers, the smaller Waioli and Waipa rivers, and two intermittent streams, the Waikoko in the west and an unnamed stream entering the northeast corner of the bay. The ocean environment, however, is the primary influence on the bay's circulation and sediment budget. Opening due north, the bay receives massive winter swells from the north Pacific with annual significant wave heights exceeding 5 m (Bodge and Sullivan, 1999), while northeast tradewinds provide seasonally variable, but nearly year-round, effects due to wind, waves, and wave-driven currents (Figure 2.2). The angles of incidence and relative strengths of these two marine energy sources vary, creating regions in the bay where deposition and erosion of various sediments form recognizable patterns. Terrestrial and marine environments converge in Hanalei Bay to create a sediment budget that is the subject of this study.

Geologic Setting

The northwestern-most of the six main Hawaiian Islands, the Kauai shield volcano is also the oldest (3.5 - 5.7 million years; Macdonald *et al.*, 1983). Fluvial erosion and mass movement have created deep valleys and large amphitheaters in the original edifice. The top of Kauai rises to 1,598 m (5,243 ft) at the summit of Kawaikini. Nearby Waialeale receives some the highest rainfall in the world ($>10 \text{ m yr}^{-1}$) as the moist tradewinds are funneled and orographically lifted over the steep-sided mountains. Such prodigious rainfall, flowing off the north side of Waialeale and into the 54.4 km² Hanalei River basin, ensures not only dense vegetation, but also a significant supply of sediment

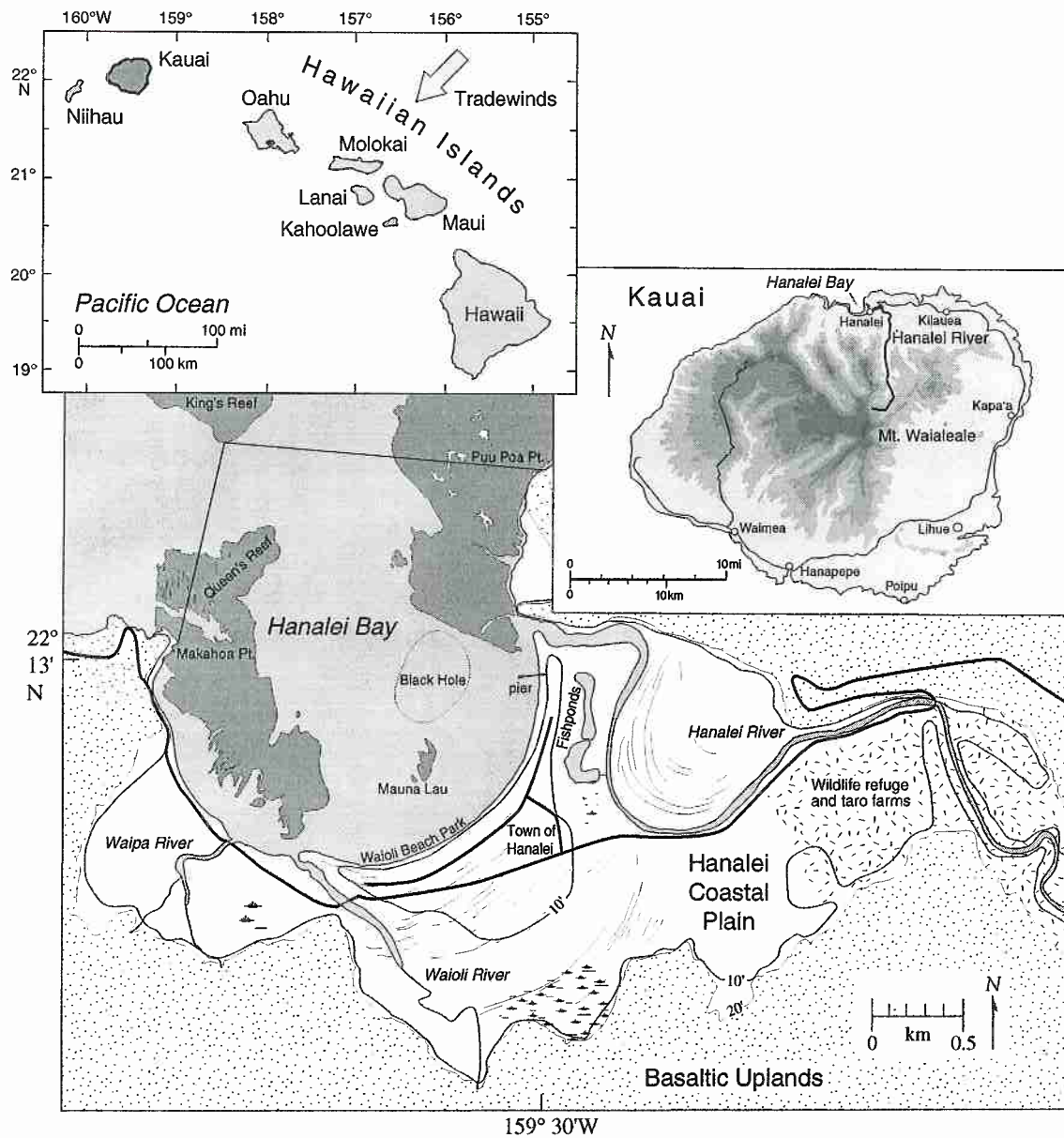


Figure 2.1. Map of Hawaiian Islands showing the island of Kauai, Hanalei Bay, and the Hanalei coastal plain on the north shore of Kauai. Also shown are the town of Hanalei, major roads, and reefs. The 10 and 20 ft (3.0 and 6.1 m) contours were obtained from U.S. Army Corps of Engineers contoured orthophotoquads (1:4800). Reef position and extent were obtained from NOAA-NOS aerial photos at an altitude of 5300 ft (1615 m) (1:8700) as well as a 100 kHz sidescan sonar survey of the region.

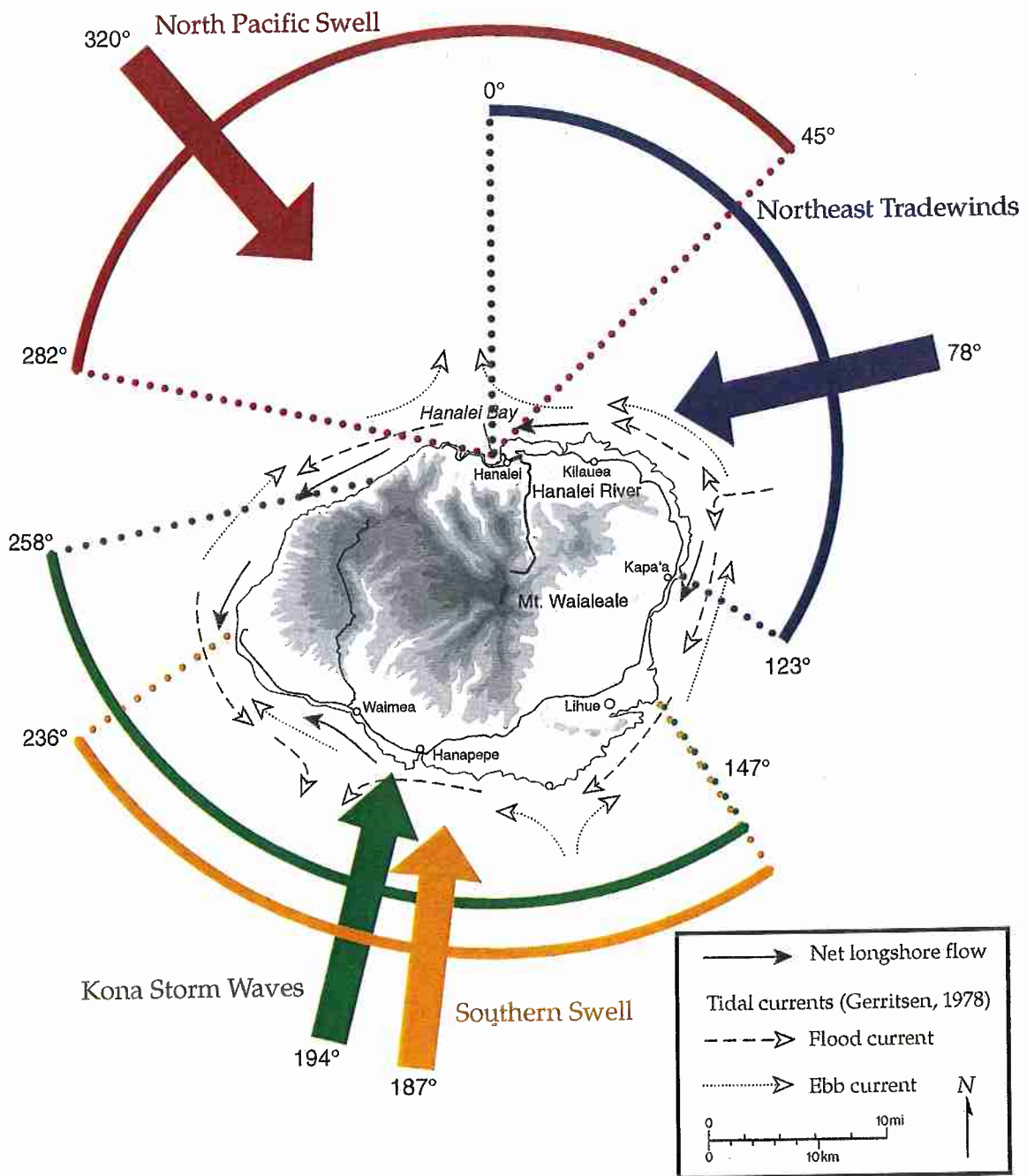


Figure 2.2. Kauai coastal energy regime (after Moberly et al., 1965) with average and extreme directions.

to Hanalei Bay through mass movement and surface erosion (Calhoun and Fletcher, in press). The Hanalei watershed is comprised predominantly of deep, steep-sided gorges, so that the 25.2 km long river has no real floodplain until below the 61 m contour.

Three wave regimes dominate sediment budget processes in Hanalei Bay. Northeast to easterly tradewind-driven waves are common throughout the year but are strongest from April to November. During the summer, tradewinds blow 90% to 95% of the time, while in the winter, they are present 55% to 65% of the time. These winds generate local waves characterized by periods of 6 to 8 s and heights of 1 to 3 m. Despite their relatively small height and short period, the persistence of the tradewinds is enough to set up steady longshore currents that can transport significant volumes of sediment in the longshore drift (Bodge and Sullivan, 1999). Although no direct measurements of longshore currents exist on the north shore of Kauai, tradewind-dominated longshore flow on the east and south shores have been measured, and vary from 6.1 cm s^{-1} to 112.8 cm s^{-1} (Inman *et al.*, 1963; Sea Engineering, 1996).

North Pacific swells, with typical deep-water heights of 2 to 5 m and periods of 12 to 20 s, enter the bay from the west-northwest to the northeast, and are produced by large winter storms in the north Pacific, most commonly between October and March (Bodge and Sullivan, 1999). These massive waves create strong currents that shift sediment around the bay and produce strong seasonal characteristics on the adjacent beaches.

Finally, Kona winds are light variable winds generally from the south and southwest that most frequently occur during the winter season. In Hanalei, periods of Kona winds, particularly common during years characterized by the onset of El Nino-Southern Oscillation conditions, are characterized by calm local conditions. They are, however, independent of north Pacific storms, and so may occur with large winter swell.

Kona storms approach Kauai from the south, and while they may produce large waves along the south shore, Hanalei Bay remains protected. Large, steep waves from

hurricanes generally do not strike Hanalei directly. Hurricanes typically threaten Hawaii from the south or east and rarely approach the north shore of Kauai from offshore so their fetch is too short to produce large waves in Hanalei (Juvik and Juvik, 1998; Kodama and Businger, 1998). Tsunamis are another relatively rare event in Hanalei. While numerous strong, damaging tsunamis have hit Hanalei in the past and almost certainly redistributed sediment, the most recent was in 1964, and any influence it had on surface sediments is not apparent 35 years later.

The entrance of Hanalei Bay is protected on each side by massive basalt headlands with barren rocky shorelines tens of meters long and over 5 m high. These stable points provide identifiable lateral boundaries for the bay. For this analysis, the oceanic limit of the bay is nominally prescribed between these two points and the landward point of an offshore paleoreef platform lacking sediment cover at 30 m depth, locally named “King’s Reef.” South of the headlands, approximately 3.2 km of continuous carbonate sand beach stretches in a semicircle around the bay. Pocket beaches on the east and west sides of the bay characterize the transition between the longer beach and the rocky headlands (Figure 2.3).

Within the 4.41 km² area of the Hanalei seafloor, unconsolidated sediments and coral-algal reef combine to provide diverse sedimentary environments. The total reef surface area capable of carbonate sediment production is 1.33 x 10⁶ m², which consists of fringing reefs flanking the east and west sides of the bay as well as two centrally located patch reefs. Additionally, small patch reefs are found on either side of the bay, and a broad, shallowly sloping depression on the east side immediately offshore from the Hanalei River and pier is locally named the “Black Hole” due to its high concentration of dark terrestrial debris. Between the reefs is a broad, gentle, seaward sloping plain of unconsolidated marine carbonate sand. Moberly *et al.* (1965) describe a single sample of sand (location not identified) from the Hanalei beach as approximately 71% carbonate and

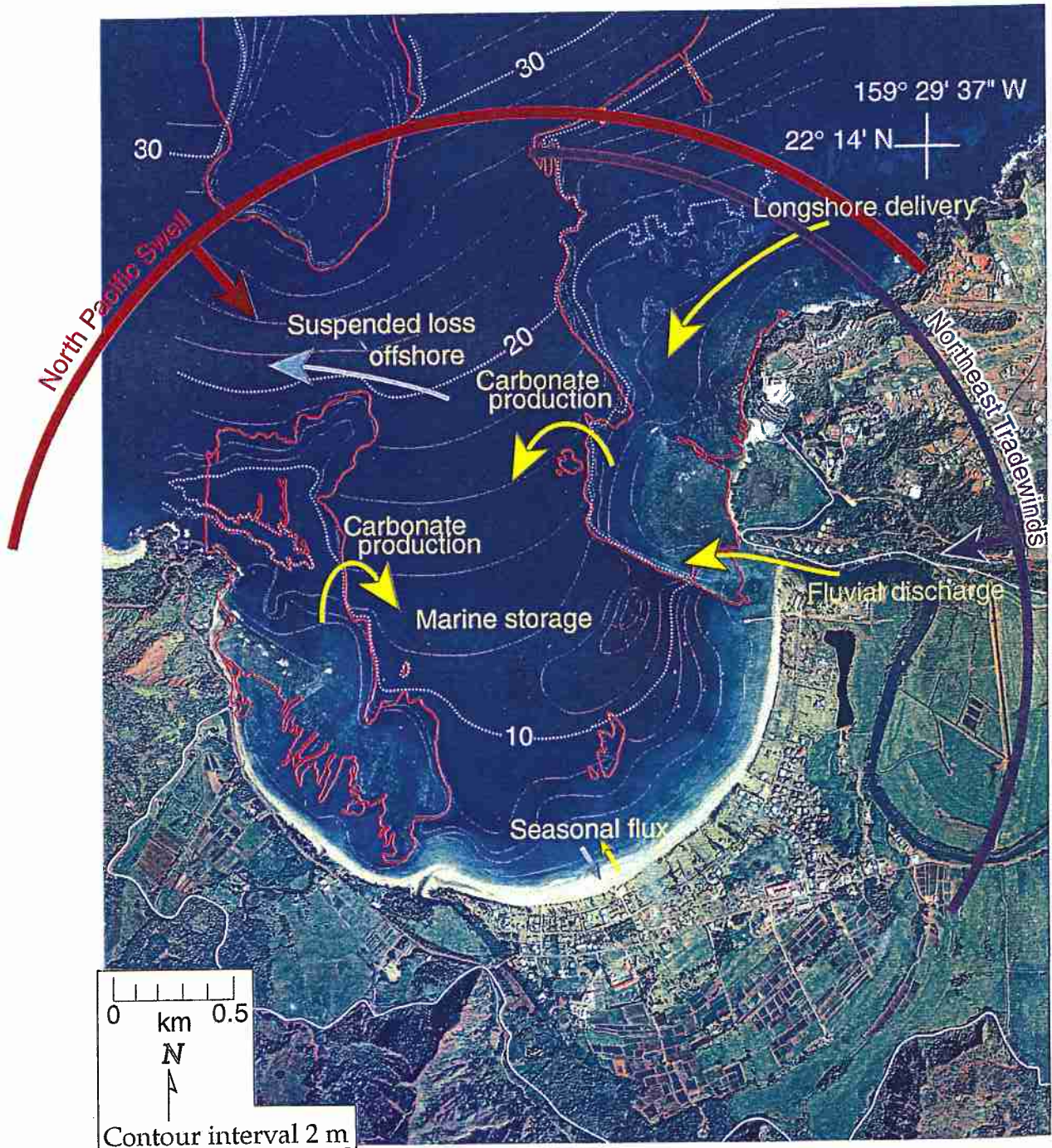


Figure 2.3. Processes shown are significant to the sediment budget of Hanalei Bay. Yellow arrows are gains to the budget and light blue arrows are losses. Additional losses include abrasion and dissolution of carbonate grains.

29% siliciclastic (defined as grains derived from the volcanics comprising the basaltic uplands of Kauai). They classified the carbonate particles as molluscs 31%, foraminifera 20%, coralline algae 16%, echinoids 7%, corals 6%, and unknown 19%. The siliciclastic grains were composed of 74% fresh lithic grains, 16% weathered lithic grains, and 10% olivine.

Sediment Budget

The purpose of defining a sediment budget is to develop an improved understanding of the natural processes governing sediment production, flux, storage, and eventual fate in order to enhance our ability to model and predict watershed, littoral, and shoreface evolution, variability, and dynamic states of stability. This knowledge will promote better management practices and the development of new and more comprehensive conservation programs.

In identifying and quantifying sediment sources and sinks, processes responsible for the flux and storage of sedimentary particles across a coastal system require characterization. Calculations based on measurements of these processes help to identify which are the most influential to sediment production, distribution, and storage, and which are not active in a particular area. Although several studies have addressed individual components and processes in Hawaiian coastal systems (Inman *et al.*, 1963; Moberly *et al.*, 1965; Sea Engineering, 1996), no comprehensive coastal sediment budgets have been described. This leaves multiple questions unanswered regarding other significant influences on sedimentary processes in a particular location. For Hanalei, the most significant sedimentary processes are addressed, and, as a result, these calculations are used to explain geological observations.

To identify and quantify the distribution and character of Hanalei sediments, a range of geophysical, geochemical, and observational methods were employed. Aerial photos

and sidescan sonar enables mapping the extent of unconsolidated sediments as well as the surface area of the carbonate producing reefs. Seismic reflection data allows the interpretation of sediment thickness throughout the bay and the characterization of underlying surfaces. Coulometry and point counting of grain-mounted thin-sections identifies grain composition and geochemistry as well as likely sources. Coastal plain stratigraphy was determined using over 100 gouge auger cores. Six years of beach profiling serves to define the seasonal flux of the beach, the connection between the bay and the coastal plain. Discharge and suspended sediment measurements from the Hanalei River are useful in quantifying the contribution of fluvial sediments to the bay. Limited current measurements show possible directions of movement for sediments within, as well as entering and exiting, the bay.

Reef Ecology

Algal turfs composed of *Dotyella*, *Centroceras*, and *Tolyptocladia* are the most common (36%) individual living substrate cover in Hanalei Bay. Encrusting coralline algae, such as *Porolithon* and *Hydrolithon*, cover a mean of 15% of the reef surface and hard corals, *Montipora*, *Porites*, *Pocillopora*, *Pavona*, *Leptastrea*, and *Fungia*, cover 18% (Friedlander *et al.*, 1997). The depths between 9.6 and 13.6 m possess the highest mean cover of coral (23%) and 7.7 m to 9.1 m the lowest (12%). Macroalgae (i.e.; *Turbinaria*, *Gibsmithia*, *Corallina*) comprise an additional 22% of living cover, and bare substrate is only 3% of the reef surface. The rugosity or microtopography of the reef structure is described by Friedlander *et al.* (1997) as ranging between 1.11 and 4.14 with a mean of 1.6 and a standard deviation of 0.60.

Methods

Sediment compositional and texture data are based on 41 benthic short-core samples from around Hanalei Bay and from 4 separate reaches of the Hanalei River acquired in late summer (August, 1993). Four beachface and nearshore sediment samples were collected during the winter. Sampling included a 15 cm diameter, open-ended, metal, cylindrical corer pushed 10-14 cm into the unconsolidated sands of the bay floor by SCUBA divers. All contents of the corer were oven-dried at approximately 120° C for 72 h. Sample sites were surveyed using digital compass triangulation with an instrument resolution of $\pm 0.5^\circ$ and a horizontal accuracy of ± 15 m. Random splits of samples were analyzed (Humboldt shaker, -1.0 to 4.0 ϕ , 0.5 ϕ intervals) for mean grain size, standard deviation, skewness, and silt and clay content ($< 4.0 \phi$). Patterns in these sediment textures were contoured by hand.

Inorganic carbon content of these benthic sediments was measured on duplicate samples using coulometry described by Engleman *et al.* (1985), except a carrier gas of potassium hydroxide scrubbed nitrogen gas was used instead of air, and samples were dried at 80° C for at least 12 h prior to weighing. The percentage of calcium carbonate in each sample was calculated with the assumption that all the inorganic carbon was calcium carbonate (Glenn *et al.*, 1995). Duplicate splits (triplicates if necessary) were run to achieve 2% reproducibility with each sample.

A 70 line 100 kHz sidescan sonar survey was conducted in the bay and its surrounding waters during the fall of 1992 by Sea Engineering, Inc. with a EGG model 260 towfish. Differences in acoustic reflections are interpreted with respect to the geology and sedimentology of the bay floor, including the extent of the reefs, other sediment-free surfaces, and variations in benthic sediment types. Interpretations were confirmed with aerial photos and "ground truthing" by SCUBA dives in the bay. Sea Engineering, Inc. also conducted a seismic reflection survey using a Datasonic bubble pulser with a

hydrophone streamer during the two days subsequent to the sidescan survey. A 600 to 4,000 Hz bandpass filter was applied to the 13 seismic lines of the survey. Because the data were recorded in analog form, no further processing was done. This survey permitted the interpretation of benthic sediment thickness and the nature of the acoustic basement (basal reflector) of the bay. The composition of benthic sediments was determined by petrographic microscope identification of 20 grain-mounted thin-sections. Patterns in the component concentrations were contoured by hand.

The 3.2 km Hanalei beach was profiled semi-annually in five locations to calculate the sand volume and describe volumetric changes. This survey was conducted with a level, a tape measure, and a stadia rod between August, 1993 and August, 1995; between March, 1996 and February, 1999, a range and angle measuring geodimeter and a prism were employed. Current directions and magnitudes were assessed with a combination of neutrally buoyant drogue measurements timed over 10 m at slack tide, sediment ripple dimension measurements, and sediment texture measurements (le Roux, 1994).

Samples ranging between 10 and 35 mg of either coral or coralline algae grains were separated from four benthic sediment samples. These eight samples were dated using the accelerated mass spectrometry (AMS) method of radiocarbon analysis at the NOSAMS facility in Woods Hole, MA (Pearson *et al.*, 1998). Calibration of the resulting dates was provided by the Radiocarbon Calibration Program Rev 3.0.3c (Stuiver and Reimer, 1993).

Results

Sedimentology

Carbonate Content

The carbonate content ranged from 42% to 92% with a bay-wide average of $66 \pm 11.7\%$ (1σ) (Table 2.1). A large region of reduced carbonate content (<60%) originates at the mouth of the Hanalei River and dominates the middle of the bay (Figure 2.4). This

Table 2.1: Hanalei Bay carbonate content from coulometry and grain size characteristics from sieving.

Sample #	Depth (m)	CaCO ₃ content (%)	Mean (ϕ)	St dev (ϕ)	Skewness	Silt and clay (%)
4		69	2.42	0.64	-2.22	0.2
5		73	2.50	0.63	-1.42	0.8
7	8.0	73	2.23	0.57	-0.36	0.4
8	4.6	85	1.83	0.69	0.11	0.4
9		51	2.75	0.91	-1.30	1.4
10	5.5	71	2.35	0.58	-1.37	0.2
11		75	2.20	0.61	-0.93	0.2
12		76	1.48	0.59	0.11	0.4
13	12.2	68	2.78	0.66	-1.09	3.5
14	18.0	61	2.65	0.64	-0.39	1.6
15	18.6	60	2.73	0.90	-0.93	6.1
16	16.8	92	0.70	1.10	0.18	0.4
17	14.6	54	2.89	0.80	-1.43	4.7
18	11.0	74	2.10	0.54	0.14	0.4
19	11.0	61	2.79	0.67	-1.00	3.9
20	10.4	61	2.65	0.57	-1.23	0.9
21	14.9	52	1.74	1.55	0.31	12.4
22	7.6	62	1.15	1.43	-0.51	0.4
23	10.4	71	2.23	0.57	-1.04	0.5
24	10.4	69	2.46	0.51	-0.56	0.6
25	9.8	76	1.29	0.57	0.61	0.3
26	7.0	73	1.34	0.66	0.42	0.5
27	15.9	60	2.46	0.65	-0.78	1.0
28	16.8	58	3.01	0.82	-0.73	10.7
29	18.0	42	2.97	0.95	-1.69	7.4
30	15.9	48	1.10	1.02	0.29	0.5
34	18.0	83	2.92	0.68	-1.00	3.8
36	14.6	44	2.95	0.68	-1.10	4.7
37	11.6	60	2.71	0.69	-1.17	1.6
38	12.2	56	2.80	0.61	-0.81	2.4
39	16.2	67	2.24	0.81	-1.03	0.5
40	12.2	78	2.47	0.73	-0.07	2.0
41	20.4	79	1.90	1.19	-0.71	1.8
43	11.0	59	0.76	1.00	0.91	0.3
44 river mouth	1.0	39	0.12	0.84	0.33	<0.1
45 river	~2.5	0.12	-0.23	0.90	0.99	0.3
46 river	~2.0	insignificant	-0.72	0.94	1.78	0.2
47 river	~2.0	insignificant	0.05	0.78	0.70	0.3
48 river	~2.0	0.50	0.24	0.93	0.95	0.6
49 beach	+2	72				
50 beach	+2	49				
51	1.5	59				
52	3.0	70				

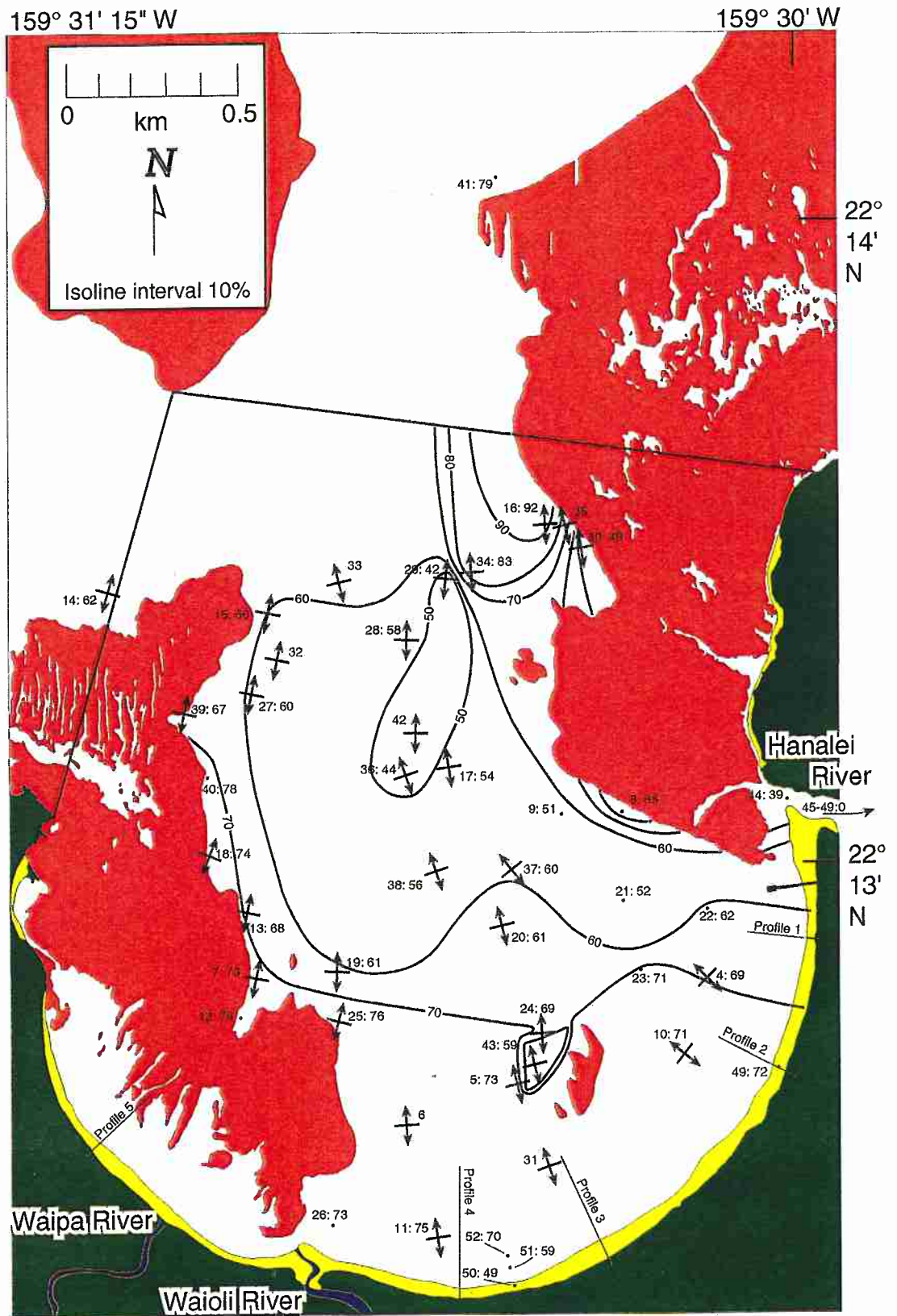


Figure 2.4. Percent calcium carbonate content (by mass) of sediment is contoured. Arrows are perpendicular to symmetric bedform crest direction; parallel to inferred current direction. Each sample site is labeled with sample number: carbonate content.

region is centered in the bay between 14.5 and 18 m water depth where the carbonate content decreases to 42%. Carbonate content rises above 70% near the western fringing reef and as the bay shallows (<10 m) toward the shoreline. Most nearshore and beach samples not proximal to the Hanalei River have carbonate contents near 70%. Two samples taken during the winter from the subaerial beach and on the offshore bar at the Waioli Beach Park have very low carbonate contents, 49% and 59% respectively, while a third sample taken at the same time from 3 m water depth seaward of the bar has a carbonate content of 70%. This pattern, perhaps, indicates preferential seasonal erosion of carbonate grains during periods of high wave energy. Samples in the northeastern corner of the bay combine to create the appearance of a high carbonate (~90%) tongue entering the bay, perhaps as a result of preferential transport and subsequent deposition of carbonate grains, in this case by the longshore current characterizing the tradewind dominated coast to the east of the bay. An isolated low carbonate patch is located on the seaward side of the patch reef in the center of the bay.

Composition

The sand in Hanalei Bay is comprised of a mixture of marine-derived carbonate grains (biogenic and chemically-altered) and terrestrially-derived volcanic grains (basalt lithics, olivine, plagioclase, and clinopyroxene) (Table 2.2). Biogenic grains are skeletal remains of marine organisms including coralline algae, coral, molluscs, foraminifera, the green algae *Halimeda*, bryozoa, and echinoderms. Altered carbonate grains are skeletal fragments that were chemically altered such that their internal structures, and hence their origin, is no longer identifiable.

The concentration of coral in sand range from 35% at the northeast corner of the bay to 3% at the northwest corner (Figure 2.5). Other areas of low coral sand concentration include the bay's southeast corner at the mouth of the Waioli River (7%), the

Table 2.2: Marine sediment composition in Hanalei Bay from 20 benthic sample sites. Sample locations are shown in Figures 2.5 and 2.6. See Appendix A for the complete summary of each sample.

Component	Mean throughout bay (%)	Standard Deviation	Range (%)	Waioli Beach Park (%) (modern beach sample)
Detrital	27	13	7 - 58	50
Coralline algae	19	8.2	11 - 42	18
Coral	17	8.4	3 - 35	10
Chemically-altered carbonate	12	4.4	3 - 20	13
Mollusc	9	3.6	3 - 15	3
Forams	6	2.1	3 - 12	5
<i>Halimeda</i>	3	2.3	0 - 8	0.3
Bryozoa	2	1.5	0 - 6	0.3
Unknown	2	2.8	0 - 9	1
Echinoderm	1	0.87	0 - 3	0.3

percentages of siliciclastic component from Waioli Beach Park:

olivine	50
lithic	43
altered lithic	3
clinopyroxene	1
plagioclase	1

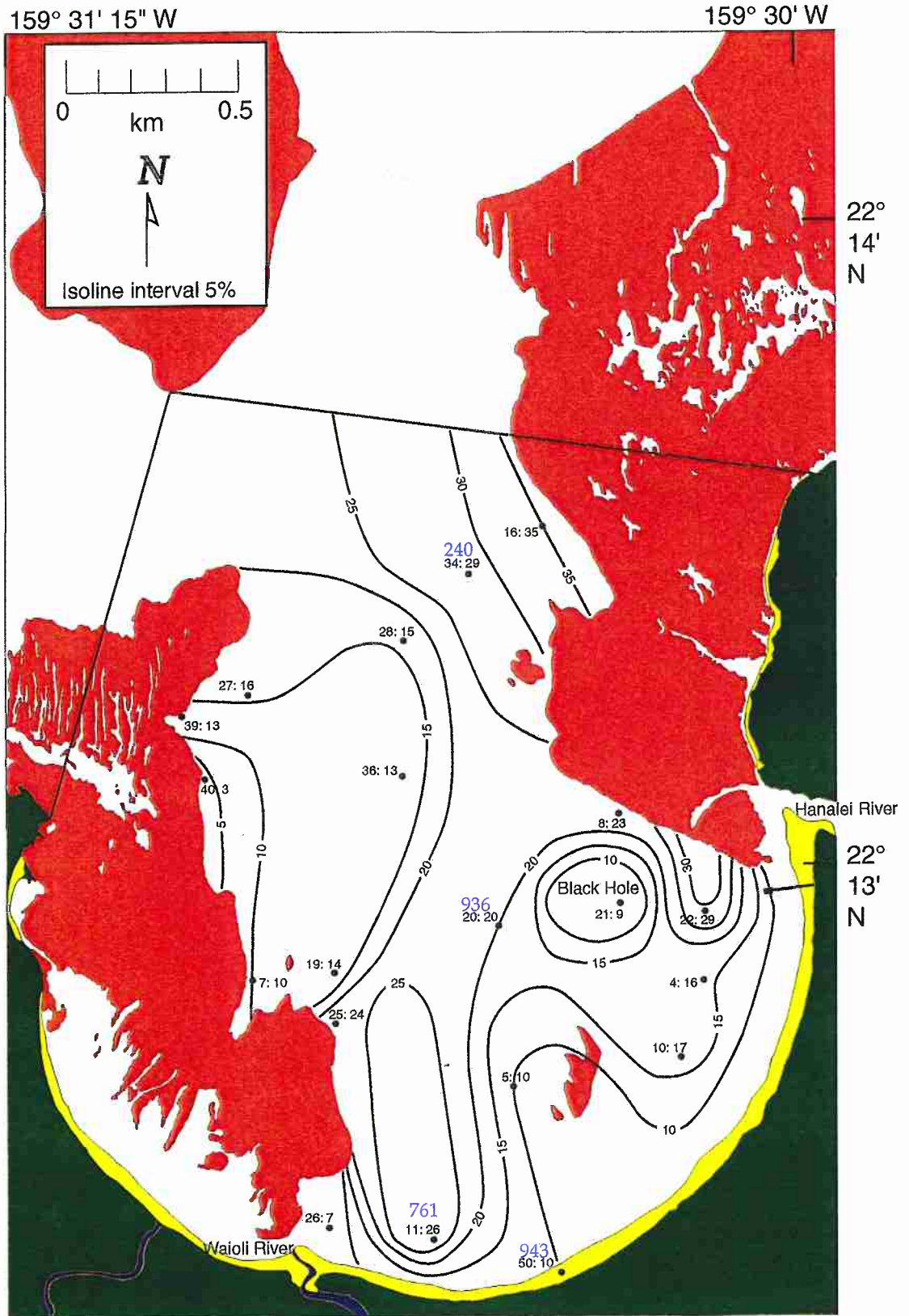


Figure 2.5. Percentage of coral grains is contoured. Each sample site is labeled with sample number: percentage of coral grains. Coral percentages range from 3 to 35% with a mean of 17.0%. Best radiocarbon ages are shown in blue.

Black Hole (9%), and much of the sand adjacent to the western fringing reef (<10%).

Areas of high coral sand concentration include between the Hanalei River mouth and the Black Hole (29%) and east of the southern end of the western fringing reef (>25%).

In general, coralline algae concentrations are high next to the fringing reefs and low in the middle of the bay. Algal grains range from a high of 42% in the southwest corner to a low of 11% in the center of the bay (Figure 2.6).

Radiocarbon dates consistently showed coralline algae grains are significantly older than coral grains from the same location (Table 2.3). The best dates for coral grains ranged from 240 BP in the northeastern corner of the bay to 936 BP near the center of the bay. Coralline algae showed best dates ranging from 1,036 BP in the northeast to 2,300 BP on the beach at Waioli Beach Park.

Siliciclastic sand grains are the most common individual grain type and range from 58% at the Black Hole to 7% at the northeast corner (Figure 2.7). High siliciclastic levels are also found in the center of the bay. The beach sample at Waioli Beach Park has a relatively high siliciclastic component of 50%. That same beach sample has an unusually low concentration of mollusc fragments (3%) (Figure 2.8). The mollusc percentage pattern also shows relatively high concentrations along the western fringing reef and around the central patch reef (>10%), and a region of low mollusc concentration entering from the northeast (<6%).

Texture

Sediment textures were computed using the method of moments described by Boggs (1995) (after Krumbein and Pettijohn, 1938). The classifications of texture are from Boggs (1995) (after Folk, 1974). The mean size of all sediments ranges from 0.12 ϕ (coarse sand) at the mouth of the Hanalei River to 3.01 ϕ (very fine sand) in the deeper water at the outer reaches of the bay (Figure 2.9). Most of the bay floor is moderately well

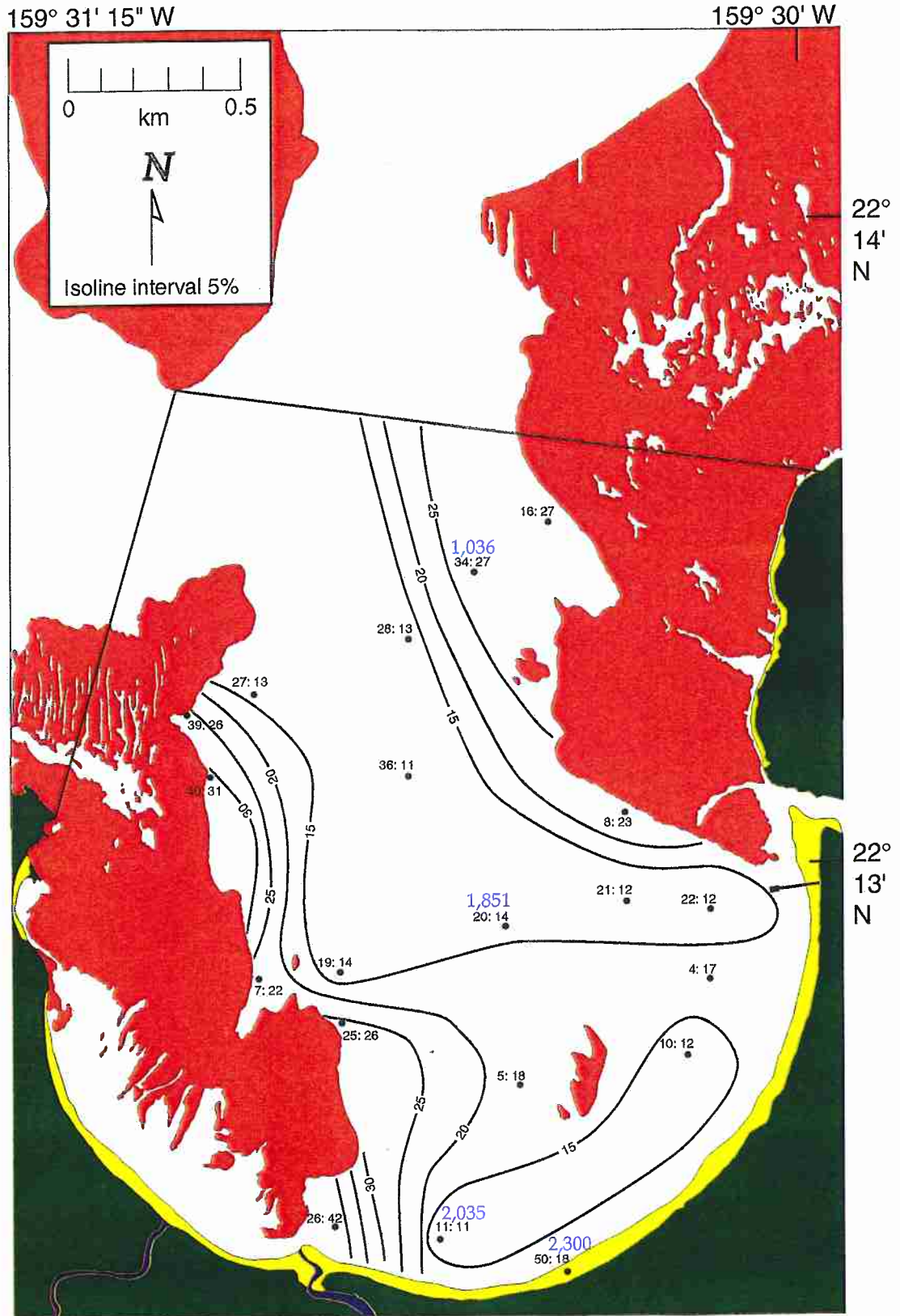


Figure 2.6. Percentage of coralline algae sand grains is contoured. Sample sites are labeled with sample number: percentage of coralline algae grains. Percentages range from 11 to 42% with a mean of 19.5%. Best radiocarbon ages are in blue.

Table 2.3: Radiocarbon dates from coral and coralline algae grains.

NOSAMS		Hanalei		Age (BP)	Age error (yr)	Calibrated Age (BP)			
Receipt accession	$\delta^{13}\text{C}$	Fm	FmError				Grain type	Age (BP)	
22265	OS-20870	2.01	0.8297	0.0032	34	coralline algae	1,500	30	1,036 (1,160 - 925)
22267	OS-20869	2.27	0.7229	0.0030	50	coralline algae	2,610	35	2,300 (2,413 - 2,115)
22269	OS-20873	2.32	0.7395	0.0029	11	coralline algae	2,420	30	2,035 (2,188 - 1,883)
22271	OS-20874	2.16	0.7546	0.0038	20	coralline algae	2,260	40	1,851 (1,994 - 1,697)
22266	OS-20871	0.03	0.9314	0.0038	34	coral	570	35	240 (294 - 45)
22268	OS-20872	0.03	0.8374	0.0032	50	coral	1,420	30	943 (1,082 - 827)
22270	OS-20867	-0.51	0.8570	0.0052	11	coral	1,240	50	761 (908 - 657)
22272	OS-20868	-0.40	0.8387	0.0033	20	coral	1,410	30	936 (1,070 - 813)

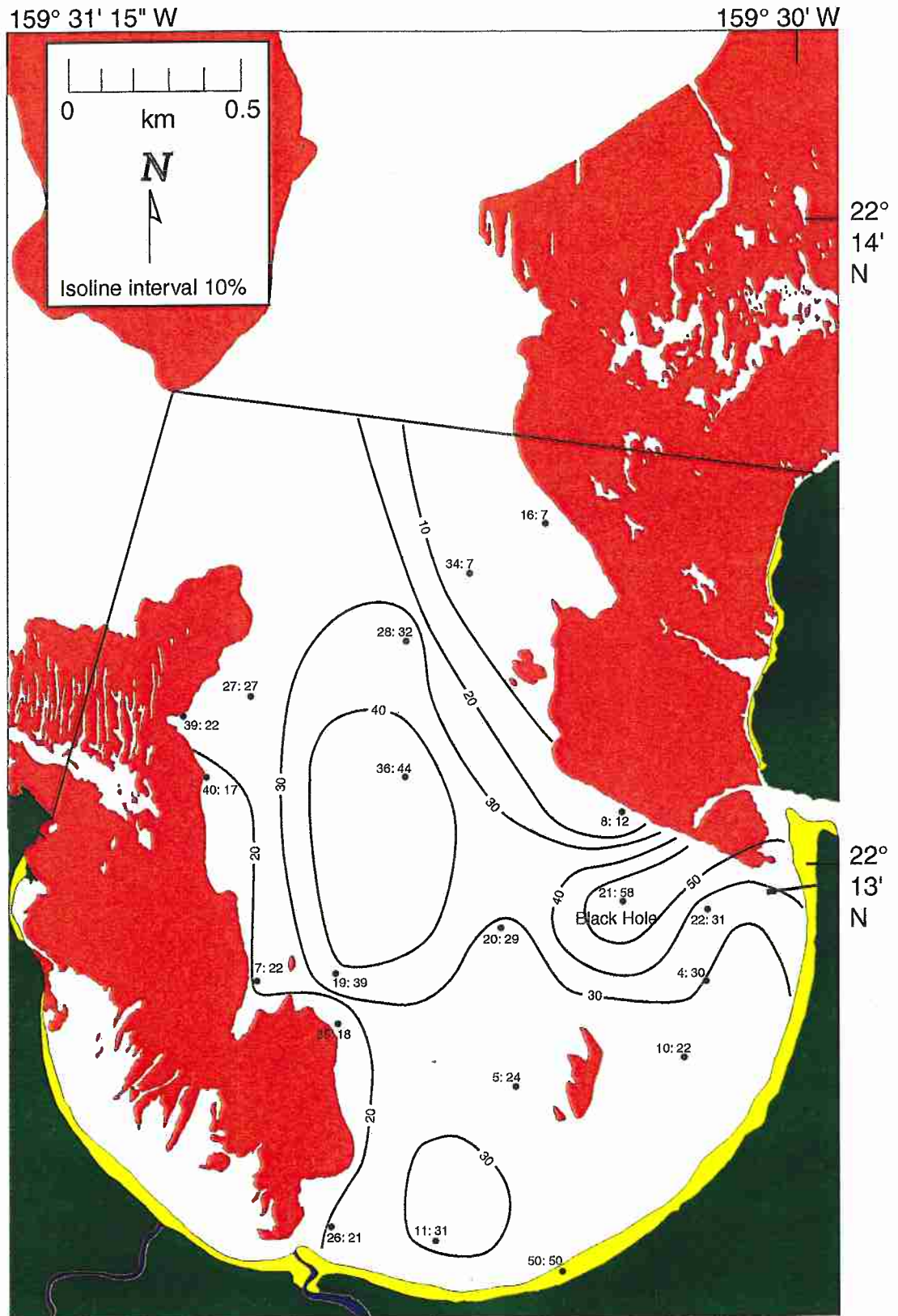


Figure 2.7. Percentage of detrital sand grains is contoured. Sample sites are labeled with sample number: percentage of detrital grains. Percentages range from 7 to 58% with a mean of 27%

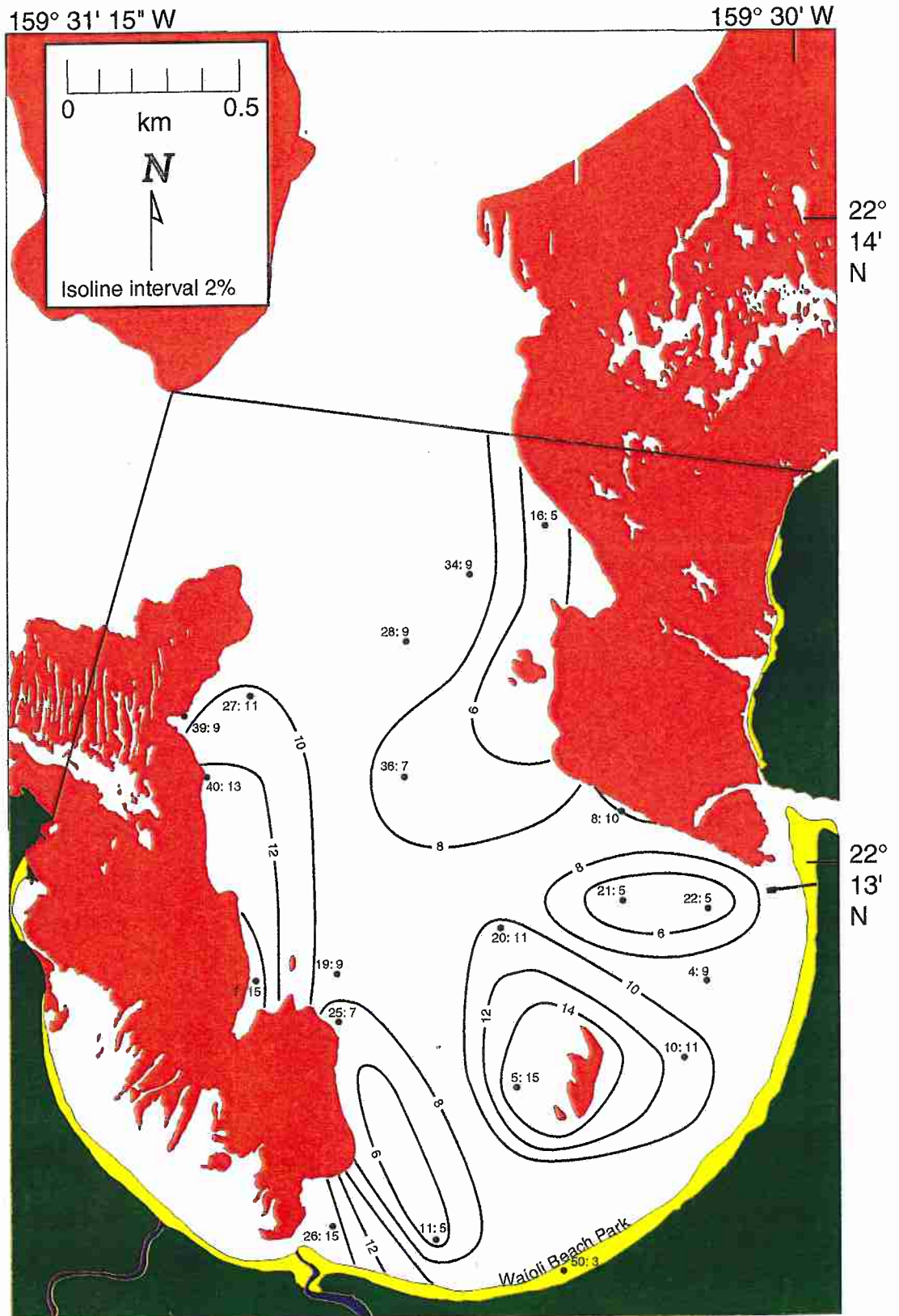


Figure 2.8. Percentage of mollusc sand grains is contoured. Sample sites are labeled with sample number: percentage of mollusc grains. Mollusc percentages range from 2.6 to 15.3% with a mean of 9.2%.

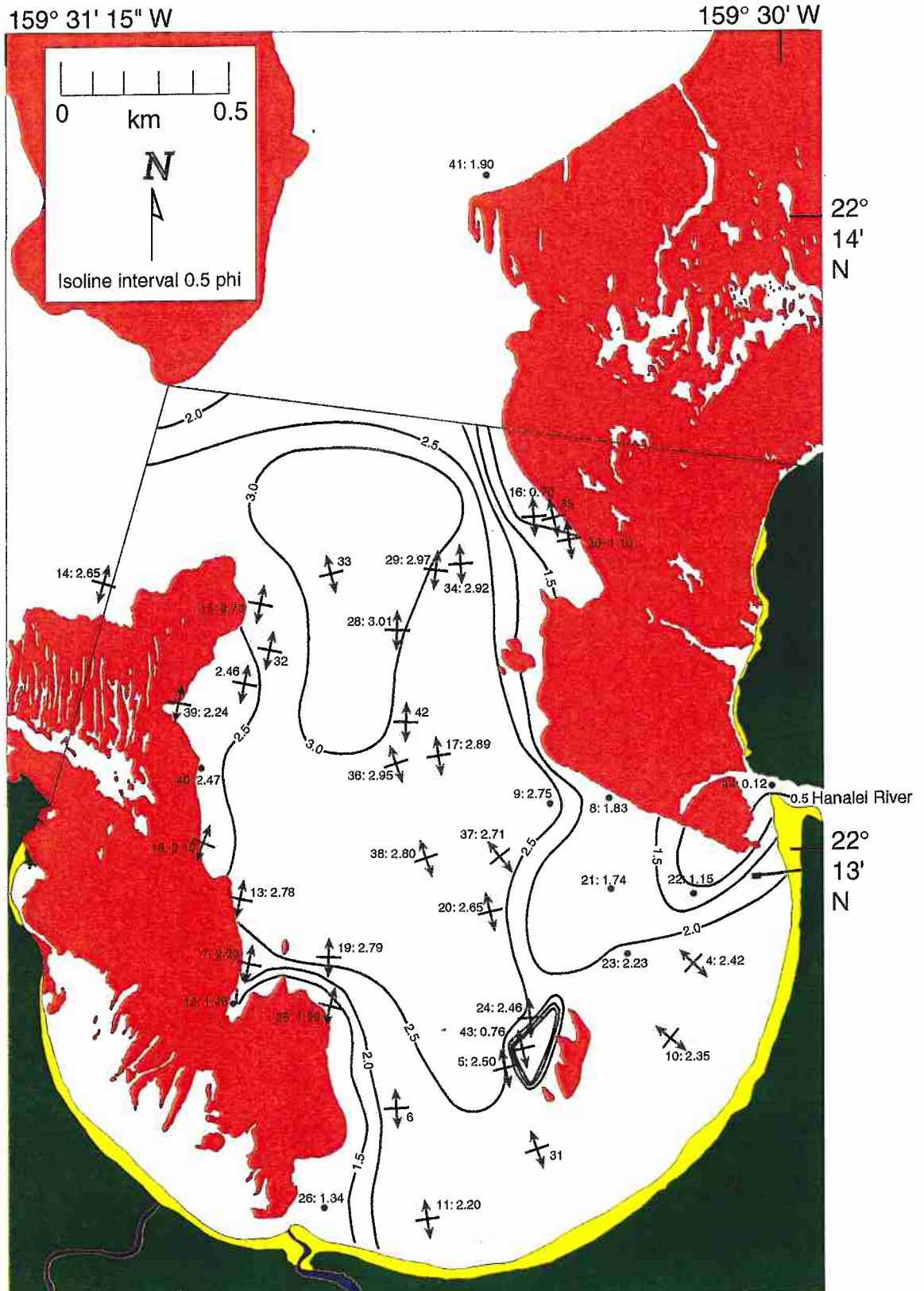


Figure 2.9. Sample number: mean sediment size (phi) and bedform direction (arrows are perpendicular to ripple crest) are shown.

sorted with standard deviations between 0.51 and 0.73 ϕ (Figure 2.10). There are several important exceptions. The deeper section of the bay (below 15-18 m) is moderately sorted with standard deviations between 0.80 and 0.95 ϕ . Three isolated locations are poorly sorted with standard deviations from 1.00 to 1.55 ϕ : along the reef edge in the northeastern corner, in the Black Hole located just off the mouth of the Hanalei River, and immediately west of the patch reef in the center of the bay. Although the sediments are mostly strongly coarse skewed, they do not appear to closely follow an established pattern (Figure 2.11). The center of the bay varies between -0.70 and -1.5 with the sediments along the reefs on either side of the bay shifting to strongly fine skewed (>0.30). A notable exception is a strongly fine skewed patch of sediment just west of the patch reef in the center of the bay. This is the same patch of sediment earlier noted as poorly sorted.

All samples collected from the inner bay (shallower than ~10.5 m) contained less than 2% silt and clay (Figure 2.12). A region of higher percentages of silt and clay, which enters the bay from deep water, is positioned slightly west of center. This region, in 17 m water depth, has a maximum silt and clay percentage of 11% and is centered between the two fringing reefs. Near the edges of the bay along the fringing reefs, breaking waves increase the turbulence and result in low mud content. The western reef is bordered by slightly higher mud percentages. The exception to this pattern is the sample taken inside the Black Hole in 15 m of water. This sample contains 12% silt and clay, the highest in the bay. Field observations of this site, which is a typical location for the Black Hole, show that it has ~20 cm of dark brown silt and clay underlain by carbonate sand. The bottom is covered in green algae and there are tree branches and fern stems with the leaves still attached indicating rapid deposition. The underlying carbonate sand was not sampled. The mud portion was not tested to determine the concentrations of carbonate and terrigenous material. It was assumed that these components had percentages similar to those found in each sample throughout the bay (carbonate 70.5%, terrigenous 27.2%).

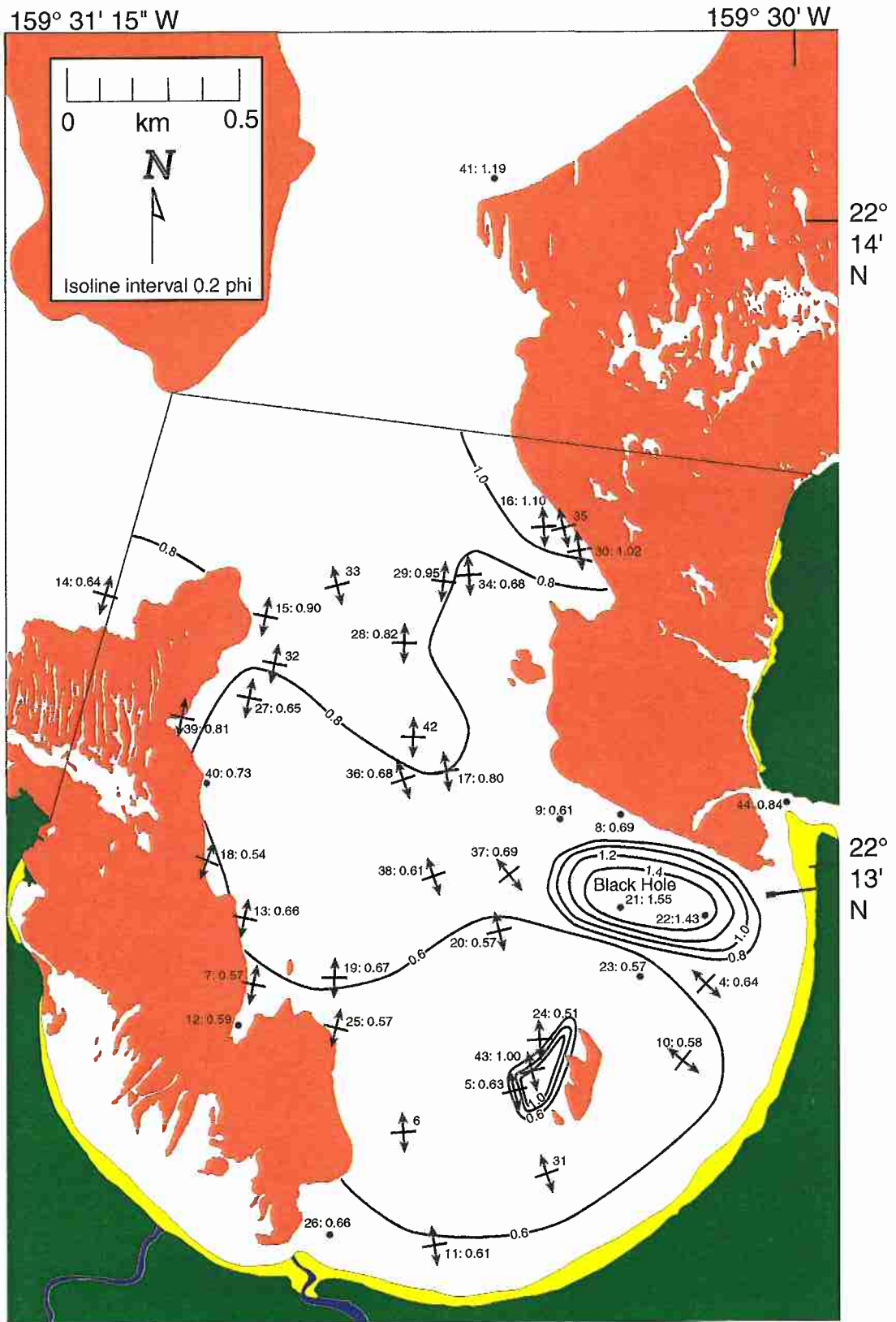


Figure 2.10. Sample number: sediment standard deviation (ϕ) and bedform direction are shown.

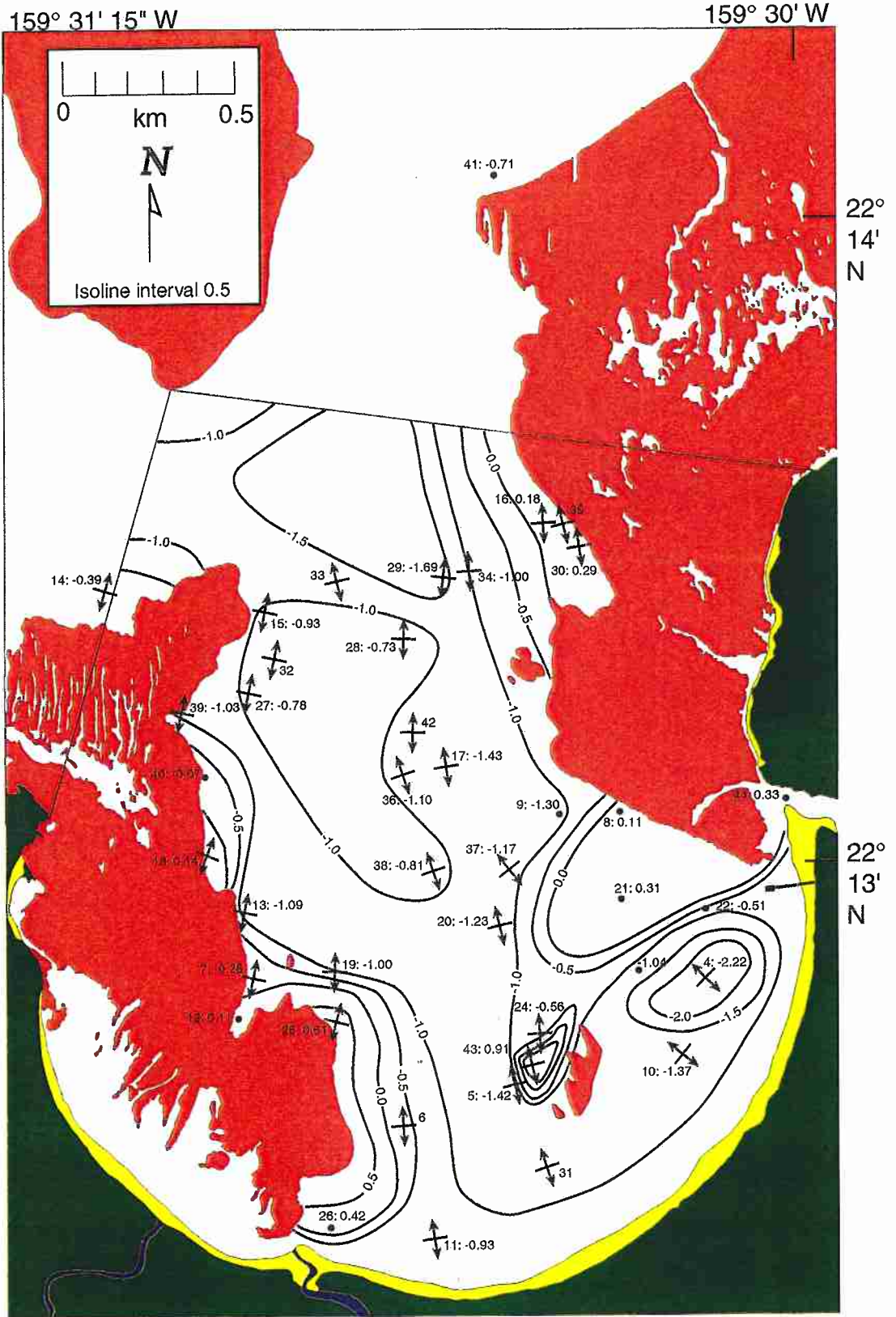


Figure 2.11. Sediment skewness and bedform direction.

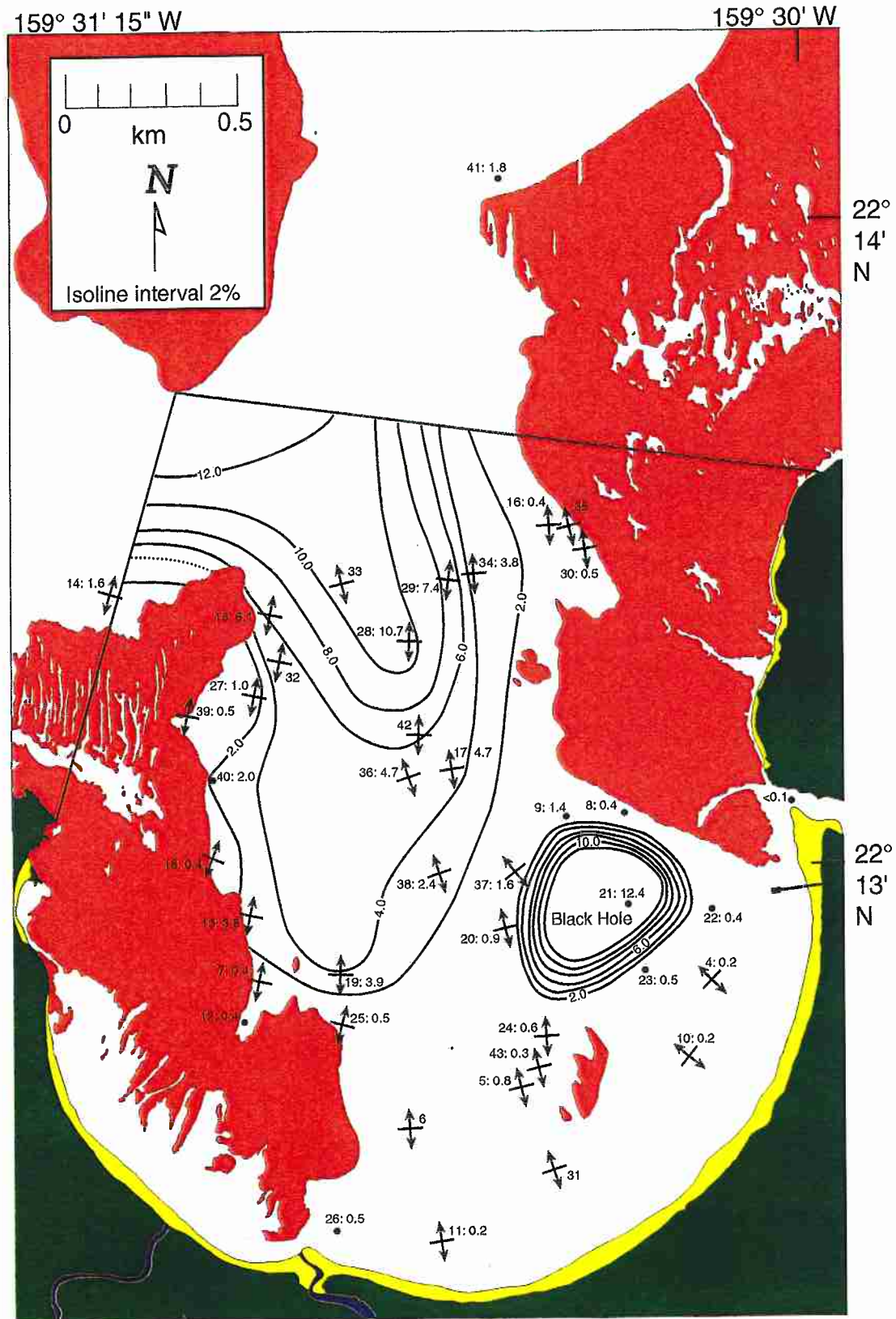


Figure 2.12. Sample number: percentage of silt and clay and bedform direction.

The patch reef in the shallow center of the bay appears to influence the local currents enough to create a distinctive patch of sand immediately to its west. The sediment patch has pronounced edges where the mean sediment size changes from approximately 2.5ϕ to 0.75ϕ over the space of a few centimeters. The bedforms in the patch are straight-crested symmetrical ripples ~10 cm in height with a wavelength of ~80 cm whereas outside the patch the ripples are only 3-5 cm in height and a few tens of centimeters in wave length. Carbonate content also changes in this area, decreasing from over 70% outside the patch to less than 60% inside. Mud percentage does not change significantly, but the standard deviation rises dramatically (to 1.00ϕ) and is very strongly fine skewed (0.91) in contrast to outside the patch which is very strongly coarse skewed (-1.42).

Beach Volumes

Five beach profile lines, starting with profile 1 ~240 m south of the Hanalei pier, are spaced approximately 350 m, 610 m, 425 m, and 1,040 m in a clockwise manner around the bay. Between August, 1993 and August, 1996, the beach sand volume fluctuated seasonally, with summer volumes above $300,000 \text{ m}^3$ and winter volumes at or below $300,000 \text{ m}^3$ (Figure 2.13). After August, 1996, the beach volume increased until July, 1998 when $460,000 \text{ m}^3$ of sand were stored in the beach prism. The seasonal variation of summer accretion and winter erosion continued through the survey period with the notable exception of March, 1997 when the beach increased in volume over the preceding summer. A least median of squares regression of the data, divided into summer and winter sets, shows a $15,900 \text{ m}^3 \text{ yr}^{-1}$ increase for both the summer and the winter.

Currents

Measurements of surface currents during summer tradewind conditions at slack tide show considerable variation throughout the bay (Figure 2.14). Sections of the eastern

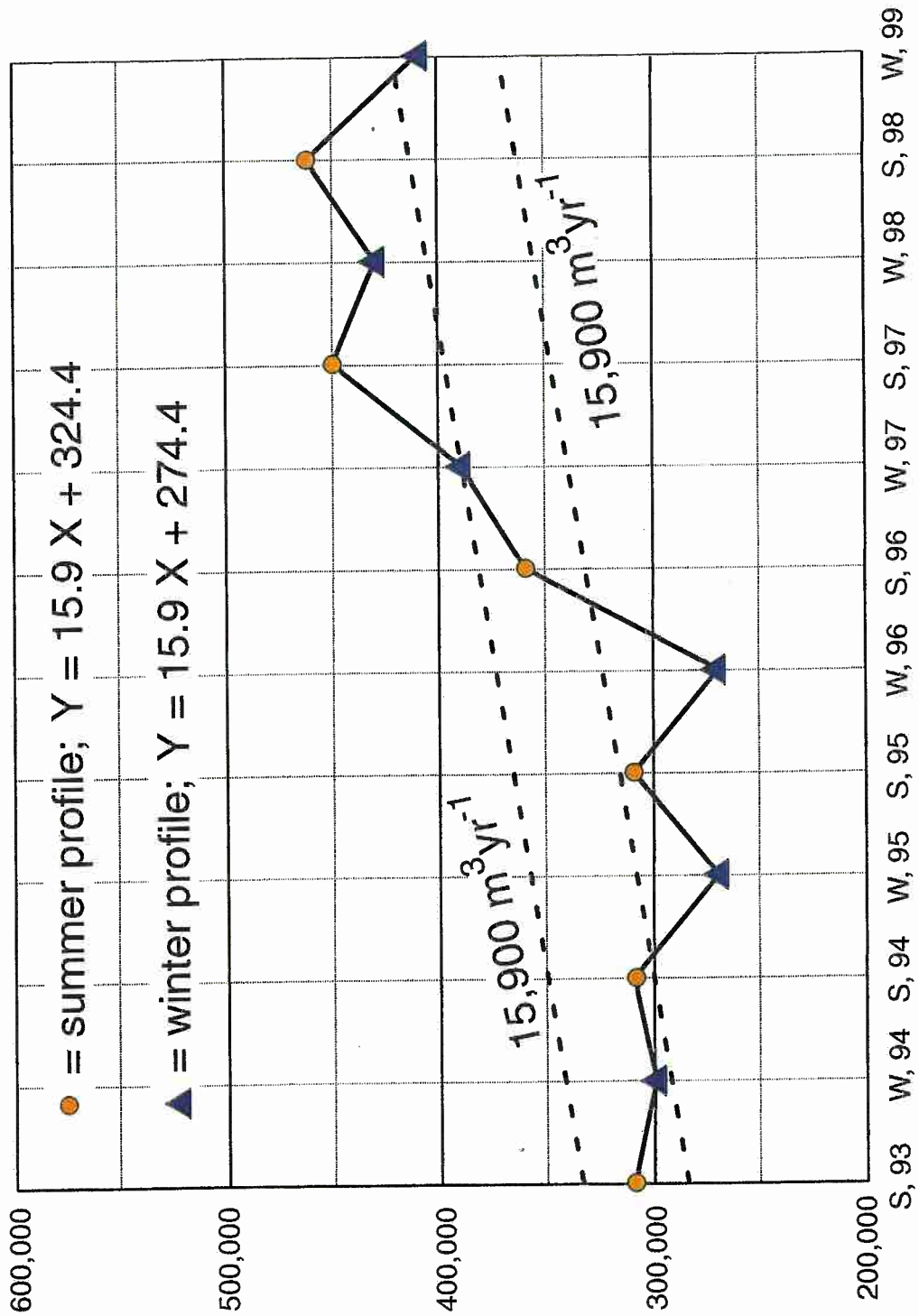


Figure 2.13. Sand volume on beach of Hanalei Bay (m^3). Regression equations and lines are based on least median of squares. S = summer volume; W = winter volume.

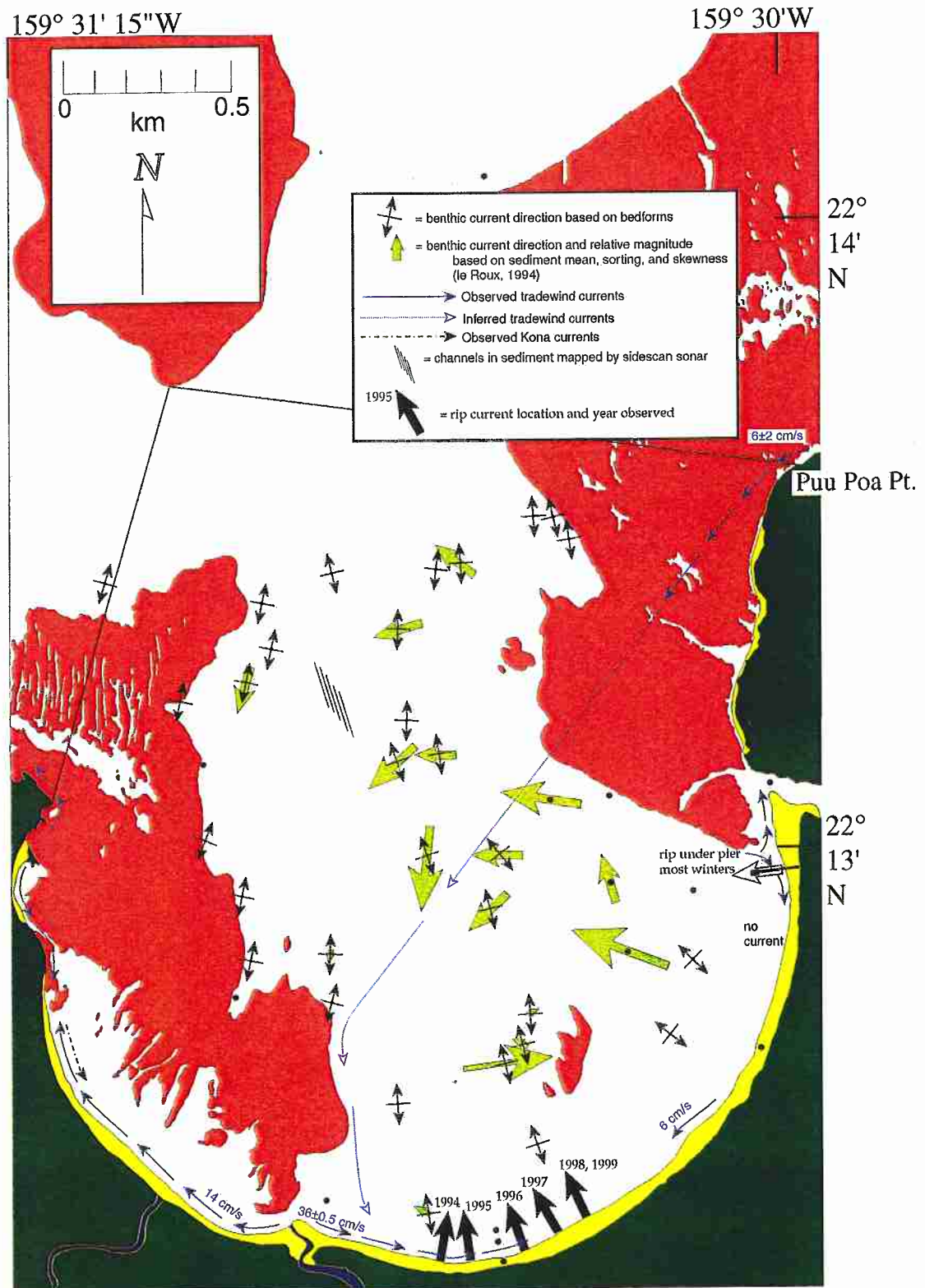


Figure 2.14. Benthic and surface currents. The magnitudes of the yellow arrows are relative only to each other. The length of blue arrows is not related to their velocities. Stable rip currents are seen only during the winter.

beach shoreline show no significant current, while the middle of the beach had an easterly moving longshore current at $36 \pm 0.5 \text{ cm s}^{-1}$. The longshore current driven by the easterly tradewinds at the eastern point of the bay (Puu Poa Point) flows into the bay rather than simply across the mouth. During periods of southerly winds, "Kona weather," most longshore currents slackened due to the loss of significant wind and wave energy. The notable exception to this was along the western beaches where longshore currents reverse direction and the stream-mouth sand spits of the Waikoko Stream and Waipa River migrate to the southeast instead of the usual northwest. Observations of sand bedforms throughout the bay show that summer tradewinds produce limited benthic currents. Small amplitude (2-5 cm), symmetrical ripples indicated a lack of sustained bottom flow. Winter conditions, with their combination of tradewinds and northerly swell, set up at least two rip current cells in the bay, one near the center of the beach, and the other on the eastern side. There is also frequently a third rip current near the mouth of the Hanalei River under the Hanalei pier. The two dominant rip currents are primarily stationary throughout a winter season, but may migrate several hundred meters between seasons. Velocities in the rip current cells reach several meters per second. These currents and the corresponding winter benthic currents are likely to be the principle causes of significant benthic sediment movement in the bay. Current directions and magnitudes indicated by sediment texture show movement into the bay along the western fringing reef and a general counter-clockwise movement of sediment in the shallower region of the bay. This methodology, described by le Roux (1994), uses mean sediment size, sorting, and skewness from four neighboring sampling sites to calculate a sediment movement trend vector for a centralized fifth sample site. The calculations assume that spatial changes in these parameters are the result of transport processes, that the three grain-size parameters are of equal importance, that sediment transport occurs along wide, unidirectional fronts, and the grain-size parameter gradients are constant between the five sampled stations.

Seismic and Sidescan Surveys

The 4.41 km² Hanalei Bay contains 1.334 km² of reef top and slope surface, including both fringing (1.31 km²) and patch (0.02 km²) reefs. The remaining 3.08 km² is covered with unconsolidated carbonate sand of variable texture and composition. Sub-bottom seismic reflection (Figure 2.15) records indicate that sand thickness varies from 4.7 m near King's Reef to 34.0 m along the eastern fringing reef (Figure 2.16). In the bay, the depth of the basal reflector below modern sea level reaches a maximum of 49.1 m next to King's Reef (Figure 2.17). In the center of the bay, the basal surface reveals a depression with a depth of nearly 41 m and what appears to be a buried valley with its axial trace exiting the bay to the northeast. Although this reflector was not cored and its composition is unknown, there are four likely possibilities: basalt basement, paleoreef (lithified carbonate) structure, a paleosol layer, or a different density in a layer of carbonate sand. It is assumed that the stratigraphic column above this reflector is marine carbonate sand, and that the reflector is predominantly one of the first three composition possibilities. This is consistent with observations that seismic lines crossing exposed paleoreef surfaces (e.g. King's Reef) show lateral continuity and contiguity between the basal reflector and exposed paleoreef hardground that are possibly middle to late Pleistocene in age (Sherman *et al.*, 1999). In this case, the entire bay holds $45.5 \pm 1.5 \times 10^6$ m³ of sand using a seismic velocity of $1,620 \pm 40$ m s⁻¹ (Fu *et al.*, 1999).

If the Bard *et al.* (1990) sea-level curve (Figure 2.18) is used as a proxy for sea-level at Hanalei, post-glacial sea-level rise first transgressed the basal reflector in Hanalei Bay during the period 11.7 to 11.2 kyr (Figure 2.19). By 5.0 kyr, the bay and coastal plain were completely inundated by the sea (Calhoun and Fletcher, 1996), and, assuming constant sediment accumulation rates and bathymetry similar to the modern bay, approximately 26.05×10^6 m³ of sand had accumulated on the bay floor. Between 5.0 kyr

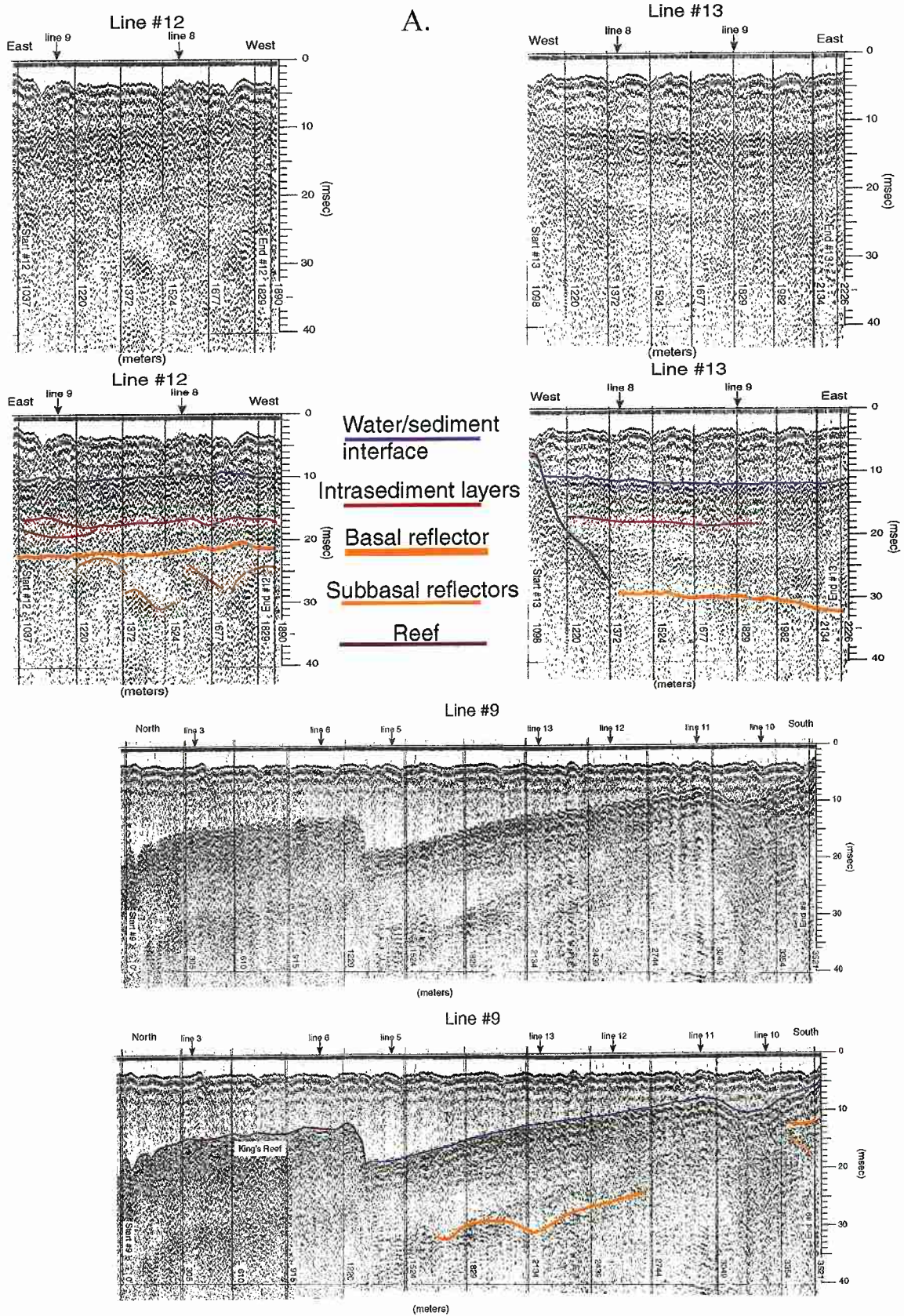


Figure 2.15. Selected seismic profiles (A) and survey track lines (B).

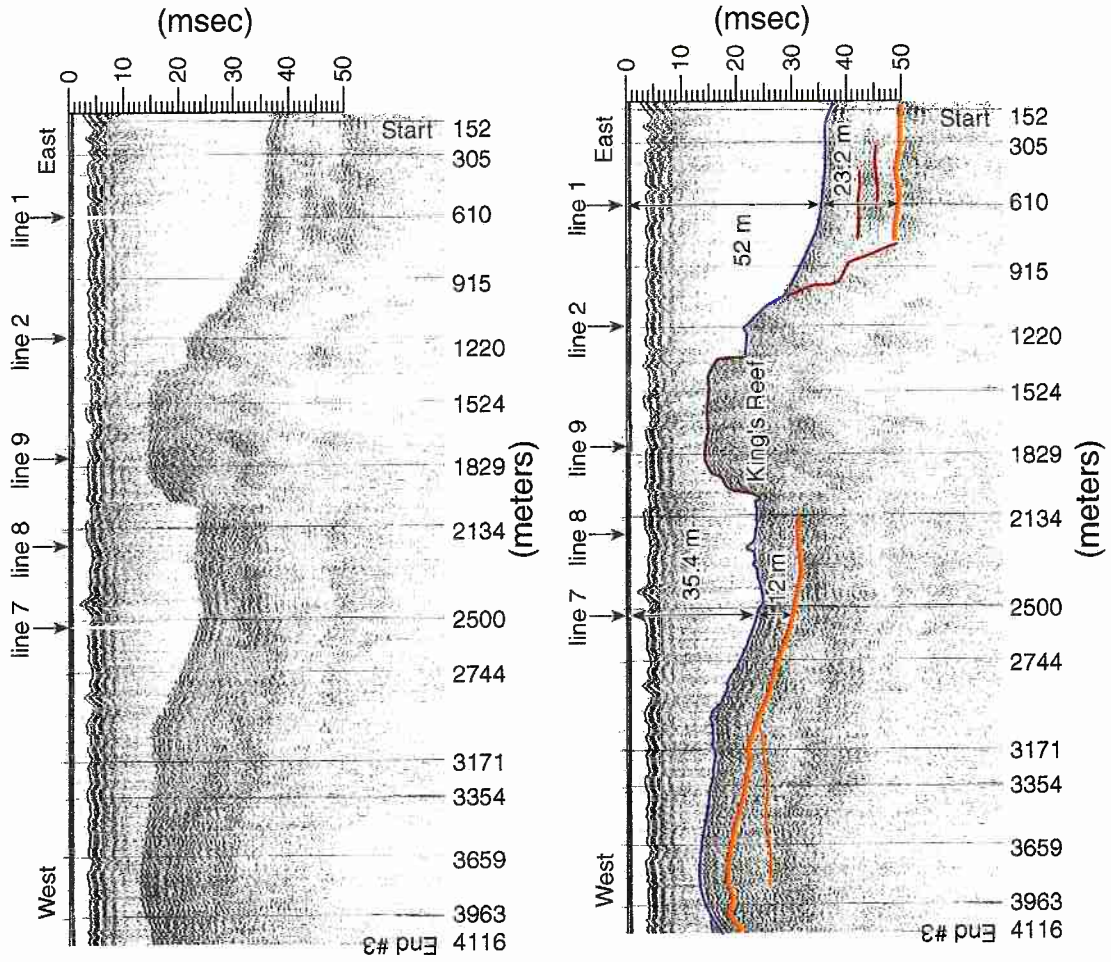


Figure 2.15A. Continued. Seismic profile 3 with examples of water depth and sediment thicknesses shown. Seismic velocity in the water column was $1,500 \text{ m s}^{-1}$ and $1,620 \pm 40 \text{ m s}^{-1}$ in the sediments (Fu et al., 1999).

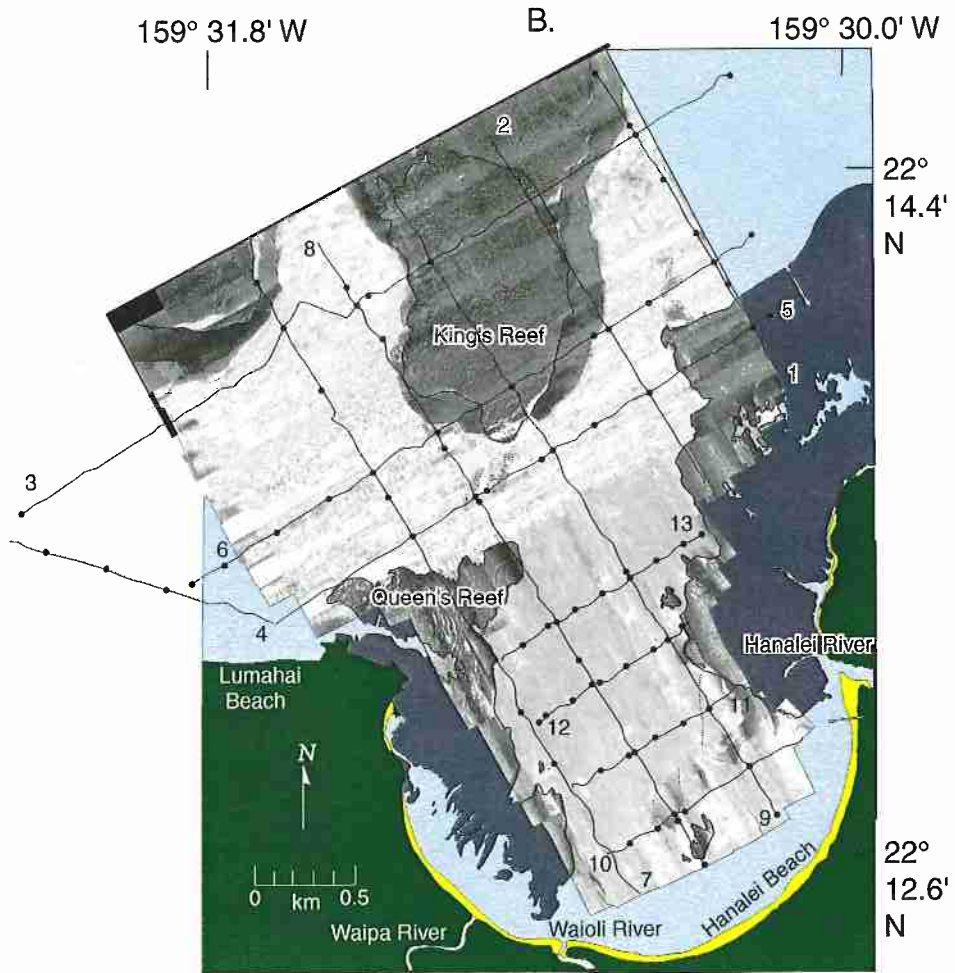


Figure 2.15B. Seismic survey track lines. Lines are labeled at their ends. Black circles show locations where sediment thicknesses were measured.

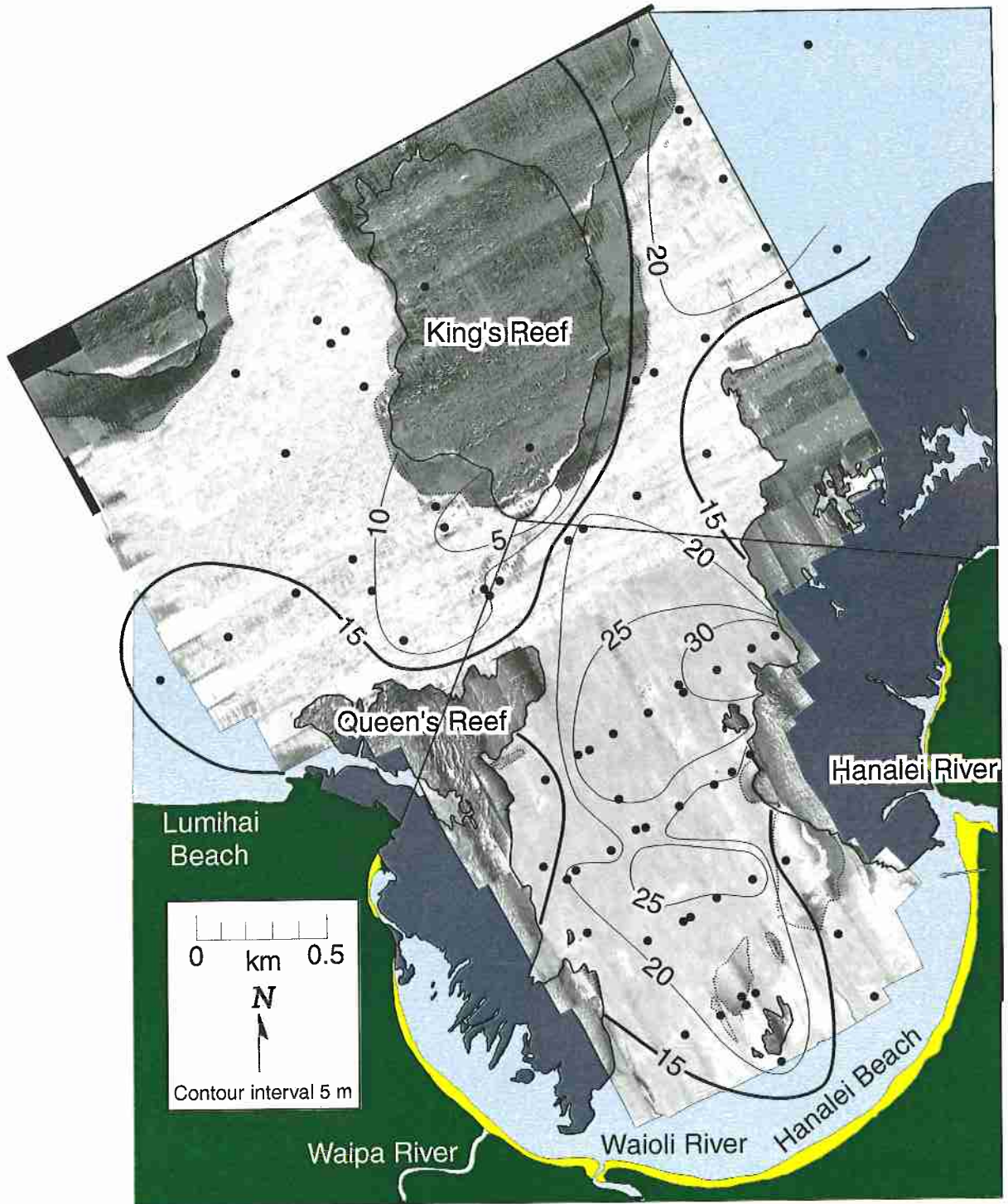


Figure 2.16. Thickness (m) of marine sediment in Hanalei Bay plotted on a sidescan sonar mosaic. Acoustic reflectance shows reefs and rubble as dark and fine sediments (sand) as light gray. • = Location where thickness is measured using seismic profiles.

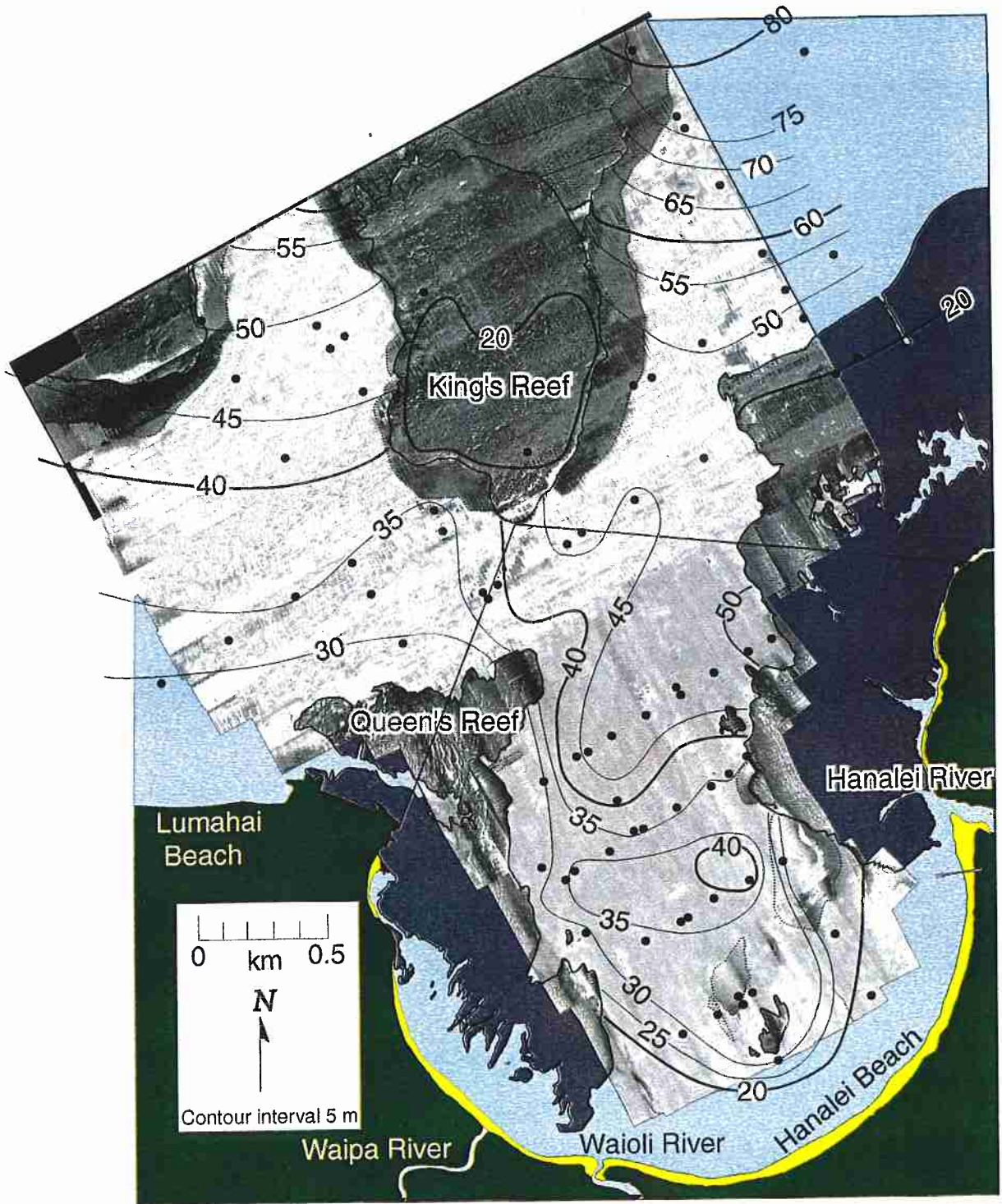


Figure 2.17. Depth (m) below modern sea level to basal reflector in seismic profiles superimposed on a sidescan sonar image of the bay. • = Location where depth was measured from seismic profiles.

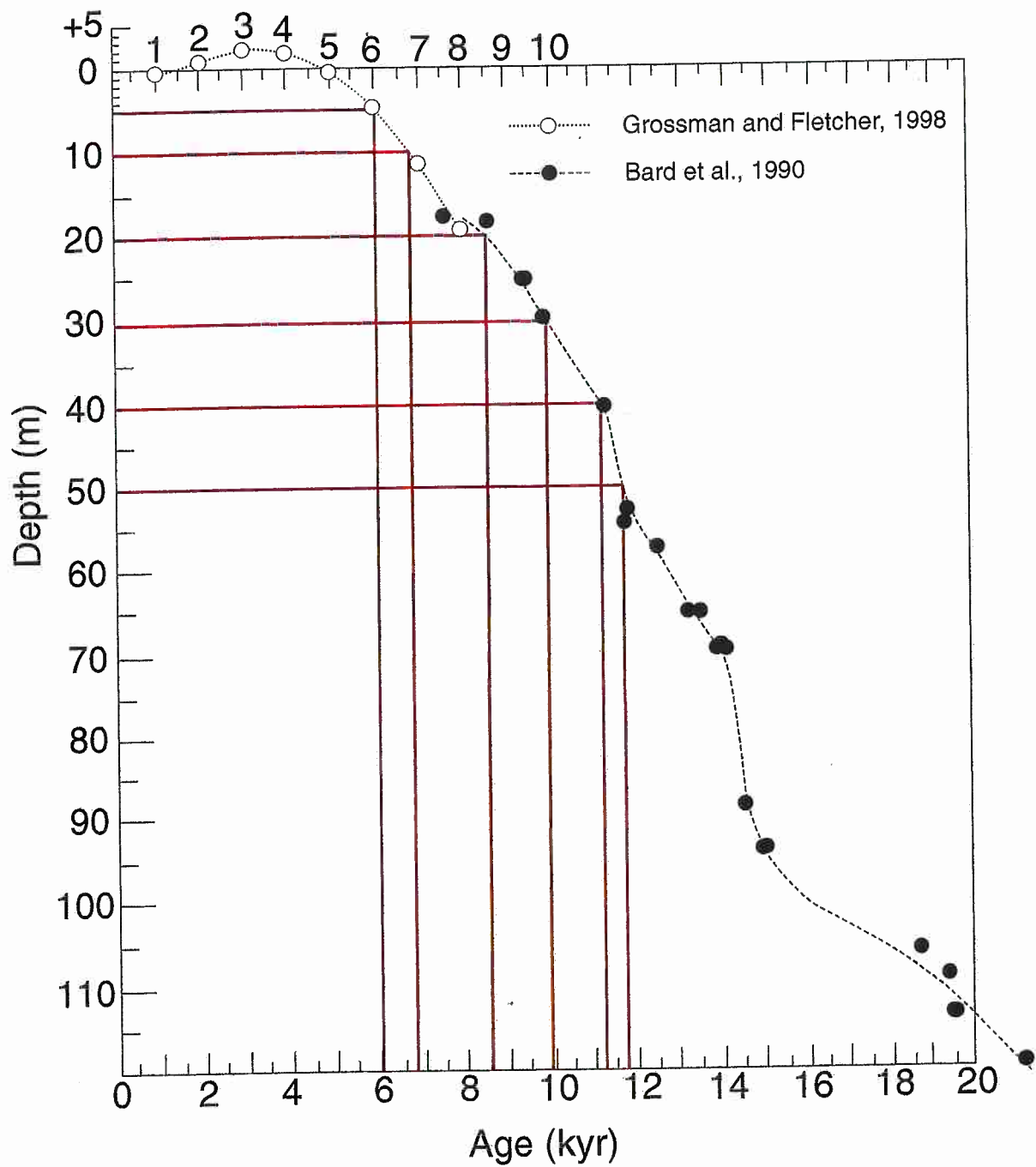


Figure 2.18. Barbados and Hawaii sea-level curves (20 kyr - present)

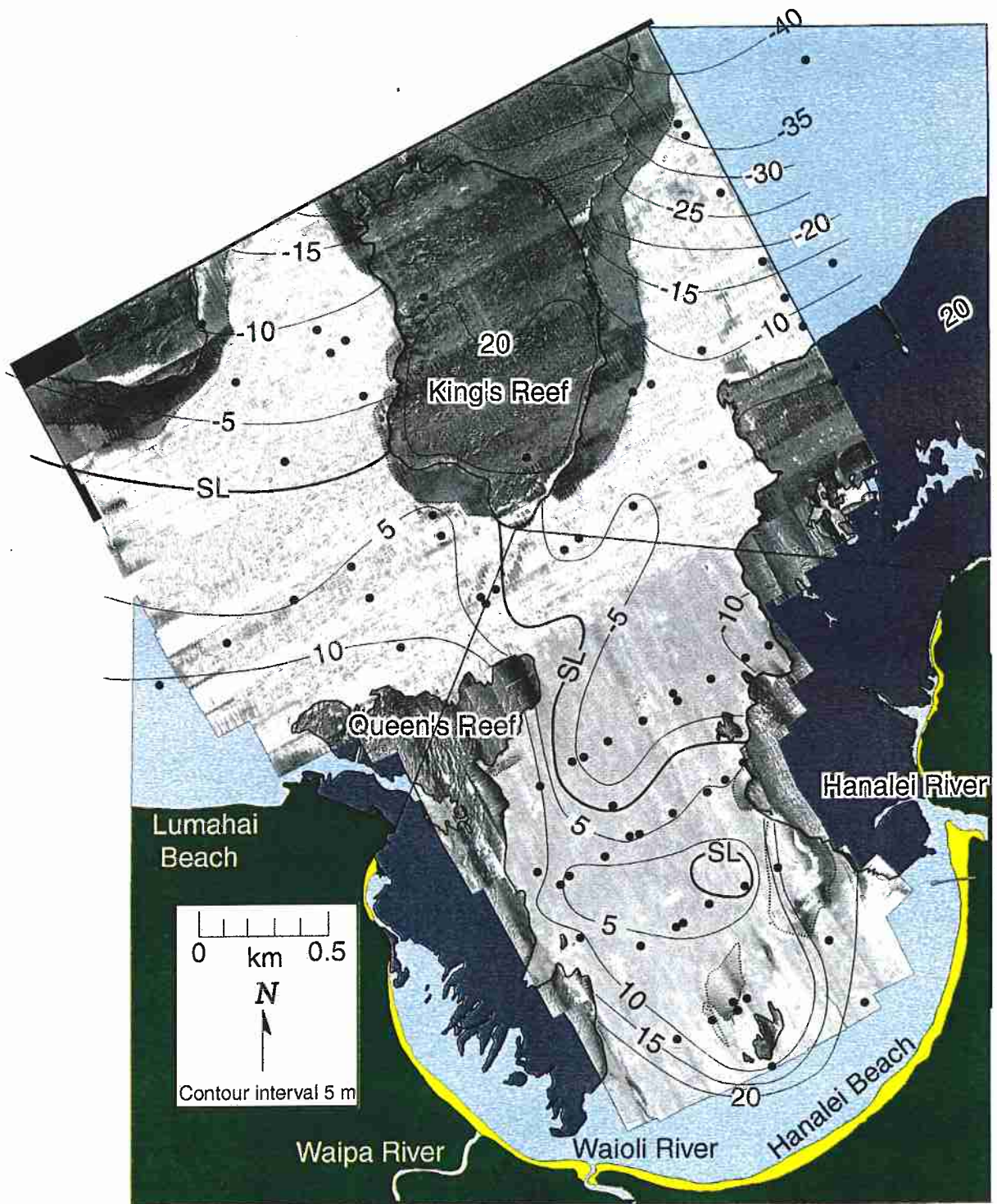


Figure 2.19. Sea level and topography at 11.2 kyr superimposed on a sidescan sonar mosaic of the bay. Sea level is 40 m below present.

and the present, $19.44 \times 10^6 \text{ m}^3$ of sand were deposited in the bay and an additional $33.66 \times 10^6 \text{ m}^3$ on the coastal plain.

Coastal Plain Deposition

From logs of wells drilled in Hanalei in the 1940s, comparisons to findings on the Kailua coastal plain on Oahu (Kraft, 1982), and consistency with marine sedimentation rates found by Calhoun and Fletcher (1996), it is estimated that the average thickness of the marine sediments on the Hanalei coastal plain (an accretional strand plain) to be approximately 6 m. Consequently, 5.61 km^2 of the formerly-inundated coastal plain contains $33.66 \times 10^6 \text{ m}^3$ of marine sand. During the late to middle Holocene regression described by Calhoun and Fletcher (1996), 1.02 km^2 of coastal plain accreted between 4.0 kyr and 3.0 kyr, 3.40 km^2 between 3.0 kyr and 2.0 kyr, and from 2.0 kyr to 1.0 kyr, the final 1.19 km^2 of the present coastal plain were accreted. During these time periods, $11,640,000 \text{ m}^3$, $8,584,000 \text{ m}^3$, and $1,792,000 \text{ m}^3$ of sand were deposited on the coastal plain, respectively, at an average annual rate varying from $11,640$ to $1,790 \text{ m}^3 \text{ yr}^{-1}$. An additional $11,640,000 \text{ m}^3$ were deposited subaqueously between 5.0 and 4.0 kyr (Table 2.4).

Discussion

The distribution of sediment components and textures in Hanalei Bay allows conclusions to be drawn regarding environmental processes and sediment sources effecting the bay. These patterns are identified on contour maps of each characteristic.

A contoured region of relatively low carbonate sand concentration, which includes most of the central bay and reaches out into deeper water, can be traced to the Hanalei River. Composed of sediment with a carbonate content of less than 60%, this region dominates the sedimentology of the entire bay and is caused by an influx of terrigenous

Table 2.4: Marine sediment accumulation in Hanalei Bay and coastal plain system.

Year (kyr)	Cumulative volume in bay (m ³)	Accumulation rate in bay (m ³ yr ⁻¹)	Cumulative volume on coastal plain (m ³)	Accumulation rate on coastal plain (m ³ yr ⁻¹)	Total accumulation rate (m ³ yr ⁻¹) in bay and on coastal plain
11.7	presumed 0	presumed 0	unknown,	unknown,	0
11.2	775,000	1,550	presumed 0	presumed 0	1,550
9.9	5,688,000	3,780	-	-	3,780
8.5	11,344,000	4,040	-	-	4,040
5.0	26,048,000	4,200	-	-	4,200
4.0	29,936,000	3,890	11,640,000	11,640	15,530
3.0	33,824,000	3,890	23,280,000	11,640	15,530
2.0	37,712,000	3,890	31,860,000	8,580	12,470
1.0	41,600,000	3,890	33,660,000	1,790	5,680
Present	45,488,000	3,890	33,660,000	0	3,890

sand and mud originating from the Hanalei River. This interpretation is reinforced by the appearance of a similar pattern when high concentrations of siliciclastic grains are contoured. The nearshore sediments, with the exception of near the Hanalei River, have carbonate content percentages consistently in the low to mid seventies. This consistency, particularly notable in close proximity to the mouth of the Waioli River, indicates that the Hanalei River is the only significant source of terrestrial sediment in the bay. Localized patches (2-4 m²) of extremely low carbonate concentrations (estimated <20%) are observed on the beach near the Waipa River. Due to the low flow and sluggish energy nature of the Waipa River, these patches appear to be beach placer deposits of basalt fragments and olivine that are the product of preferential carbonate sand erosion.

Areas of high carbonate content sediment (>70%) along both fringing reefs indicate that these reefs are a prime source of carbonate sediment in the bay. An additional source is the deep water outside the bay along the eastern fringing reef. Very high carbonate content sediments (>80%) form a plume here that appears to reflect the transportation of carbonate sediments into the bay.

The distribution of silt and clay in the sediments appears to be fairly simple. Areas of high energy due to currents or breaking waves have low silt and clay percentages (<2%). Waves break all along both fringing reefs creating high turbulence and preventing deposition of fine grains in these areas. Mud content is slightly lower along the eastern reef suggesting slightly higher energy, perhaps due to its orientation relative to the average approach direction of winter swell (320°) (Gerritsen, 1978). This provides more energy to be expended in one location, at the seaward-most reef edge, rather than spread over a larger length of reef front as would occur if the reef front had a more open exposure to the swell.

Hanalei Bay may be inferred to act as a sediment trap or sink for sediments moving west along the north shore of Kauai under the influence of the longshore current produced by the northeast tradewinds. The energy from this longshore current is greatly reduced as

the bathymetry suddenly increases off the fringing reef surface onto the outer bay floor. Any sediment in motion under the influence of this longshore flow from the east will likely be deposited near the base of the reef slope. High wave energy probably also accounts for the lack of mud in the shallow portions of the bay (<12 m). Even relatively small tradewind waves provide sufficient energy to maintain silt and clay in suspension where the water is shallow. As the bay deepens, the benthic wave energy drops, and mud content of the sediments begins to increase. Most samples reflect summer season (tradewind) energy regimes. It may be inferred that during the winter, when wave energy is high, mud content decreases.

The major exception to this pattern of mud distribution is the Black Hole. The mud content here is the highest in the bay (12%) and, from surface observations as well as conversations with local boaters, is present throughout the year. The Black Hole is in a broad, shallowly sloping depression with a maximum depth of approximately 17 m while the surrounding bay reaches approximately 12 m. This deepening, and the resulting decrease in benthic wave energy, as well as the depression's protected location shoreward from the eastern fringing reef, may cause mud to be retained here while it is being removed from the rest of the bay by large wave events. Additionally, because the depression is located directly off the mouth of the Hanalei River, there is a ready supply of fine sediment.

The distribution of mean sediment size shows patterns similar to the silt and clay percentages. Regions of high wave and current energy display medium to coarse sands and the low energy center of the bay is characterized by very fine sand. A plume of medium to coarse sand appears to extend from the Hanalei River out through the Black Hole. Coarser sediment lies in a thin band along the edges of both fringing reefs and in a broad plain in the nearshore environment. The eastern sediments are slightly coarser (coarser than 2.0 ϕ) than the western sediment (coarser than 2.5 ϕ) indicating higher energy and/or a proximal source of larger grains.

Observations at all benthic sample sites found either small (1-5 cm height) symmetrical straight crested ripples or a planar bed. This suggests that wave energy is responsible for the majority of benthic sediment movement and is therefore more important for the distribution of sediments than currents. Additionally, no areas of hard substrate were found, outside of reef surfaces, which would result in regions swept clean by currents. All reefs are substantially raised above their surrounding unconsolidated sediments and so are not likely to be periodically buried. Living coral and coralline algae is common on these reef crests and would not likely survive prolonged burial. One exception to these observations is in the nearshore environment during high wave events. These waves set up longshore and rip currents that redistribute beach and nearshore sediments and form asymmetrical ripples and dunes, some with wave lengths of several meters. These currents, however, are restricted to the region between the breaker zone and the shoreline, their formation limited to extreme conditions, and they do not appear to exert a significant influence on the remainder of the bay.

Although benthic processes redistribute sediments, the texture and compositional variations still allow patterns to be discerned and processes to be characterized. Coralline algae concentration levels are high near the fringing reefs and a pronounced low concentration area is in the center of the bay indicating that both reefs are sources of coralline algae sediment. Coral concentrations are high along the eastern fringing reef in the same location where total carbonate concentrations show a region of high carbonate concentration sediment entering the bay. Coral concentrations are, however, low along most of the western fringing reef indicating that this reef may not be a source of coral. From this, coral sediment may be inferred to be entering the bay from the east where there is a several kilometer long fringing reef and that the bay itself may not have produced the majority of the coral sediment within it. In a reversed pattern, mollusc fragments generally appear to be concentrated around the reefs except to the northeast where coral sands are

highly concentrated. This suggests that mollusc sediments are being produced in the bay rather than carried into it by the longshore current.

The radiocarbon dates from coral grains are consistent with the primary source of coral sediment being in the northeast corner of the bay and the counterclock-wise rotation of the sediment redistribution in the shallow region of the bay. The oldest sample in the middle of the bay may be at the distal end of the bay gyre with the start at the northeast corner and the southwest corner of the bay in the middle. Coralline algae may show an increase in the age of its grains as shore is approached because it has both fringing reefs as its sources.

Sediment Budget

Calculations of the total sediment volume in Hanalei Bay, based on seismic reflection, sidescan sonar, and aerial photography, indicate that the bay holds approximately $45.5 \pm 1.5 \times 10^6 \text{ m}^3$ of unconsolidated sediment. Hard reef structure, which is the most likely modern habitat source for marine carbonate sediment production, measures $1.334 \times 10^6 \text{ m}^2$. This reef surface has been submerged, and therefore productive, for only the past 5.0 kyr (Calhoun and Fletcher, 1996), although there may have been other reef surfaces in Hanalei Bay producing carbonate sediments during Holocene (Jones, 1992). The 70% of the sediment that is carbonate and has been deposited in the bay or on the coastal plain equals $31.248 \times 10^6 \text{ m}^3$ of calcium carbonate (with measured 44% porosity). Based on extrapolations to Hanalei Bay from other studies (Hallock, 1981; Agegian, 1985; Hubbard *et al.*, 1990; Harney and Fletcher, 1999), total carbonate sediment production supported by the reef substrate within Hanalei Bay is estimated to total $2.148 \pm 1.674 \times 10^6 \text{ m}^3$ during the past 5.0 kyr (Table 2.5). As a result, there appears to be an excess of carbonate sand stored in the Hanalei Bay and coastal plain system compared to the volume likely produced within its boundaries over the available

Table 2.5: Calcium carbonate sediment production rates. See Appendix B for step-by-step calculations.

Authors	Rate based on	CaCO ₃ production rates (m.yr ⁻¹)	Location	CaCO ₃ production rate (m ³ yr ⁻¹) extrapolated to Hanalei Bay	CaCO ₃ sediment production rate (m ³ yr ⁻¹) extrapolated to Hanalei Bay	Excess CaCO ₃ entering bay (m ³ yr ⁻¹)
Hallock, 1981	foraminifera	0.00005	Oahu, Hawaii	770±211	770±211	3,420±211
Agegian, 1985	coralline algae	0.00033	Oahu, Hawaii	1,590±211	390±52	3,800±212
Hubbard et al., 1990	reef wide	0.00085	St. Croix	1,130±214	280±53	3,910±215
Hubbard et al., 1990	coral	0.00065	St. Croix	3,600±214	890±53	3,300±214
Hubbard et al., 1990	coralline algae	0.00003	St. Croix	140±211	35±52	4,160±212
Harney and Fletcher, 1999	total carbonate	0.000614	Oahu, Hawaii	820±214	200±53	3,990±215
				mean: 430±330		mean: 3,760±330

time period. Approximately $5,820 \text{ m}^3 \text{ yr}^{-1}$ excess carbonate has been deposited in the coastal plain and bay during the last 5.0 kyr, and, contrary to Calhoun and Fletcher (1996), it appears likely that this excess has contributed significantly, although not necessarily exclusively, to the progradation of the Hanalei shoreline.

If the Bard *et al.* (1990) and Grossman and Fletcher (1998) sea-level curves are accepted as a proxy for sea-level in Hanalei Bay, the above calculations ignore the fact that marine deposition has been taking place over the 11.7 kyr that the sea has flooded at least part of the bay. Additionally, carbonate sediment production has likely only been occurring at a rate similar to that of today for the past 5.0 kyr after major portions of the fringing reefs submerged. If, however, the sediments in the bay are divided into equal accumulation rate thicknesses and reflect modern bathymetric characteristics, deposition during the late Holocene still outpaces production in the bay. Deposition of marine sediment began slowly ($1,550 \text{ m}^3 \text{ yr}^{-1}$), although this rate may be too low if sea-level did not actually reach into the bay until 11.4 kyr. Accumulation in the bay stabilized at approximately $4,000 \text{ m}^3 \text{ yr}^{-1}$ from 11.2 to 5.0 kyr (Figure 2.20). Because Hanalei Bay has been fully inundated by the sea only since 5.0 kyr (Calhoun and Fletcher, 1996; Fletcher and Jones, 1996; Grossman and Fletcher, 1998), all unconsolidated marine sediments underlying the modern coastal plain have been deposited since then. Between 5.0 and 3.0 kyr, corresponding to the middle Pacific Kapapa Stand of the sea at +1-2 m (Grossman and Fletcher, 1998), marine deposition on the coastal plain and in the bay increased to $15,500 \text{ m}^3 \text{ yr}^{-1}$ before decreasing to slightly under $4,000 \text{ m}^3 \text{ yr}^{-1}$ from 1.0 kyr to the present. This variation in deposition is not simply a function of available area for deposition. The marine sediments found in the bay and on the coastal plain are a similar combination of carbonate grains from marine organisms and siliciclastic grains predominantly terrigenous in origin.

Estimates of excess carbonate sediment entering Hanalei Bay rely heavily on published carbonate production rates. Each published rate (in mm yr^{-1}) was multiplied by

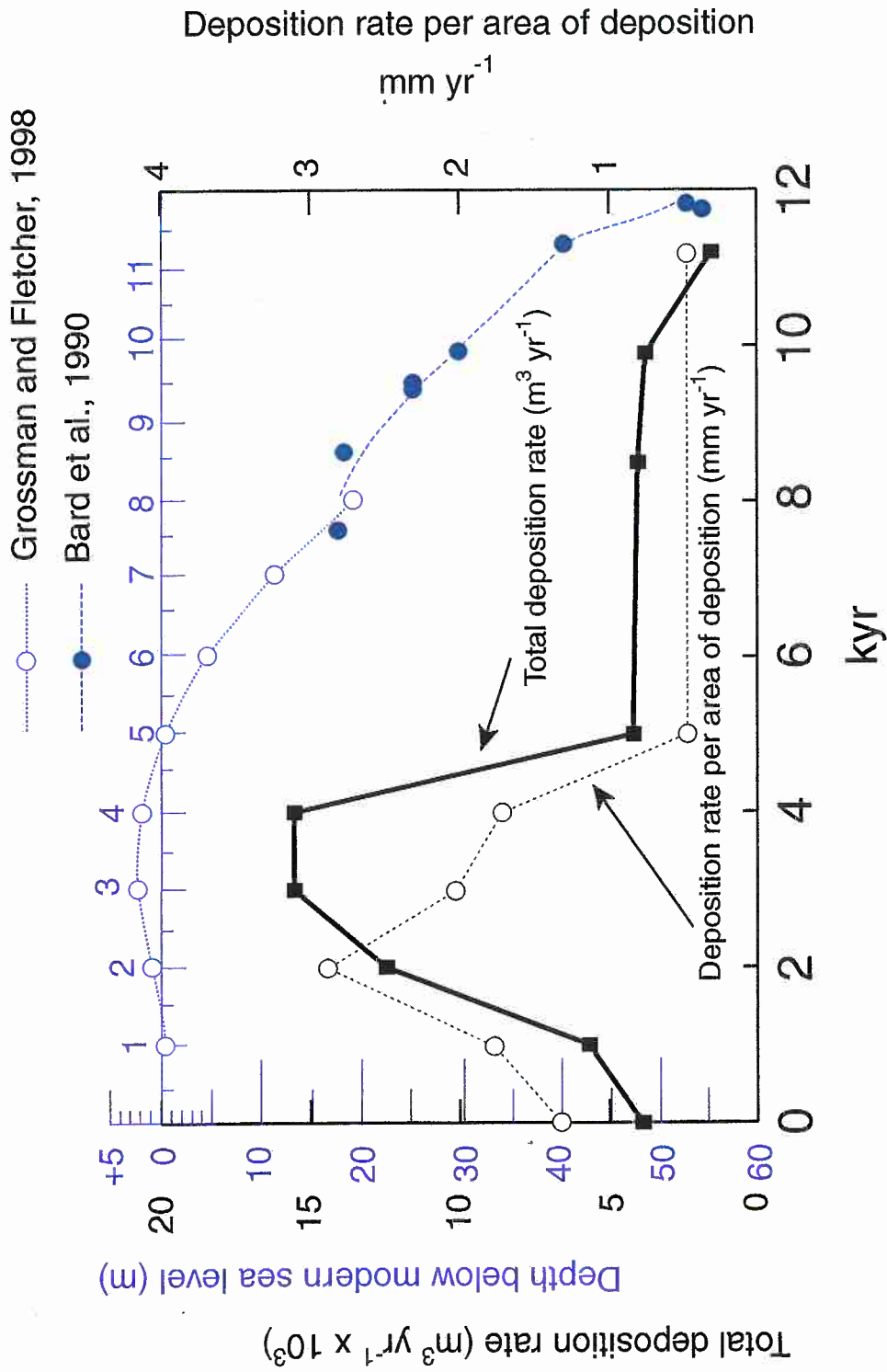


Figure 2.20. Sediment accumulation rate in Hanalei Bay and coastal plain. Grossman and Fletcher (1998) and Bard et al. (1990) sea-level curves are in blue and show the timing of sea-level rise compared to the deposition rate.

the reef surface area in Hanalei ($1.3342 \times 10^6 \text{ m}^3$) to calculate the total carbonate produced in Hanalei. If the published rate was based on a single organism (i.e. only coral), then total carbonate number was divided by the abundance percentage of that organism found in the sediments (17% for coral). If the organism was a reef framework building organism (coral or coralline algae), the total carbonate production was multiplied by 0.248 (the net sediment production expressed as a fraction of total carbonate production) to determine carbonate sediment production (Hubbard *et al.*, 1990). The carbonate sediment production rates using six different methodologies (or rationals) are then subtracted from the average annual volume of stored sediment during the past 5,000 yrs ($4,190 \text{ m}^3$) to infer the excess carbonate sediment entering the bay. The mean calculated excess is approximately $3,760 \pm 330 \text{ m}^3 \text{ yr}^{-1}$.

Because excess carbonate was calculated by the subtracting one measured volume from another and not directly measured, this excess carbonate volume is termed an “unmeasured residual” by Kondolf and Matthews (1991). They warn that, while it is difficult to measure all components of a budget, care must be taken when unmeasured residuals are used, particularly if the residual comprises a large portion of the budget. In the case of Hanalei Bay, 90% of the CaCO_3 is credited to the unmeasured residual or 64% of the total sediment. Errors in measuring the subtrahend and minuend will be transferred to the residual. These hidden errors are difficult to identify without proper accounting of the errors involved with the original measurements.

Hallock (1981) calculated a carbonate production rate of 0.05 mm yr^{-1} using foraminifera from 16 sites on the Hawaiian Island of Oahu. Apparent mortality of individual foraminifera was added over time and then converted to g CaCO_3 using diameter-mass ratios to determine a carbonate production rate. Hubbard *et al.* (1990) calculated three carbonate production rates based on the growth of coral, coralline algae, and all carbonate producers across a reef. Coral production was calculated with x-rayed

coral samples showing annual growth and multiple transects to determine coral abundance and surface area coverage. Due to the lack of coralline algae in reef cores, Hubbard *et al.* (1990) assumed bioerosion of coralline algae was similar to its gross carbonate production. Bioerosion was calculated by multiplying the abundance of coralline algae fragments by the total sediment production. Total sediment production was calculated by dividing gross carbonate production minus carbonate that remains in the reef structure by the abundance of coral fragments found in the sediments. Agegian (1985) measured coralline algae growth by staining specimens and then letting them grow for a given period of time before measuring the subsequent additional growth.

In using these previous studies for the carbonate production rates, several important assumptions are made. First, that the growing conditions for the studied organisms were similar to those found in Hanalei Bay. Second, that the abundance of each component in the Hanalei sediment as a whole has remained close to constant over time. Finally, that it is possible to extrapolate the rate of total carbonate sediment production from an individual component.

The Hanalei River has been calculated to discharge $4,310 \pm 1,810 \text{ m}^3 \text{ yr}^{-1}$ of fluvial suspended sediment (Calhoun and Fletcher, in press). This would result in $50.427 \pm 21.177 \times 10^6 \text{ m}^3 \text{ yr}^{-1}$ discharged over 11,700 years. This far exceeds the approximately $6.939 \pm 0.23 \times 10^6 \text{ m}^3$ of terrigenous sediment found in the modern bay (27% of $45.5 \pm 1.5 \times 10^6 \text{ m}^3$ with 44% porosity). It is also far above the total when $5.135 \pm 1.712 \times 10^6 \text{ m}^3$ of siliciclastic sediments are added from the coastal plain (27% of $33.66 \pm 11.22 \times 10^6 \text{ m}^3$ with 44% porosity). Since the terrigenous component is likely to be significantly higher on the coastal plain due to its juxtaposition to the Hanalei River and its more protected nature, the total terrigenous material on the coastal plain and in the bay may be greater than the apparent $12.074 \pm 1.942 \times 10^6 \text{ m}^3$ calculated. From these calculations however, $15.234 \times 10^6 \text{ m}^3$ to $61.472 \times 10^6 \text{ m}^3$ or $1,300$ to $5,250 \text{ m}^3 \text{ yr}^{-1}$ of terrigenous

sediment are lost from the Hanalei system to the open ocean (Figure 2.21). From point counting of thin-sections data, $590 \text{ m}^3 \text{ yr}^{-1}$ of terrigenous sediment have been deposited in the bay during the past 5,000 years (27% of $10.89 \times 10^6 \text{ m}^3$). Since these data were based on sand-size grains, this figure may be considered to represent bedload discharge from the Hanalei River. Additionally, the silt and clay-size particles represent 2.26% of the sediment in the bay and those that are terrigenous (27%) may be considered suspended sediment from the Hanalei River. This results in only $10 \pm 20 \text{ m}^3 \text{ yr}^{-1}$ of the suspended sediment discharged from the Hanalei River staying in the bay and the remaining $4,300 \pm 1,830 \text{ m}^3 \text{ yr}^{-1}$ of suspended sediment from the Hanalei River being lost to the open ocean.

The increase in beach sediment volume over the six years of data collection appears dramatic. It is, however, difficult to claim that this increase is a significant long-term trend on such a brief temporal scale. It should be noted, however, that the beach volume in Hanalei does appear to be in a stable state. Due to the normal wide seasonal fluctuations in beach volume, at least a part of this short-term stability may be credited to the absence of anthropogenic impacts on the sediment budget. The question of whether this brief period of beach accretion is consistent with long-term shoreline trends must be addressed with the analysis of recent and historical aerial photos (Coyne *et al.*, 1999).

Conclusions

From the characteristics of sediment in Hanalei Bay, it appears that the bay has one significant source of terrigenous material, the Hanalei River, and two significant sources of carbonate sediments, the fringing reefs on either side of the bay and longshore delivery by tradewind driven flow along the coast to the east of Hanalei Bay. These two materials (carbonate:terrigenous) comprise the sediments in Hanalei Bay with an average ratio of 2:1. The nearshore Hanalei marine environment generally has carbonate contents above 70%,

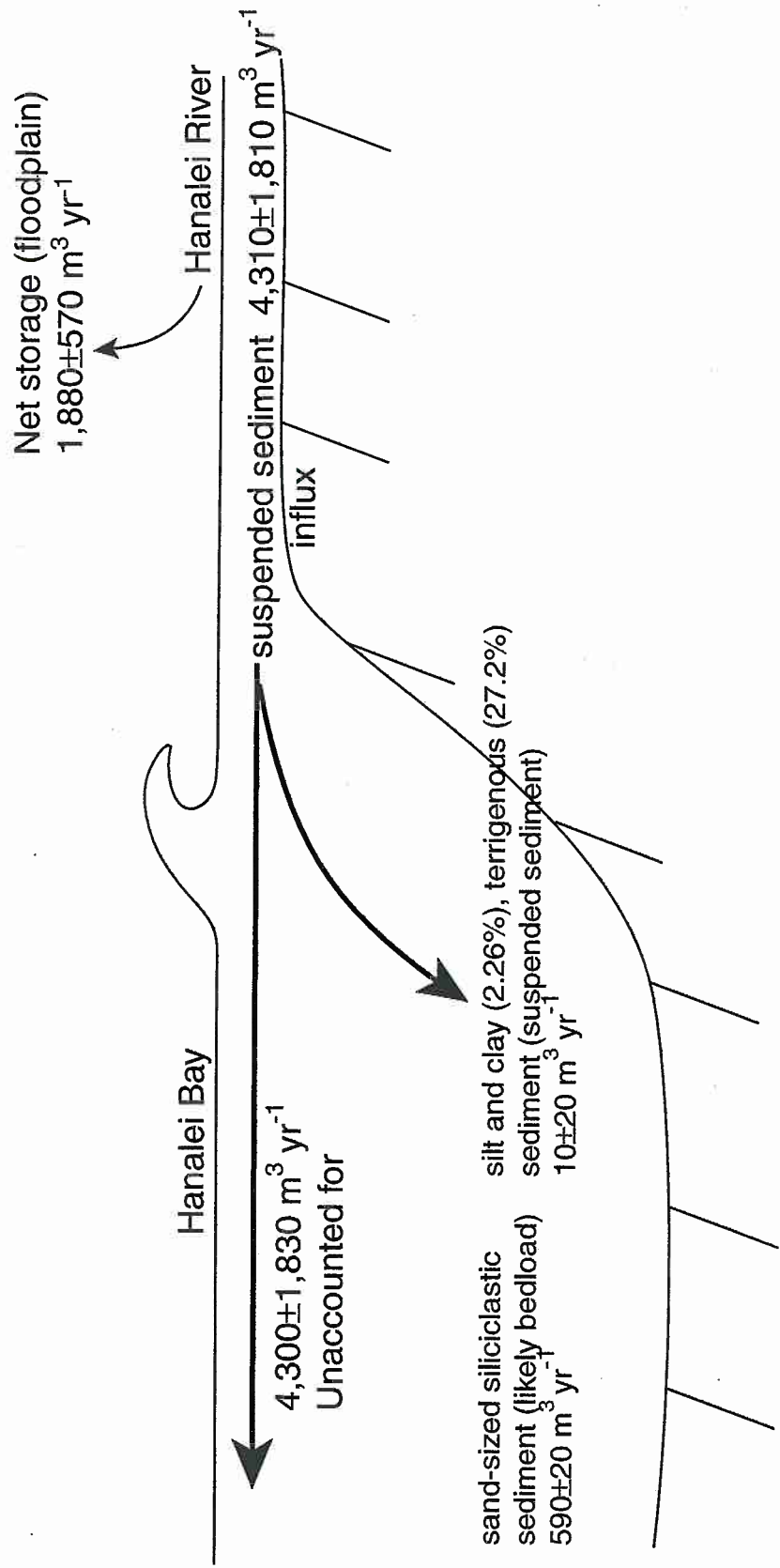


Figure 2.21. Terrigenous sediment budget for Hanalei Bay (5.0 kyr - present).

and offshore environments generally have carbonate percentages below 60%. Specific locations along the beach may vary due to placer deposits resulting from preferential movement of carbonate particles during the higher energy winter swell regime.

Wave stress is a more important source of energy for sediment movement than sustained current flow. The exception to this is in the surf zone during the winter high-wave environment. During these times, longshore and rip currents are set up and transport sediments from the beach face to the nearshore environment.

The inundation of Hanalei Bay began soon after 11.7 kyr. Marine sediments have been deposited in the bay since then, peaking at $15,500 \text{ m}^3 \text{ yr}^{-1}$ between 5.0 and 3.0 kyr. Sediments presently total $45.5 \pm 1.5 \times 10^6 \text{ m}^3$ in the bay and approximately $33.7 \pm 11.2 \times 10^6 \text{ m}^3$ on the coastal plain. This volume represents more carbonate sediment than can be readily accounted for by inferred rates of local carbonate sediment production. To balance the volume of stored and produced carbonate sediment, since 5.0 kyr, approximately $3,760 \pm 330 \text{ m}^3 \text{ yr}^{-1}$ of carbonate sediment must be brought into Hanalei Bay from the east. This excess sediment has likely been a significant factor in the mid to late Holocene progradation of the Hanalei shoreline.

Conclusions

Systematic observations of the sediments in Hanalei Bay and its environs show that terrigenous and marine sediments are arranged in distinct patterns. The sole significant source of terrigenous sediment, the Hanalei River, discharges $4,310 \pm 1,810 \text{ m}^3 \text{ yr}^{-1}$ of suspended sediment in the bay. An additional $1,880 \pm 570 \text{ m}^3 \text{ yr}^{-1}$ are deposited on the floodplain during overbank events by the river. Due to the nature of the observations, these volumes must be considered minimum values. While these volumes do compare favorably with other denudation studies conducted in Hawaii (Li, 1988; McMurtry *et al.*, 1995), more detailed field measurements must be taken of high discharge events to better define these volumes.

The USLE does not describe the Hanalei watershed adequately enough to be of practical use. This is primarily due to the significant size of the errors involved with calculating the fluvial sediment discharge and the USLE factors in addition to the local importance of such processes as mass movement for which the USLE does not account.

While approximately $590 \pm 20 \text{ m}^3$ of terrigenous sediment are deposited annually in the bay, it comprises only 27% of the sediment in the bay. The remaining the sediments are the skeletal remains of marine organisms (coralline algae, coral, diagenetic grains, mollusks, foraminifera, *Halimeda*, bryozoa, and echinoderms). The source of all these marine sediments is a principal concern to the management of the bay environment. The carbonate sediments are inferred to be produced on the fringing reefs in the bay at a rate of $420 \pm 330 \text{ m}^3 \text{ yr}^{-1}$. This is not enough to account for the $45.5 \pm 1.5 \times 10^6 \text{ m}^3$ found in the modern bay and presumed deposited since 11.7 kyr when the marine environment first entered Hanalei Bay during the post-glacial maximum sea-level transgression. Since 5.0 kyr when the bay and coastal plain were completely inundated, an additional $33.7 \pm 11.2 \times 10^6 \text{ m}^3$ have been deposited on the coastal plain. To balance the volume of stored sediment and the volume of carbonate sediment produced locally, approximately $3,760 \pm 330 \text{ m}^3$ are

inferred to be transported into the bay annually from the east by the tradewind induced longshore current. This additional sediment has likely been a significant factor in the mid to late Holocene progradation of the Hanalei shoreline. Figure 2.22 is a summary of the processes significant to the sediment budget of Hanalei Bay with particular emphasis on 5.0 kyr to present.

Improved management practices may be implemented based on the these conclusions concerning the most significant sedimentary processes in Hanalei Bay. From this new understanding, future research may include investigation of CaCO_3 production within the bay, cores through the sediments in the bay to determine the exact nature of the basal reflector observed in the seismic profiles, and a geophysical survey, possibly including ground-penetrating radar, to search for additional buried paleoreefs under the modern coastal plain.

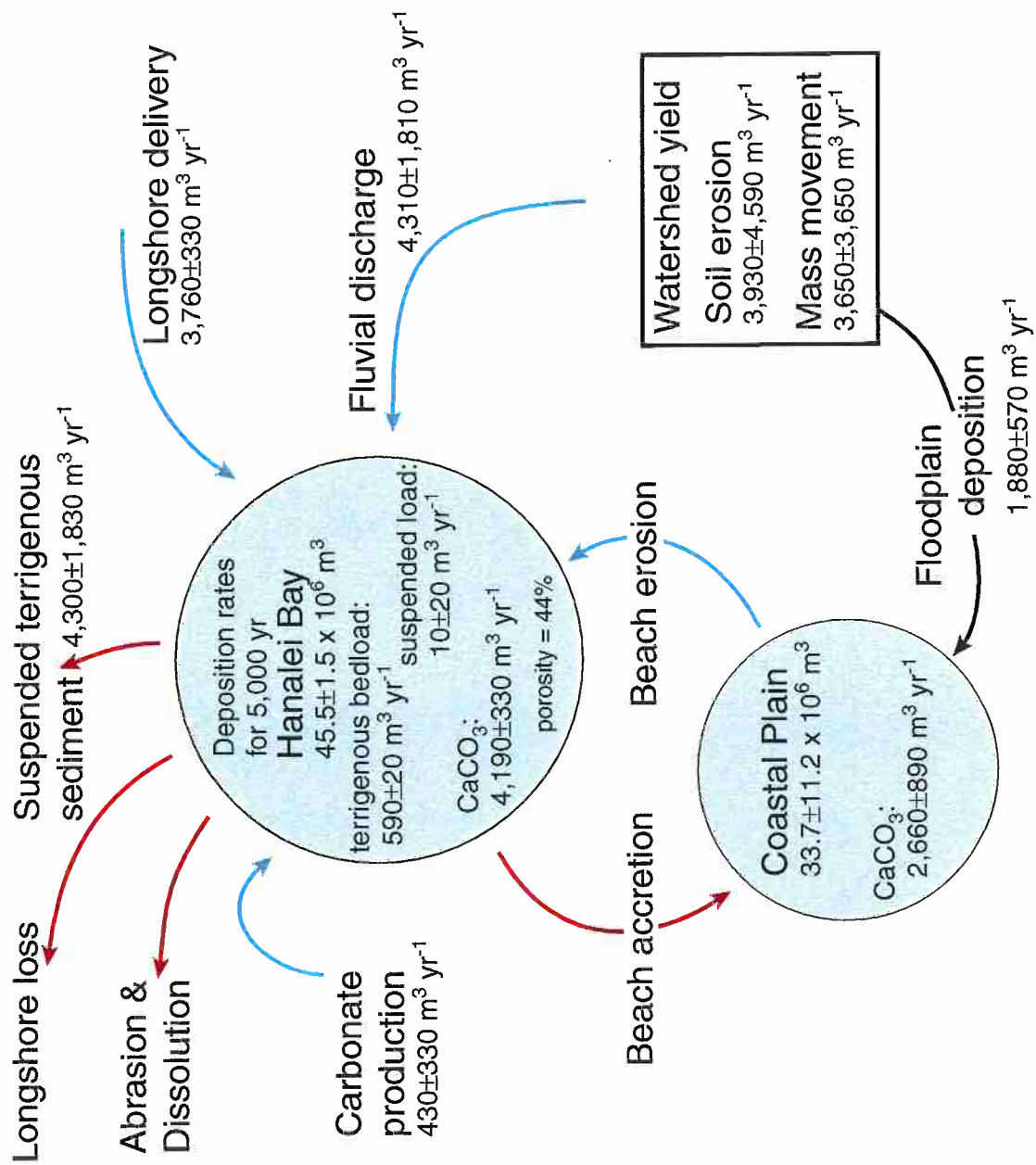


Figure 2.22. The processes and volumes significant to the sediment budget of Hanalei Bay are shown with particular emphasis on 5.0 kyr to present. Blue arrows are gains to the budget and red arrows are losses.

Appendix A. Percentages of sediment components from thin-section point counts.

Sample #											Chemically- altered
	Coralline algae	Coral	Mollusc	Foraminifera	Echiderm	Halimeda	Siliciclastic	Unknown			
4	17.00	16.00	9.67	6.33	1.67	2.33	30.00	0.33	13.67		
5	18.00	10.33	15.33	5.67	2.67	5.00	24.33	1.33	11.00		
7	22.00	10.00	14.33	5.33	1.00	3.33	21.67	0.00	18.00		
8	22.67	23.00	10.00	5.00	2.00	2.00	12.00	2.00	16.67		
10	12.33	17.00	11.33	5.33	0.67	7.67	21.67	2.67	18.67		
11	11.33	26.00	5.67	6.33	0.67	0.00	31.33	8.33	8.67		
16	27.33	35.00	4.67	6.67	2.00	0.00	7.33	7.33	9.67		
19	14.33	14.00	9.00	5.00	0.67	1.33	39.33	1.00	12.33		
20	14.33	19.67	10.67	8.00	0.67	2.33	29.67	0.33	11.00		
21	12.00	9.00	5.67	3.33	1.67	6.00	58.33	0.00	3.67		
22	12.00	29.33	4.33	4.33	1.00	0.00	31.00	9.33	7.67		
25	25.67	23.67	7.00	4.33	2.00	1.00	18.33	4.33	12.00		
26	42.00	6.80	14.80	6.00	2.40	0.40	20.80	0.00	3.20		
27	13.00	15.67	10.33	4.00	0.67	6.00	27.33	1.33	20.00		
28	13.33	15.33	9.00	10.67	0.33	1.67	32.33	1.00	13.67		
34	27.33	28.67	9.00	5.00	3.33	2.00	7.00	1.33	15.00		
36	11.00	13.33	6.67	7.33	0.67	1.00	43.67	0.33	14.67		
39	25.33	13.33	9.67	6.67	1.67	4.00	22.33	2.67	11.00		
40	30.67	3.00	13.33	12.00	2.33	3.67	16.67	1.33	13.33		
50	17.67	10.00	2.67	5.00	0.33	0.33	49.67	1.33	12.67		

Siliciclastic components from Waioli Beach Park beach surface sample (#50):

olivine	50.34	lithic	42.95	altered lithics	2.68	clinopyroxene	0.67	plagioclase	0.67
---------	-------	--------	-------	-----------------	------	---------------	------	-------------	------

Appendix B. Calcium carbonate production rate calculations.

Part 1: Calculation of excess CaCO₃ sediment in bay.

Authors, producing organism

that rates are based on:

	A	B	=	C	D	÷	E	=	F	G	=	H	I
Hallock, 1981 foraminifera	0.05	÷ 1000	=	0.00005	• 1,334,200	÷	0.0865	=	770±211	• 1	=	770±211	3,420±211
Agegian, 1985 coralline algae	0.33	÷ 1000	=	0.00033	• 1,334,200	÷	0.277	=	1,590±211	• 0.248	=	390±52	3,800±212
Hubbard et al., 1990 all carbonate producers	0.85	÷ 1000	=	0.00085	• 1,334,200	÷	1	=	1,130±214	• 0.248	=	280±53	3,910±215
Hubbard et al., 1990 coral	0.65	÷ 1000	=	0.00065	• 1,334,200	÷	0.241	=	3,600±214	• 0.248	=	890±53	3,300±214
Hubbard et al., 1990 coralline algae	0.03	÷ 1000	=	0.00003	• 1,334,200	÷	0.277	=	140±211	• 0.248	=	35±52	4,160±212
Harney and Fletcher, 1999 all carbonate producers	0.614	÷ 1000	=	0.000614	• 1,334,200	÷	1	=	820±215	• 0.248	=	200±53	3,990±215
												means:	430±330 3,760±330

A = CaCO₃ production rates (mm yr⁻¹) from source

B = conversion from mm yr⁻¹ to m yr⁻¹

C = CaCO₃ production rates (m yr⁻¹)

D = surface area of reef in Hanalei Bay (m²)

E = percentage of carbonate sediment composed of producing organism in Hanalei Bay

F = CaCO₃ production rate (m³ yr⁻¹) extrapolated to Hanalei Bay

G = percent of carbonate produced that becomes sediment (used only when coral or coralline algae is producer)

H = CaCO₃ sediment production rate extrapolated (m³ yr⁻¹) to Hanalei Bay

I = volume of CaCO₃ sediment deposited in bay (m³ yr⁻¹) greater than volume expected from local source; calculated by 4,190 (m³ yr⁻¹) - H

Appendix B. Part 2. Calculation of calcium carbonate deposition rate in Hanalei system during last 5,000 yrs ($4,190 \text{ m}^3 \text{ yr}^{-1}$).

$$\frac{\text{J}}{19.44 \times 10^6 \cdot 0.705 \cdot 0.56} = \frac{\text{K}}{7.675 \times 10^6} + \frac{\text{L}}{(33.66 \times 10^6 \cdot 0.705 \cdot 0.56)} + \frac{\text{M}}{20.96 \times 10^6} + \frac{\text{N}}{13.289 \times 10^6} + \frac{\text{O}}{5,000} + \frac{\text{P}}{5,000} + \frac{\text{Q}}{5,000} + \frac{\text{R}}{5,000} + \frac{\text{S}}{5,000} + \frac{\text{T}}{5,000}$$

J = volume of sediment (m^3) estimated to have been deposited within the area of modern Hanalei Bay assuming a constant rate of deposition and bathymetry similar to the modern bay

K = percentage of CaCO_3 grains in the sediments of Hanalei Bay

L = percentage of sediment volume that is sediment with porosity of 44%

M = mass of CaCO_3 sediment (m^3) estimated to be in modern Hanalei Bay and deposited between 5.0 kyr and present

N = volume of marine sediment (m^3) estimated to be under modern Hanalei coastal plain

O = percentage of CaCO_3 grains in the sediments under Hanalei coastal plain assuming similar percentage to the modern bay

P = percentage of sediment volume that is sediment with porosity of 44% assuming similar porosity to the modern bay

Q = mass of CaCO_3 sediment (m^3) estimated to be under modern Hanalei coastal plain and deposited between 5.0 kyr and present

R = mass of CaCO_3 sediment (m^3) estimated in Hanalei system (bay and coastal plain) and deposited between 5.0 kyr and present

S = years of deposition

T = mass of deposition of CaCO_3 per year in Hanalei system ($\text{m}^3 \text{ yr}^{-1}$)

References

- Aegean, C.R. 1985. The biogeochemical ecology of *Porolithon gardineri* (Foslie). Ph.D. Dissertation, University of Hawaii, Honolulu, HI, 178 pp.
- Bard, E., B. Hamelin, R.G. Fairbanks, and A. Zindler. 1990. Calibration of the ^{14}C timescale over the past 30,000 years using mass spectrometric U-Th ages From Barbados corals. *Nature*, 345, 405-410.
- Best, T.C. and G.B. Griggs. 1991. A sediment budget for the Santa Cruz littoral cell, California. In: From Shoreline to Abyss, R. Osborne (Ed.), SEPM Special Publication No. 46, 35-50.
- Bhowmik, N.G. and M. Demissie. 1989. Sedimentation in the Illinois River Valley and backwater lakes. *Journal of Hydrology*, 105, 187-195.
- Blum, M.D. and S. Valastro, Jr. 1994. Late Quaternary sedimentation, lower Colorado River Gulf Coastal Plain of Texas. *G.S.A. Bulletin*, 106, 1002-1016.
- Bodge, K.R. and S.P. Sullivan. 1999. Hawaii pilot beach restoration project: Coastal engineering investigation. Prepared for State of Hawaii, Department of Land and Natural Resources.
- Boggs, S. Jr. 1995. Principles of Sedimentology and Stratigraphy. Prentice Hall, Upper Saddle River, New Jersey, 774 pp.
- Calhoun, R.S. and C.H. Fletcher. 1996. Late Holocene coastal plain stratigraphy and sea-level history at Hanalei, Kauai, Hawaiian Islands. *Quaternary Research*, 45, 47-58.
- Calhoun, R.S. and C.H. Fletcher. in press. Measured and predicted sediment yield from a subtropical, heavy rainfall, steep-sided river basin: Hanalei, Kauai, Hawaiian Islands. *Geomorphology*.
- Clarkin, K.L., M.D. Harvey, A. Elkin, S.C. McIntyre. 1986. Sediment storage and delivery - eastern Colorado. Proceedings of the 4th Federal Interagency Sedimentation Conference, Las Vegas, Nevada, Volume 1, 3-54 - 3-63.
- Cooley, K.R. and J.R. Williams. 1985. Applicability of the universal soil loss equation (USLE) and the modified USLE to Hawaii. In: S.A. El-Swaify, W.C. Moldenhauer, and A. Lo (Editors), International Conference on Soil Erosion and Conservation, "Malama Aina 83". University of Hawaii, Dept of Agron. and Soil Science, Honolulu, HI, Soil Conservation Society of America, Ankeny, IA, 509-522.
- Coyne, M.A., C.H. Fletcher, and B.M. Richmond. 1999. Mapping coastal erosion hazard areas in Hawaii: Observations and errors. *Journal of Coastal Research, Special Issue #28*, 171-184.
- Cundy, A.B. and I.W. Croudace. 1995. Sedimentary and geochemical variations in a salt marsh/mud flat environment from the mesotidal Hamble estuary, southern England. *Marine Chemistry*, 51, 115-132.

- Dean, R.G. 1988. Managing sand and preserving shorelines. *Oceanus*, 31, 49-55.
- Desloges, J.R. and R. Gilbert. 1994. Sediment source and hydroclimatic inferences from glacial lake sediments: The postglacial sedimentary record of Lillooet Lake, British Columbia. *Journal of Hydrology*, 159, 375-393.
- Dissmeyer, G.E. and G.R. Foster. 1980. A guide for predicting sheet and rill erosion on forest land. United States Department of Agriculture Technical Publication SA-TP 11, Atlanta, GA, 40 pp.
- Dissmeyer, G.E. and G.R. Foster. 1981. Estimating the cover-management factor (C) in the universal soil loss equation for forest conditions. *Journal of Soil and Water Conservation*, 36, 235-240.
- Ellen, S.D., R.K. Mark, S.H. Cannon, and D.L. Knifong. 1993. Map of debris-flow hazard in the Honolulu District of Oahu, Hawaii. US Geological Survey, Open-File Report 93-213, 25 pp.
- Ellison, J.C. 1994. Paleo-lake and swamp stratigraphic records of Holocene vegetation and sea-level changes, Mangaia, Cook Islands. *Pacific Science*, 48, 1-15.
- Engleman, E.E., L.L. Jackson, and D.R. Norton. 1985. Determination of carbonate carbon in geological materials by coulometric titration. *Chemical Geology*, 53, 125-128.
- Fletcher, C.H. and A.T. Jones. 1996. Sea-level highstand recorded in Holocene shoreline deposits on Oahu, Hawaii. *Journal of Sedimentary Research*, 66, 632-641.
- Fletcher, C.H., R.A. Mullane, and B.M. Richmond. 1997. Beach loss along armored shorelines on Oahu, Hawaiian Islands. *Journal of Coastal Research*, 13, 209-215.
- Folk, R.L. 1974. Petrology of Sedimentary Rocks. Hemphill, Austin, Texas, 182 pp.
- Foster, G.R. and W.H. Wischmeier. 1974. Evaluating irregular slopes for soil loss prediction. *Transactions ASAE*, 17, 305-309.
- Friedlander, A.M., R.C. DeFelice, J.D. Parrish, and J.L. Frederick. 1997. Habitat Resources and Recreational Fish Population at Hanalei Bay, Kauai. Final Report to State of Hawaii, Department of Land and Natural Resources, Division of Aquatic Resources, 320 pp.
- Frihy, O.E., A.M. Fanos, A.A. Khafagy, and P.D. Komar. 1991. Patterns of nearshore sediment transport along the Nile Delta, Egypt. *Coastal Engineering*, 15, 409-429.
- Fu, S.S., M. Prasad, R.H. Wilkens, and L.N. Frazer. in press. Hamilton parameters and acoustic properties for carbonate sands, Waikiki, Hawaii. *Journal of the American Acoustic Society*.

- Gerritsen, F. 1978. Beach and Surf Parameters in Hawaii. Sea Grant Technical Report: UNIHI-SEAGRANT-TR-78-02, pp.178.
- Glenn, C.R., S. Rajan, G.H. McMurtry, and J. Benaman. 1995. Geochemistry, mineralogy, and stable isotopic results from Ala Wai estuarine sediments: Records of hypereutrophication and abiotic whittings. *Pacific Science*, 49, 367-399.
- Goodfriend, G.A. and D.J. Stanley. 1996. Reworking and discontinuities in Holocene sedimentation in the Nile delta: documentation from amino acid racemization and stable isotopes in mollusk shells. *Marine Geology*, 129, 271-283.
- Grossman, E.E. and C.H. Fletcher. 1998. Sea level higher than present 3500 years ago on the northern main Hawaiian Islands. *Geology*, 26, 363-366.
- Hallock, P. 1981. Production of carbonate sediments by selected large benthic foraminifera on two Pacific coral reefs. *Journal of Sedimentary Petrology*, 51, 467-474.
- Harney, J.N. and C.H. Fletcher. 1999. Understanding the carbonate factory: A comprehensive, high-resolution, sediment budget for a windward Pacific reef, Kailua Bay, Oahu, Hawaiian Islands. unpublished manuscript.
- Hill, B.R., C.C. Fuller, and E.H. DeCarlo. 1997. Hillslope soil erosion estimated from aerosol concentrations, North Halawa Valley, Oahu, Hawaii. *Geomorphology*, 20, 67-79.
- Hubbard, D.K., A.I. Miller, and D. Scaturro. 1990. Production and cycling of calcium carbonate in a shelf-edge reef system (St. Croix, U.S. Virgin Islands): Applications to the nature of reef systems in the fossil record. *Journal of Sedimentary Petrology*, 60, 335-360.
- Inman, D.L. and R. Dolan. 1989. The outer banks of North Carolina: Budget of sediment and inlet dynamics along a migrating barrier system. *Journal of Coastal Research*, 5, 193-237.
- Inman, D.L., W.R. Gayman, and D.C. Cox. 1963. Littoral sedimentary processes on Kauai, a subtropical high island. *Pacific Science*, 17, 106-130.
- Jones, A.T. 1992. Holocene coral reef on Kauai, Hawaii: Evidence for a sea-level highstand in the central Pacific. In: Quaternary Coasts of the United States: Marine and Lacustrine Systems, C.H. Fletcher and J.F. Wehmiller (Eds.), SEPM Special Publication No. 48, p 267-271. SEPM, Tulsa.
- Jones, B.L., S.S.W. Chinn, and J.C. Brice. 1984. Olokele rock avalanche, island of Kauai, Hawaii. *Geology*, 12, 209-211.
- Juvik, S. and J. Juvik (Eds.). 1998. Atlas of Hawaii, third edition. University of Hawaii Press, Honolulu, 333 pp.

- Kana, T.W. 1995. A mesoscale sediment budget for Long Island, New York. *Marine Geology*, 126, 87-110.
- Kodama, K.R. and S. Businger. 1998. A brief overview of weather and forecasting in the Pacific Region of the National Weather Service. *Weather and Forecasting*, 13, 523-546.
- Komar, P.D. 1996. The budget of littoral sediments - Concepts and application. *Shore and Beach*, 64, 18-26.
- Komar, P.D. 1998. Beach Processes and Sedimentation. Prentice Hall, Upper Saddle River, New Jersey, 544 pp.
- Kondolf, G.M. and W.V.G. Matthews. 1991. Unmeasured residuals in sediment budgets: A cautionary note. *Water Resources Research*, 27, 2483-2486.
- Kraft, J.C. 1982. Terrigenous and carbonate clastic facies in a transgressive sequence over volcanic terrain. *AAPG Bulletin*, 66, 589.
- Krumbein, W.C. and F.J. Pettijohn. 1938. *Manual of Sedimentary Petrology*. Appleton-Century Crofts, New York, pp. 549.
- Larcombe, P. and C.F. Jago. 1994. The late Devensian and Holocene evolution of Barmouth Bay, Wales. *Sedimentary Geology*, 89, 163-180.
- le Roux, J.P. 1994. An alternative approach to the identification of net sediment transport paths based on grain-size trends. *Sedimentary Geology*, 94, 97-107.
- Li, Y.-H. 1988. Denudation rates of the Hawaiian Islands by rivers and groundwater. *Pacific Science*, 42, 253-266.
- Lo, A., S.A. El-Swaify, E.W. Dangler, and L. Shinshiro. 1985. Effectiveness of EI₃₀ as an erosivity index in Hawaii. In: S.A. El-Swaify, W.C. Moldenhauer, and A. Lo (Editors), *International Conference on Soil Erosion and Conservation, "Malama Aina 83"*. University of Hawaii, Dept of Agron. and Soil Science, Honolulu, HI, Soil Conservation Society of America, Ankeny, IA, 384-392.
- Ly, C.K. 1980. The role of the Akosombo Dam on the Volta River in causing coastal erosion in central and eastern Ghana (West Africa). *Marine Geology*, 37, 323-332.
- Macdonald, G.A., A.T. Abbott, and F.L. Peterson. 1983. Volcanoes in the Sea: The Geology of Hawaii. University of Hawaii Press, Honolulu, 517 pp.
- Macdonald, G.A., D.A. Davis, and D.C. Cox. 1960. Geology and ground-water resources of the island of Kauai, Hawaii. Hawaii Division of Hydrography, Bulletin 13, 212 pp., colored geologic map.

- McMurtry, G.M., A. Snidvongs, and C.R. Glenn. 1995. Modeling sediment accumulation and soil erosion with ^{137}Cs and ^{210}Pb in the Ala Wai Canal and central Honolulu watershed, Hawaii. *Pacific Science*, 49, 412-451.
- Meade, R.H., T.R. Yuzyk, and T.J. Day. 1990. Movement and storage of sediment in rivers of the United States and Canada. In: *The Geology of North America*, vol O-1, Surface Water Hydrology, The Geological Society of America, p. 255-279.
- Moberly, R. Jr. 1963. Rate of denudation in Hawaii. *Journal of Geology*, 71, 371-375.
- Moberly, R. Jr., D. Baver, Jr., and A. Morrison. 1965. Source and variation of Hawaiian littoral sand. *Journal of Sedimentary Petrology*, 35, 3, pp. 589-598.
- Pearson, A., A.P. McNichol, R.J. Schneider, K.F. von Reden, and Y. Zheng. 1998. Microscale AMS ^{14}C measurement at NOSAMS. In: *Proceedings of the 16th International ^{14}C Conference*, W.G. Mook and J. van der Plicht, *Radiocarbon*, 20, p. 0.
- Pederstad, K., E. Roaldset, and T.M. Ronningsland. 1993. Sedimentation and environmental conditions in the inner Skagerrak-outer Oslofjord. *Marine Geology*, 111, 245-268.
- Peterson, C.D., M.E. Darienzo, D.J. Pettit, P.L. Jackson, and C.L. Rosenfeld. 1991. Littoral-cell development in the convergent Cascadia margin of the Pacific Northwest, USA. In: *From Shoreline to Abyss*, R. Osborne (Ed.), SEPM Special Publication No. 46, 17-34.
- Peterson, D.M., S.D. Ellen, and D.L. Knifong. 1993. Distribution of past debris flows and other rapid slope movements from natural hillslopes in the Honolulu District of Oahu, Hawaii. US Geological Survey, Open-File Report 93-514, 32 pp.
- Phillips, J.D. 1991. Fluvial sediment delivery to a coastal plain estuary in the Atlantic drainage of the United States. *Marine Geology*, 98, 121-134.
- Prestegard, K.L. 1988. Morphological controls on sediment delivery pathways. *Sediment Budgets* (Proceedings of the Porto Alegre Symposium). IAHS Publication number 174, 533-540.
- Renard, K.G., J.M. Laflen, G.R. Foster, and D.K. McCool. 1994. The Revised Universal Soil Loss Equation. In: R. Lal (Editor), *Soil Erosion Research Methods*, Soil and Water Conservation Society, St. Lucie Press, Delray Beach, FL., pp 105-124.
- Scott, G.A.J. 1969. Relationships between vegetation and soil avalanching in the high rainfall areas of Oahu, Hawaii. Honolulu, Hawaii, University of Hawaii. M.A. Thesis, 98 pp.

- Scott, G.A.J. and J.M. Street. 1976. The role of chemical weathering in the formation of Hawaiian amphitheatre-headed valleys. *Zeitschrift für Geomorphologie*, 20, 171-189.
- Sea Engineering, Inc. 1996. Sediment transport at Kikiaolo Harbor, island of Kauai, Hawaii. Prepared for U.S. Army Engineer Division, Pacific Ocean Fort Shafter, Hawaii, Contract No. DACW83-94-D-0007, Delivery Order: 0009.
- Shepard, F.P. 1973. Submarine Geology. Harper and Row Publishers, New York.
- Sherman, C.E., C.H. Fletcher, and K.H. Rubin. 1999. Marine and meteoric diagenesis of Pleistocene carbonates from a nearshore submarine terrace, Oahu, Hawaii. *Journal of Sedimentary Research*, 69, 1083-1097.
- Showers, V. 1979. World Facts and Figures. John Wiley and Sons, New York, NY.
- Stearns, H.T. and K.N. Vaksvik. 1935. Geology and ground-water resources of the island of Oahu, Hawaii. Territory of Hawaii, Division of Hydrography, Bulletin 1, 478 pp.
- Stuiver, M. and P.J. Reimer. 1993. Extended ^{14}C data base and revised Calib 3.0 ^{14}C age calibration program. *Radiocarbon*, 35, 215-230.
- Taylor, R.J. 1982. An Introduction to Error Analysis: The Study of Uncertainties in Physical Sciences. University Science Books, Mill Valley, CA.
- Umitsu, M. 1993. Late Quaternary sedimentary environments and landforms in the Ganges delta. *Sedimentary Geology*, 83, 177-186.
- U.S. Geological Survey Water-Data Reports. 1963-1995. Water resources data Hawaii and other Pacific areas. Water year reports 1963-1995. Prepared in cooperation with the State of Hawaii, Division of Land and Natural Resources, Water Resource Management.
- U.S. Soil Conservation Service. 1972. Soil Survey of Islands of Kauai, Oahu, Maui, Molokai, and Lanai, State of Hawaii. U.S.D.A. Soil Conservation Service and University of Hawaii Agricultural Experiment Station, Washington D.C.
- Van Weering, T.C.E., G.W. Berger, and E. Okkels. 1993. Sediment transport, resuspension, and acculamation rates in the northeastern Skagerrak. *Marine Geology*, 111, 269-285.
- Walling, D.E. 1994. Measuring sediment yield from river basins. In: R. Lal (Editor) Soil Erosion Research Methods, Soil and Water Conservation Society, St. Lucie Press, Delray Beach, FL., 39-80.
- Wentworth, C.K. 1943. Soil avalanches on Oahu, Hawaii. *Bulletin of the Geological Society of America*, 54, 53-64.

- White, S.E. 1949. Processes of erosion on steep slopes of Oahu, Hawaii. American Journal of Science, 247, 168-186.
- Williams, J.R. 1975. Sediment-yield prediction with universal equation using runoff energy factor. In: Present and Prospective Technology for Predicting Sediment Yield and Sources. Sed. Yield Work. Proc., Oxford, Miss., Agriculture Research Service, U.S.D.A. . Science and Education Admin., Washington D.C., ARS-S-40, pp. 244-252.
- Wischmeier, W.H. 1975. Estimating the soil loss equation's cover and management factor for undisturbed areas. In: Present and Prospective Technology for Predicting Sediment Yield and Sources. Sed. Yield Work. Proc., Oxford, Miss., Agriculture Research Service, U.S.D.A. . Science and Education Admin., Washington D.C., ARS-S-40, pp. 118-124.
- Wischmeier, W.H. and D.D. Smith. 1978. Predicting rainfall erosion losses - a guide to conservation planning. U.S.D.A. Agric. Handbook No. 537, 58 pp.